Heat Convection from a Horizontal Cylinder Rotating in a Quiescent Fluid

by

Syed Manzoor Ahmed

A Thesis Presented to the

FACULTY OF THE COLLEGE OF GRADUATE STUDIES

KING FAHD UNIVERSITY OF PETROLEUM & MINERALS

DHAHRAN, SAUDI ARABIA

In Partial Fulfillment of the
Requirements for the Degree of

MASTER OF SCIENCE

In

MECHANICAL ENGINEERING

October, 1985

Order Number 1360409

Heat convection from a horizontal cylinder rotating in a quiescent fluid

Ahmed, Syed Manzoor, M.S.

King Fahd University of Petroleum and Minerals (Saudi Arabia), 1985

U·M·I
300 N. Zeeb Rd.
Ann Arbor, MI 48106

HEAT CONVECTION FROM A HORIZONTAL CYLINDER ROTATING IN A QUIESCENT FLUID

BY

SYED MANZOOR AHMED

A Thesis Presented to the
FACULTY OF THE COLLEGE OF GRADUATE STUDIES

UNIVERSITY OF PETROLEUM & MINERALS
DHAHRAN, SAUDI ARABIA

In Partial Fulfillment of the
Requirements for the Degree of

MASTER OF SCIENCE
IN

MECHANICAL ENGINEERING

OCTOBER 1985

PRINTED BY: UPM PRINTING PRESS

UNIVERSITY OF PETROLEUM AND MINERALS

DHAHRAN, SAUDI ARABIA

This thesis, written by

SYED MANZOOR AHMED

under the direction of his Thesis Committee, and approved by all its members, has been presented to and accepted by the Dean, College of Graduate Studies, in partial fulfillment of the requirements for the degree of

MASTER OF SCIENCE IN MECHANICAL ENGINEERING

Dean, College of Graduate Studies

Date 12/2/1986

11/2/86

Dr. Jasim Al-Ansari

Department chairman

THESIS COMMITTEE

Chairman (Dr. Hasan M. Badr)

Member (Dr. I. K. Madni)

Member (Dr. A. F. M. A. Ali)

بسم الله الرحمن الرحيم

This thesis is

dedicated

to my parents.

ACKNOWLEDGEMENT

Thanks are due to the University of Petroleum and Minerals for the support provided to carry out this research.

I wish to express my thanks and appreciation to my major thesis advisor Dr. Hasan M. Badr, Associate Professor of Mechanical Engineering, whose help made this thesis possible. I also extend thanks to other members of my thesis committee Dr. Abdul Ali A.F.M. and Dr. Imtiaz K. Madni.

Thanks are also due to many of my friends particularly Mr. Shamoon A. Samad, Mr. Nousher and Mr. Aleem for their help in typing the manuscript.

Finally, I thank Mr. S.I. Jameel, secretary in Mechanical Engineering department, for his sincere help and cooperation.

TABLE OF CONTENTS

NOMENCLATURE

a,	cylinder radius;
c,	specific heat;
f_n, F_n,	functions defined in (44);
F_r, F_θ,	radial and transverse body force components;
g,	acceleration due to gravity;
g_n, G_n,	functions defined in (44);
Gr,	Grashof number, $g\beta(T_s-T_\infty)(2a^3)/\nu^2$;
h, $\bar{h}$,	local and average heat transfer coefficients;
h_n, H_n,	functions defined in (44);
k,	coefficient of thermal conductivity;
Nu, $\overline{Nu}$,	local and average Nusselt numbers;
p,	dimensionless pressure defined defined in (60);
Pe,	Peclet number, Re Pr;
P_n,	function defined in (66);
Pr,	Prandtl number, $\mu c/k$;
q,	rate of heat transfer per unit area;
Q_n,	function defined in (66);
r,	radial coordinate, r'/a;
Ra,	Rayleigh number, Gr Pr;
Re,	Reynolds number, $2a^2\omega/\nu$;
t,	dimensionless time, $t'u_s/a$;

T, temperature;

T_s, surface temperature of the rotating cylinder;

T_∞, temperature of the surrounding fluid;

V_r, V_θ, radial and transverse velocity components;

u_s, surface velocity of the rotating cylinder;

Greek symbols

α, thermal diffusivity, $k/\rho c$;

β, coefficient of volumetric thermal expansion;

δ, Kronecker's delta, a constant defined in Appendix (A);

ξ, logarithmic radial coordinate, ln r;

ρ, density;

ω, angular velocity of the rotating cylinder;

ν, kinematic viscosity;

ϕ, dimensionless temperature, $(T - T_\infty)/(T_s - T_\infty)$;

ψ, dimensionless stream function, ψ'/au_s;

θ, angular coordinate;

ζ, dimensionless vorticity, $a\zeta'/u_s$.

LIST OF TABLES

LIST OF FIGURES

ABSTRACT

This work aims to carry out a theoretical investigation to the problem of heat transfer from an isothermally heated horizontal cylinder rotating in quiescent fluid of infinite extent. The study is based on the solution of the conservation equations of mass, momentum and energy for the two dimensional flow of a Boussinesq fluid. The effect of the various parameters which influence the heat transfer process namely the Reynolds number and Grashof number are considered while the Prandtl number is held constant. The investigation is carried out for different values of Reynolds number while the Grashof number is varied in the range $0<Gr/Re^2<1.5$, the Prandtl number $Pr = 0.7$ is held at a constant value. The highest value of the Reynolds number considered in the present study is 840. Streamline and isotherm patterns are obtained from the mathematical model and the results are compared with previous experimental data. A satisfactory agreement was found.

ملخـــــص

تهدف هذه الدراسة الى اجراء بحثا نظريا لمشكلة انتقال الحـــرارة من أسطوانة أفقية ذات درجة حرارة منتظمة تدور في مائع ساكن غير محـــــدود . وتعتمد الدراسة على حل معادلات حفظ الكتلة وكمية الحركة والطاقة لسريـــان مائع في مجال ثنائي الأبعاد . وتشمل هذه الدراسة تأثير المتغيرات المختلفة التي تؤثر في عملية انتقال الحرارة وعلى وجه التحديد رقم رينولـــــــــد (Reynolds number) ورقم قراشوف (Grashof number) مع بقـــاء رقم براندتل (Prandtl number) ثابتا . وقد أجري هذا البحث لعـــدة قيم لرقم رينولد كما يتغير رقم قراشوف بحيث يكون ١٠٥ > رقم قراشـــوف / (رقم رينولد)٢ > صفر

أما رقم براندتل فكانت قيمته ٠.٧ كما أن أعلى قيمة لرقم رينولـــد في هذه الدراسة هي ٨٤٠ . وقد تم الحصول على خطوط الانسياب وكذلك خطوط تساوي درجة الحرارة من النموذج الحسابي كما تم مقارنة النتائج مع النتائج العمليـــة السابقة حيث كان التوافق بينهما مرضيا .

CHAPTER 1

1.1 INTRODUCTION

The thermal behavior of different machine elements involves the analysis of various modes of heat transfer such as conduction heat transfer between solid parts, convection between solid parts and the adjacent fluids and the radiative heat transfer between different machine elements. The convective heat transfer comprises mainly of the fluid flow over the stationary or moving machine elements. Convection heat transfer between a rotating machine element and the surrounding fluid presents a type of convection problem which is quite different and much more complicated than the typical problems of flow through ducts or over stationary external surfaces. Such a problem arises frequently in connection with the thermal behavior of shafting, flywheels, turbine rotors and many other similar machine parts.

Heat transfer from stationary horizontal cylinders to the surrounding fluid has been studied both theoretically and experimentally by many researchers. Vander Hegge Zijnen [1], Kyte [2] and others experimentally studied this problem and developed empirical correlations for the heat transfer coefficient for different ranges of Rayleigh number, Ra. Lately, Tsubouchi and Masuda [3] and Churchill and Chu [4] studied the same problem and obtained empirical correlations

for the heat transfer coefficient with further improvements.

The heat transfer from rotating machine elements consists of two major classes of problems, the first one associated with the rotating cylinders and the second associated with the rotating disks. The amount of research work available for the theoretical analysis of flow is small for the case of isothermally heated rotating horizontal cylinders. Several experimental investigations were conducted during 1950's to ascertain the thermal behaviour of isothermally heated rotating horizontal cylinders in different fluids of infinite extent. The results showed that the heat transfer coefficient was influenced mainly by the speed of rotation and the natural convection. All the researchers found that free convection has strong effect at low rotational speeds and then as rotational speed increases, the heat transfer coefficient was found to be entirely dependent on the rotational speed and not upon free convection effects. Empirical correlations were deduced for the heat transfer coefficient where it was found to be influenced only by the high speed of rotation.

The primary objective of the present work is to obtain a complete theoretical analysis of this problem of heat transfer from an isothermally heated horizontal cylinder rotating in a quiescent fluid of infinite extent. Importance is given to the low speed range in which the free convection

mechanism dominates and the flow is laminar.

1.2 LITERATURE REVIEW

Free convection heat transfer from horizontal cylinders has been a subject of both theoretical and experimental research due to its numerous engineering applications. Most of the previous research involved the experimental investigation for the heat transfer by natural convection from stationary cylindrical bodies immersed in different fluids which are infinite in extent. The empirical correlations developed for the heat transfer coefficient [1-8] for different ranges of Rayleigh number, Ra are summarised in Table 1.

Recently, Farouk and S.I. Guceri [9] studied the problem of laminar natural convection heat transfer from a stationary isothermal horizontal cylinder. A finite difference scheme involving successive substitution technique was employed. Finite difference equation were obtained by integration over finite cells, instead of using standard Taylor's series expansion. The results obtained were compared with the results obtained by Kuehn and Goldstein [10] and were found to be in good agreement. The results in [10] also showed that the boundary layer solutions do not adequately describe the flow and heat transfer at low and moderate values of Rayleigh number, Ra, due to neglecting curvature effects and the breakdown of

TABLE 1. Correlations for Heat Transfer by Natural Convection from Horizontal Isothermal Cylinder

1. Vander Hegge Zingen [1]

$$Nu = 0.35 + 0.25\ Ra^{0.125} + 0.45\ Ra^{0.25}, \qquad 10^{-7} < Ra < 10^{9} \qquad (1)$$

2. Kyte [2]

$$\left.\begin{aligned} Nu &= 2/\ln[1 + 7.09/Ra^{0.37}], && 10^{-7} < Ra < 10^{1.5} \\ Nu &= 2/\ln[1 + 5.01/Ra^{0.26}], && 10^{1.5} < Ra < 10^{9} \end{aligned}\right\} \qquad (2)$$

3. Tsubouchi and Masuda [3]

$$\left.\begin{aligned} Nu &= 0.36 + 0.52\ Ra^{0.25}, && 10^{-6} < Ra < 10 \\ Nu &= 0.36 + 0.048\ Ra^{0.125} + 0.52\ Ra^{0.25}, && 10^{-6} < Ra < 10^{9} \end{aligned}\right\} \qquad (3)$$

4. Churchill and Chu [4]

$$Nu = 0.36 + 0.518\ Ra^{0.25}\left[1 + (0.559/Pr)^{9/16}\right]^{-4/9}, \qquad 10^{-6} < Ra < 10^{9} \qquad (4)$$

5. Rice [5]

$$Nu = 2/\ln[1 + 2/(0.47\ Ra^{0.25})], \qquad (5)$$

6. Senftleben [6]

$$Nu = 2\{1 - [(1 + xy)^{0.5} - 1]/(xy)\}/x, \qquad (6)$$

where $x = \ln[1 + 4.5/Ra^{0.25}]$, $y = Ra^{0.25}/0.033$

7. Morgan [7]

$$\left.\begin{aligned} Nu &= 0.675\ Ra^{0.058}, && 10^{-10} < Ra < 10^{-2} \\ &= 1.020\ Ra^{0.148}, && 10^{-2} < Ra < 10^{+2} \\ &= 0.850\ Ra^{0.188}, && 10^{+2} < Ra < 10^{4} \\ &= 0.480\ Ra^{0.250}, && 10^{4} < Ra < 10^{7} \\ &= 0.125\ Ra^{0.333}, && 10^{7} < Ra < 10^{12} \end{aligned}\right\} \qquad (7)$$

contd .. Table 1

8. Raithley and Hollands [8]

$$Nu^{3.337} = [2/\ell n\{1 + 2.59/C(\ell)Ra^{0.25}\}]^{3.337} + [0.72\, C(t)Ra^{1/3}]^{3.337}$$

$$10^{-2} < Ra < 10^{12} \qquad (8)$$

$$C(\ell) = (2/3)/[1 + (0.49/Pr)^{9/16}]^{4/9},$$

$$C(t) = \min(0.15,\ 0.14\ Pr^{0.084}).$$

boundary layer assumptions in the region of the plume.

A detailed theoretical investigation of the problem of laminar mixed convection from an isothermally heated horizontal cylinder is presented by Badr [11,12]. Different flow directions were considered. The investigations were based on the solution of full vorticity transport equation together with the streamfunction and energy equations. The results obtained for different Reynolds number and Grashoff number were compared with available experimental correlations and the agreement was found to be satisfactory. Information on the effect of the flow direction on mixed convection from a horizontal cylinder [13] is also presented by the same author for Reynolds number, Re upto 40 and Grashoff numbers of $Gr = Re^2$. The results obtained agreed well with the experimental data obtained by other investigators.

The amount of research work conducted on the theoretical analysis of flow in the laminar free convection dominated regime is considerably small especially for the case of isothermally heated horizontal cylinders rotating in different fluids. Following 1950, several experimental investigations were performed to study the development of velocity and thermal fields around the isothermally heated rotating horizontal cylinder in a fluid of infinite extent. These studies have been restricted to the consideration of

the mean heat transfer coefficient without paying much attention to the details of the flow and thermal fields. These experimental studies further revealed that the heat transfer coefficient may be located in any one of the three distinct regions.

(1) in a region where its value does not depend on speed of rotation.

(2) in a region where its value is dependent on both free convection and speed of rotation and

(3) in a region where its value depends only on the speed of rotation.

Correlations were developed for the heat transfer coefficient where it was found to be influenced only by the high speed of rotation.

Anderson and Saunders [14] found that upto a critical value of Reynolds number, Re, the Nusselt number, Nu was almost independent of the surface velocity of the rotating cylinder. The Reynolds number which is based upon the surface velocity of cylinder was expected to reach a critical value when the tangential velocity of the surface of the cylinder becomes approximately equal to the upward free convection velocity. The critical Reynolds number Re_{cr} was found to be

$$Re_{cr} = 1.09\ Gr^{\frac{1}{4}} \qquad (9)$$

The heat transfer below this critical value was mainly due to free convection. Above this value, the Nusselt number Nu increases with the increase of Reynolds number and the heat transfer by free convection becomes negligibly small.

Dropkin and Carmi [15] conducted experiments for the same problem and concluded that for Reynolds number above 15000, Nusselt number may be computed from the equation

$$Nu = 0.073\ Re^{0.7} \tag{10}$$

The entire region in which the heat transfer coefficient is influenced by rotation was expressed as

$$Nu = 0.095\ (0.5\ Re^2 + Gr)^{0.35} \tag{11}$$

Etemad [16] studied experimentally the heat transfer and flow over horizontal cylinders rotating in air. The Interferometric studies revealed that the laminar couette flow broke down at a critical Reynolds number, Re of 900. At Reynolds number above the critical value, a three dimensional secondary flow begins to develop which showed some resemblance to the secondary flow between two concentric cylinders when the inner cylinder is rotated. Such a flow was observed by Taylor [17]. Using theoretical considerations, he obtained for Reynolds number above 8000, a correlation for Nusselt number

$$Nu = 0.076\ Re^{0.7} \tag{12}$$

In the intermediate range between 1000 and 8000, both Grashoff number and Reynolds number influenced the heat transfer rate

$$Nu = 0.11[(0.5\ Re^2 + Gr)Pr]^{0.35} \tag{13}$$

Kays and Bjorklund [18] studied the heat transfer from a horizontal cylinder rotating in air with and without cross flow. In case of no cross flow, it was found that the Nusselt number could be predicted by the equation

$$Nu = \frac{Re \cdot Pr \cdot \sqrt{\frac{C_D}{2}}}{5\ Pr + 5\ \ell n(3\ Pr + 1) + \left(\frac{1}{\sqrt{\frac{C_D}{2}}}\right) - 12} \tag{14}$$

The Friction factor C_D was obtained from the data of Theoderson and Regier [19].

Information about the heat transfer from a horizontal cylinder rotating in fluids other than air was reported by Becker [20] and Seban and Johnson [21]. Becker [20] studied the rate of heat transfer from a horizontal cylinder rotating in water. The experimental results obtained were

correlated with the equation

$$Nu = 0.133\ Re^{\frac{2}{3}} \cdot Pr^{\frac{1}{3}} \qquad (15)$$

The range of Prandtl number was 2.2 to 6.4 and the Reynolds number was between 1000 and 46000. Seban and Johnson [21] studied experimentally the heat transfer from a horizontal cylinder rotating in a tank of oil. The results covered the Prandtl number 130 to 670 and Reynolds number upto 15000. The results showed an increasing dependence of free convection heat transfer on rotation as the Prandtl number was increased by reducing the oil temperature.

A comprehensive experimental work regarding combined , forced and natural convection with low-speed air flow over isothermally heated horizontal cylinders was carried out by A.P. Hatton et.al [22]. The region in which both the natural convection and the forcing velocity have considerable influence on the mean heat transfer coefficient is extremely complex since the natural convection causes the fluid to move vertically upwards whereas the forcing velocity may be in any direction. In their work, a special emphasis was given to the hot wire anemometry application and accordingly, the heat transfer measurements were performed for Reynolds number, Re upto 45 and Rayleigh number, Ra in the range $10^{-3}<Ra<10$ for different flow directions. An experimental correlation based on the

vectorial summation of forced and natural convection was deduced. An equation of the following form was proposed for the natural convection regime

$$Nu \left[\frac{Tf}{T_\infty}\right]^{-0.154} = 0.384 + 0.59\ Ra^{0.184} \qquad (16)$$

where $[T_f/T_\infty]^{-0.154}$ is a temperature correction factor.

Shimomura [23] conducted experimental investigation on the region where the heat transfer coefficent is influenced by both the speed of rotation and the free convection mechanism. The study was focussed on the low speed range in which free convection mechanism dominates and the flow regime is laminar. Later L. Goettler and J.A. Filo [24] examined heat transfer from a slowly rotating horizontal cylinder to ambient air both analytically and experimentally. The approach was based on boundary layer assumptions where the boundary layer equations were deduced on the basis of order of magnitude analysis. However, because of the thick boundary layer prevailing around the cylinder surface specially at low rotational speeds, the above assumptions become questionable. Moreover the boundary layer assumptions are valid only upto the point of seperation after which the boundary layer thickness increases in all cases. The use of boundary layer assumptions in the region of plume was also shown to be

invalid by Kuehn and Goldstein [10] at low and moderate values of Rayleigh number, Ra. Hence the full conservation equations must be solved in the region after seperation. The results obtained in [24] show a considerable difference when compared with the experimental results of Shimomura [23].

When a horizontal cylinder, initially at the same temperature as that of the surrounding fluid, is subjected to a sudden uniform increase in tempertaure, it has been observed that the heat transfer to the surrounding medium was initially by pure conduction and then by natural convection [25-29]. Ostroumov [25] utilized an optical technique to observe the transient pattern of the temperature field around a 0.1 mm diameter platinum wire. The experimental setup had a resistance bridge to actually measure the temperature response of the wire. From the data obtained, he concluded that the transition time from pure conduction to natural convection was proportional to $Q^{0.6}$, where Q is the power delivered to the wire per unit length. It was also observed optically that the isotherms around the wire appeared to remain approximately concentric for a certain time called the 'delay time' before they were distorted by the buoyancy driven convective motion. The delay time was considered as the time for which a volume of liquid must be heated, characterised by the penetration depth of the temperature field, until its buoyancy exceeds

the viscosity of the surrounding liquid. At that point the hot fluid breaks away from the wire. Overshoot was also found to occur in some of the wire response data. Vest and Lawson [26] studied this transient temperature field in the fluid surrounding a suddenly heated thin horizontal wire using a precision Mach-Zehnder interferometer with a He-Ne light source. They found that transition time was proportional to $Q^{-2/3}$. The transition phenomenon was explained as hydrodynamic instability. In other words, the transition takes place when the Rayleigh number, Ra based on the penetration depth of the fluid reaches a critical value. The data indicated that the overshoot in heat transfer occurs for the case of horizontal cylinders and is related to thermal instability. Parsons and Mulligan [27] investigated experimentally the transient heat transfer due to step increase in temperature for 0.03mm and 0.127mm platinum wires in air. They confirmed the theory of Vest and Lawson with a suggestion to include the wire heat capacity and thermal conductivity effects. Parsons and Mulligan [28] also studied the onset of transient natural convection from a suddenly heated horizontal cylinder (6.32mm diameter steel) in air. The thermal stability analysis was confirmed which indicated localised natural convection before the global motion. The transition from conduction to convection was investigated again for horizontal cylinders, platinum wires in various liquids, subjected to internal heat

generation increasing linearly with time by Faw et.al [29]. Shadowgraph and interferometric images were obtained and the transition times were determined . The results showed that the time of transition was inversely proportional to the cubic root of the rate of increase in heat generation, and independent of wire diameter.

The transient experiments of Vest and Lawson, and Ostroumov, were optical in nature. The experimental studies [27-29] confirmed the transition from conduction to convection for the case of stationary horizontal cylinders only. No theoretical or experimental studies have been presented as yet for the case of isothermally heated rotating horizontal cylinder to confirm this transition from initial conduction to convective motion.

1.3 OBJECTIVE

The present work is aimed to conduct a complete theoretical analysis of the problem of heat transfer from an isothermally heated horizontal cylinder rotating in a quiescent fluid. The study is based on the solution of the three conservation principles namely the conservation of mass, conservation of momentum and the conservation of energy. The effect of various parameters on the heat transfer coefficient including the Reynolds number, Re and Grashoff number, Gr are considered. The time development of the velocity and thermal boundary layers until reaching the steady conditions are to be investigated. Variation of the local Nusselt number and vorticity over the whole cylinder surface as well as the streamline and isotherm patterns are to be plotted in order to study the different aspects of the phenomenon. Special emphasis is given to ascertain whether the initial heat transfer is due to pure conduction only as was reported for the case of isothermally heated stationary horizontal cylinders.

CHAPTER 2

2.1 PROBLEM STATEMENT

In this work, the problem of heat convection from a horizontal cylinder rotating in a quiescent fluid is considered. The solution is based on the solution of the three conservation principles namely the conservation of mass,the conversation of momentum and the conservation of energy. The most important assumptions utilized for the analysis of the present problem are as follows

(1) The flow is laminar.

(2) The cylinder is of infinite length assumed to be immersed in a fluid of infinite extent.

(3) The end effects of the cylinder on the velocity and temperature fields are neglected and hence the flow is assumed two dimensional.

(4) The effect of temperature variation on fluid properties are considered negligible except for the body force term in the momentum equation. This is commonly referred to as the 'Boussinesq approximation'.

(5) Effect of viscous dissipation is neglected.

(6) Radiation heat transfer effects are neglected.

2.2 GOVERNING EQUATIONS AND BOUNDARY CONDITIONS

The model considered here is a smooth horizontal circular cylinder of infinite length and radius, a, heated isothermally to a uniform surface temperature T_s. The cylinder is rotating counterclockwise at a constant angular velocity ω about its own axis and is assumed to be completely immersed in a quiescent fluid of constant temperature T_∞. Fluid motion is mainly due to

(1) Rotation of the cylinder and

(2) Buoyancy effects.

Assuming time dependent flow, the governing equations [30] in cartesian coordinates are

(1) EQUATION OF CONTINUITY:

$$\nabla \cdot \underline{U} = 0 \tag{17}$$

(2) EQUATION OF MOMENTUM:

$$\rho \left[\frac{\partial \underline{U}}{\partial t} + (\underline{U} \cdot \nabla)\underline{U} \right] = \underline{F} - \nabla p + \mu \nabla^2 \underline{U} \tag{18}$$

(3) EQUATION OF ENERGY:

$$\frac{\rho c}{k} \frac{DT}{Dt} = \nabla^2 T \tag{19}$$

where $\nabla^2 = \frac{\partial^2}{\partial x^2} + \frac{\partial^2}{\partial y^2} + \frac{\partial^2}{\partial z^2}$

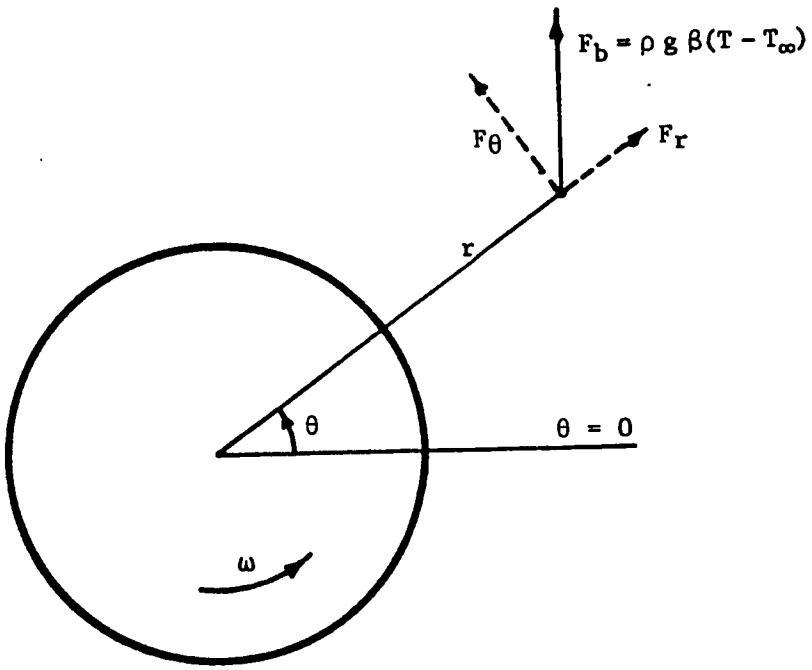

Fig. 1. The coordinate system used showing the radial and transverse body force components F_r and F_θ.

Now, introducing the vorticity vector $\underline{\zeta}'$ which is defined as

$$\underline{\zeta}' = \nabla \times \underline{U} \tag{20}$$

In case of two dimensional flow, the vorticity ζ' is given by

$$\zeta' = \left[\frac{\partial v'}{\partial x'} - \frac{\partial u'}{\partial y'}\right] \tag{21}$$

where ψ' is the stream function defined as

$$u' = \frac{\partial \psi'}{\partial y'} \qquad \text{and} \qquad v' = -\frac{\partial \psi'}{\partial x'} \tag{22}$$

to satisfy the continuity equation (17).

Utilizing this definition of vorticity in the momentum equation (18), an expression for the rate of change of vorticity can be obtained. This is achieved by taking the curl of the two sides of equation (18) which results in the famous Helmholtz vorticity transport equation

$$\rho\left[\frac{\partial \underline{\zeta}'}{\partial t'} + (\underline{U} \cdot \nabla)\underline{\zeta}'\right] = \nabla \times \underline{F} - \nabla \times \nabla p + \mu \nabla^2 \zeta' + \rho(\underline{\zeta}' \cdot \nabla)\underline{U} \tag{23}$$

Knowing that $\nabla \times \nabla p = 0$, equation (23) for the case of two dimensional flow yields

$$\frac{\partial \zeta'}{\partial t'} + u' \frac{\partial \zeta'}{\partial x'} + v' \frac{\partial \zeta'}{\partial y'} = \frac{1}{\rho}\left[\frac{\partial F_{y'}}{\partial x'} - \frac{\partial F_{x'}}{\partial y'}\right] + \nu \nabla^2 \zeta' \tag{24}$$

where the vorticity ζ' is related to the stream function ψ' by

$$\zeta' = - \nabla^2 \psi' \tag{25}$$

In cylindrical coordinates, the above two equations along with the energy equation can be expressed as

$$\frac{\partial \zeta'}{\partial t'} + v_{r'} \frac{\partial \zeta'}{\partial r'} + \frac{v_{\theta}'}{r'} \frac{\partial \zeta'}{\partial \theta} = \nu \nabla^2 \zeta' - \left(\frac{1}{\rho}\right)\left(\frac{\partial F_{\theta}}{\partial r'} - \frac{1}{r'} \frac{\partial F_{r'}}{\partial \theta} + \frac{F_{\theta}}{r'}\right) , \tag{26}$$

$$\zeta' = \nabla^2 \psi' , \tag{27}$$

$$\frac{\partial T}{\partial t'} + v_{r'} \frac{\partial T}{\partial r'} + \frac{v_{\theta}'}{r'} \frac{\partial T}{\partial \theta} = \left(\frac{K}{\rho c}\right) \nabla^2 T . \tag{28}$$

where $\nabla^2 = \frac{\partial^2}{\partial r'^2} + \frac{1}{r'} \frac{\partial}{\partial r'} + \frac{1}{r'^2} \frac{\partial^2}{\partial \theta^2}$

$F_{r'}$ and F_{θ} represent the radial and transverse body force components. These are defined as

$$\left.\begin{aligned} F_{r'} &= \rho g \beta (T - T_{\infty}) \sin\theta , \\ F_{\theta} &= \rho g \beta (T - T_{\infty}) \cos\theta . \end{aligned}\right\} \tag{29}$$

where β is the coefficient of volumetric thermal expansion defined as

$$\beta = \frac{1}{v}\left(\frac{\partial v}{\partial T}\right)_p = -\frac{1}{\rho}\left(\frac{\partial \rho}{\partial T}\right)_p \qquad (30)$$

The stream function ψ' and vorticity ζ' in cylindrical coordinates are defined as

$$v'_{r'} = \frac{1}{r'}\frac{\partial \psi'}{\partial \theta} \quad , \quad v'_\theta = -\frac{\partial \psi'}{\partial r'} \qquad (31)$$

and

$$\zeta' = -\frac{1}{r'}\left[r'\frac{\partial v'_\theta}{\partial r'} + v'_\theta - \frac{\partial v'_{r'}}{\partial \theta}\right] \qquad (32)$$

2.3 NORMALISING THE GOVERNING EQUATIONS

Since it is convenient to work with dimensionless quantities, the governing equations along with the boundry conditions are made dimensionless by redefining the dependent and the independent variables. This is achieved by dividing these dependent and independent variables by constant reference properties appropriate to the flow. The variables used are

$$v_r = \frac{v'_{r'}}{u_s} \quad ; \quad v_\theta = \frac{v'_\theta}{u_s} \quad ; \quad t = t'\frac{u_s}{a}$$

$$r = \frac{r'}{a} \quad ; \quad \psi = \frac{\psi'}{a\, u_s} \quad ; \quad \zeta = \zeta' \frac{a}{u_s}$$

and $$\phi = \frac{T - T_\infty}{T_s - T_\infty} \ .$$

where $u_s = a\omega$ is the surface velocity of the rotating cylinder.

Introduction of the dimensionless variables in equations (26)-(28) yields the following equations for the vorticity ζ, the stream function ψ and temperature ϕ

$$\frac{\partial \zeta}{\partial t} + V_r \frac{\partial \zeta}{\partial r} + \frac{V\theta}{r} \frac{\partial \zeta}{\partial \theta} = \left(\frac{2}{Re}\right) \nabla^2 \zeta - \frac{Gr}{2Re^2} \left[\cos\theta \frac{\partial \phi}{\partial r} - \frac{\sin\theta}{r} \frac{\partial \phi}{\partial \theta}\right] , \qquad (33)$$

$$\zeta = \nabla^2 \psi \ , \qquad (34)$$

$$\frac{\partial \phi}{\partial t} + V_r \frac{\partial \phi}{\partial r} + \frac{V\theta}{r} \frac{\partial \phi}{\partial \theta} = \frac{2}{Pe} \nabla^2 \phi \ . \qquad (35)$$

The radial and tangential velocity components V_r and V_θ can now be expressed in terms of ψ as

$$V_r = \frac{1}{r} \frac{\partial \psi}{\partial \theta} \quad \text{and} \quad V_\theta = - \frac{\partial \psi}{\partial r} \ . \qquad (36)$$

and the vorticity ζ is

$$\zeta = -\frac{1}{r}\left[r\,\frac{\partial v_\theta}{\partial r} + v_\theta - \frac{\partial v_r}{\partial \theta} \right] . \qquad (37)$$

The above equations were deduced using the following definitions for the dimensionless numbers

Reynolds number, $Re = 2a^2\omega/\nu$ based on the peripheral velocity of the rotating cylinder.

Prandtl number, $Pr = \mu\, c/k$ and

Grashoff number, $Gr = g\beta\,(T_s - T_\infty)(2a^3)/\nu^2$

2.4 BOUNDARY CONDITIONS

The different boundary conditions for the present problem are

i) at $r' = a$

$$V'_{r'} = 0 \;;\; V'_\theta = a\omega \quad \text{and} \quad T = T_s .$$

ii) as $r' \to \infty$

$$V'_{r'} \to 0 \;,\; V'_\theta \to 0 \;;\; T \to T_\infty \quad \text{and} \quad \zeta' \to 0 .$$

Utilizing the non-dimensional variables, the above boundary conditions reduce to

$$\left.\begin{aligned} &\text{i) at } r = 1 \\ &\qquad V_r = 0 \quad ; \quad V_\theta = 1 \quad \text{and} \quad \phi = 1 \\ &\text{ii) as } r \to \infty \\ &\qquad V_r \to 0 \quad ; \quad V_\theta \to 0 \quad ; \quad \phi \to 0 \quad \text{and} \quad \zeta \to 0 \end{aligned}\right\} \qquad (38)$$

These conditions are based on impermeability, no-slip and the isothermal conditions on the cylinder surface. V_r and V_θ both approach zero as r approaches infinity because of quiescent ambient fluid surrounding the rotating circular cylinder.

CHAPTER 3

THE METHOD OF SOLUTION

The method used for the solution of present problem is based on integrating the time dependent governing equations of motion and energy till the steady velocity and temperature fields are obtained. The procedure adopted for the solution involves the use of certain initial conditions and then integrating for a sufficient time till a steady state solution is reached. The approach is similar to the one adopted successfully for studying the laminar mixed convection from a horizontal isothermal circular cylinder in a cross stream [11] and laminar combined convection from an isothermal horizontal circular cylinder for the cases when the forced flow was directed either vertically upwards (parallel flow) or vertically downwards (contraflow) [12]. The same approach was used furthur to study the problem of laminar forced convection from an isothermally heated horizontal circular cylinder rotating about its own axis and placed in a uniform stream [31].

The method of solution is a generalization of the method developed by Badr and Dennis [32] to include the buoyancy term in the vorticity equation and to solve the energy equation simultaneously to obtain the time dependent temperature field. In the present problem, the cylinder is assumed to be initially rotating with no temperature

difference between its surface and the surrounding quiescent fluid. The cylinder is then suddenly heated (t>0) to a constant temperature T_s. In the initial stage immediately following the temperature increase, the temperature change is confined to the immediate neighborhood of the cylinder surface. Accordingly, the body force term will not have any effect on the solution since the temperature is same everywhere. In the later stage, due to temperature difference which exists between surface of cylinder and the surrounding fluid, both velocity and temperature fields develop with time until reaching the steady conditions.

3.1 THE SERIES TRUNCATION METHOD

To account for the boundary conditions that exist far away from the cylinder surface, the modified polar coordinates (ξ,θ) are utilized such that

$$\xi = \ln(r'/a) = \ln r$$

The equations (33)-(35) are now transformed accordingly to

$$e^{2\xi}\frac{\partial\zeta}{\partial t} = \frac{2}{Re}\left(\frac{\partial^2\zeta}{\partial\xi^2} + \frac{\partial^2\zeta}{\partial\theta^2}\right) - \frac{\partial\psi}{\partial\theta}\frac{\partial\zeta}{\partial\xi} + \frac{\partial\psi}{\partial\xi}\frac{\partial\zeta}{\partial\theta}$$

$$- e^{\xi}\frac{Gr}{2Re^2}\left[\cos\theta\frac{\partial\phi}{\partial\xi} - \sin\theta\frac{\partial\phi}{\partial\theta}\right], \qquad (39)$$

$$e^{2\xi}\zeta = \frac{\partial^2\psi}{\partial\xi^2} + \frac{\partial^2\psi}{\partial\theta^2}, \qquad (40)$$

$$e^{2\xi}\frac{\partial\phi}{\partial t} = \frac{2}{Pe}\left(\frac{\partial^2\phi}{\partial\xi^2} + \frac{\partial^2\phi}{\partial\theta^2}\right) - \frac{\partial\psi}{\partial\theta}\frac{\partial\phi}{\partial\xi} + \frac{\partial\psi}{\partial\xi}\frac{\partial\phi}{\partial\theta} \tag{41}$$

where

$$v_r = e^{-\xi}\frac{\partial\psi}{\partial\theta} \tag{42}$$

and

$$v_\theta = -e^{-\xi}\frac{\partial\psi}{\partial\xi} .$$

The transformed boundary conditions now are

$$\frac{\partial\psi}{\partial\theta} = 0 \quad , \quad \frac{\partial\psi}{\partial\xi} = -1 \quad \text{and} \quad \phi = 1 \quad \text{at} \quad \xi = 0$$

$$e^{-\xi}\frac{\partial\psi}{\partial\theta} \to 0 \quad ; \quad -e^{-\xi}\frac{\partial\psi}{\partial\xi} \to 0 , \tag{43}$$

$$\phi \to 0 \quad \text{and} \quad \zeta \to 0 \quad \text{as} \quad \xi \to \infty .$$

Although the buoyancy driven flow is symmetric about the line $\theta = \pi/2$ and the flow resulting from the rotational motion of the cylinder is axisymmetric, the superposition of the two motion results in an asymmetric flow field. Following the series truncation method developed by Badr and Dennis [32], the dimensionless vorticity ζ, stream function ψ, and temperature ϕ are expressed in terms of Fourier series as

$$\left.\begin{aligned}
\psi &= \frac{1}{2} F_o + \sum_{n=1}^{N} [f_n \sin n\theta + F_n \cos n\theta] , \\
\zeta &= \frac{1}{2} G_o + \sum_{n=1}^{N} [g_n \sin n\theta + G_n \cos n\theta] , \\
\phi &= \frac{1}{2} H_o + \sum_{n=1}^{N} [h_n \sin n\theta + H_n \cos n\theta] .
\end{aligned}\right\} \qquad (44)$$

where F_o, f_n, F_n, G_o, g_n, G_n, H_o, h_n and H_n are all functions of ξ and t.

Substituting equation (44b) in equation (39) and then integrating both sides of the resulting equation from 0 to 2π yields the following equation for the function $G_o(\xi,t)$

$$e^{2\xi} \frac{\partial G_o}{\partial t} = \left(\frac{2}{Re}\right) \frac{\partial^2 G_o}{\partial \xi^2} + S_o \qquad (45a)$$

To obtain the governing equation of $g_n(\xi,t)$, equation (44b) is substituted in equation (39) and both sides of the resulting equation are multiplied by sin $n\theta$. It is then integrated between 0 and 2π which yields after rearranging

$$2e^{2\xi} \frac{\partial g_n}{\partial t} = \left(\frac{4}{Re}\right)\left(\frac{\partial^2 g_n}{\partial \xi^2} - n^2 g_n\right) + n F_n \frac{\partial G_o}{\partial \xi} - n G_n \frac{\partial F_o}{\partial \xi} + S_{n_1} \qquad (45b)$$

Again after substituting (44b) in (39) and multiplying the resulting equation by cos nθ on both sides, the integration carried out as before between 0 and 2π yields an equation in terms of $G_n(\xi,t)$

$$2e^{2\xi}\frac{\partial G_n}{\partial t} = \left(\frac{4}{Re}\right)\left(\frac{\partial^2 G_n}{\partial \xi^2} - n^2 G_n\right) - n\, f_n \frac{\partial G_o}{\partial \xi} + n\, g_n \frac{\partial F_o}{\partial \xi} + S_{n_2} \qquad (45c)$$

where S_o, S_{n1} and S_{n2} are all functions of ξ and t and are defined in Appendix (A).

To obtain relationships between $F_o(\xi,t)$, $f_n(\xi,t)$ and $F_n(\xi,t)$ on one hand and $G_o(\xi,t)$, $g_n(\xi,t)$ and $G_n(\xi,t)$ on the other, equation (44a) is used together with equation (40). Both sides of the resulting equation are integrated directly between 0 and 2π to obtain the following relationship between F_o and G_o

$$\frac{\partial^2 F_o}{\partial \xi^2} = e^{2\xi} G_o \qquad (46a)$$

To obtain a relationship between F_n and G_n, equation (44a) is substituted in equation (40) and then both sides of the resulting equation are multiplied by cos nθ. The integration is performed on both sides between 0 and 2π which yields

$$\frac{\partial^2 F_n}{\partial \xi^2} - n^2 F_n = e^{2\xi} G_n \qquad (46b)$$

The relationship between f_n and g_n is obtained when both sides of equation (after substituting equation (44a) in equation (40)) are multiplied by sin $n\theta$ and integrated between 0 and 2π

$$\frac{\partial^2 f_n}{\partial \xi^2} - n^2 f_n = e^{2\xi}\, g_n \tag{46c}$$

Finally, using (44c) together with equation (41) and following the same mathematical procedure as was described for obtaining expressions (45) and (46), one can get the following expressions

$$e^{2\xi}\frac{\partial H_o}{\partial t} = \left(\frac{2}{Pe}\right)\frac{\partial^2 H_o}{\partial \xi^2} + Z_o\,, \tag{47a}$$

$$2e^{2\xi}\frac{\partial h_n}{\partial t} = \left(\frac{4}{Pe}\right)\left(\frac{\partial^2 h_n}{\partial \xi^2} - n^2 h_n\right) + n F_n \frac{\partial H_o}{\partial \xi} - n H_n \frac{\partial F_o}{\partial \xi} + Z_{n_1} \tag{47b}$$

$$2e^{2\xi}\frac{\partial H_n}{\partial t} = \left(\frac{4}{Pe}\right)\left(\frac{\partial^2 H_n}{\partial \xi^2} - n^2 H_n\right) - n f_n \frac{\partial H_o}{\partial \xi} + n h_n \frac{\partial F_o}{\partial \xi} + Z_{n_2} \tag{47c}$$

where the functions Z_o, Z_{n1}, Z_{n2} are all functions of ξ and t and are defined in Appendix (B). It must be mentioned here that the equations (45)-(47) obtained are similar to the equations obtained earlier by Badr [11].

The different boundary conditions for all the functions present in equations (45)-(47) are deduced by substituting the boundary conditions (43) in equation (44). This leads to

$$
\left.
\begin{aligned}
&\text{i) at } \xi = 0 \; ; \quad t > 0 \\
&\qquad F_n = f_n = h_n = H_n = 0 \quad ; \quad H_o = 2 \\
&\qquad \frac{\partial F_o}{\partial \xi} = -2 \; ; \; \frac{\partial f_n}{\partial \xi} = 0 \quad \text{and} \quad \frac{\partial F_n}{\partial \xi} = 0 \\
&\text{ii) as } \xi \to \infty \; ; \quad t > 0 \\
&\qquad F_n, \; f_n, \; H_o, \; h_n, \; H_n, \; G_o, \; g_n, \; G_n \to 0 \\
&\qquad \frac{\partial F_o}{\partial \xi} \to 0 \quad ; \quad \frac{\partial f_n}{\partial \xi} \to 0 \quad \text{and} \quad \frac{\partial F_n}{\partial \xi} \to 0
\end{aligned}
\right\} \qquad (48)
$$

3.2 INTEGRAL CONDITIONS

In order to ensure the continuity of pressure around the cylinder surface, Badr [11,12] and Collins and Dennis [33] found that the use of integral conditions were more efficient and easier to implement than the differential conditions in equation (48). Integrating equation (46a) with respect to ξ from $\xi = 0$ to $\xi = \infty$ and then applying the boundary conditions (48), one can obtain the integral condition (49a)

$$\int_0^\infty e^{2\xi} G_o \, d\xi = 2 \tag{49a}$$

By multiplying both sides of (46b) and (46c) with $e^{-n\xi}$ and then integrating from $\xi = 0$ to $\xi = \infty$ subject to boundary conditions (48), one obtains equations (49b) and (49c)

$$\int_0^\infty e^{(2-n)\xi} g_n \, d\xi = 0 \tag{49b}$$

$$\int_0^\infty e^{(2-n)\xi} G_n \, d\xi = 0 \tag{49c}$$

A similar approach has also been used by Ingham [34] to study the problem of free convective hear transfer from a stationary isothermal horizontal cylinder. The solution procedure in the present study is divided into two stages, the first one being the initial phase wherein the motion of

the fluid is only due to the rotation of cylinder with no temperature difference between the cylinder surface and the surrounding fluid and the second phase in which the surface of the rotating cylinder is heated instantaneously to a constant temperature T_s.

3.3 INITIAL PHASE

In the initial phase since the cylinder is assumed to be only rotating with no temperature difference between its surface and the surrounding fluid ($T_s = T_\infty$), the body force terms in equation (26) have no significance. Due to rotational symmetry and assuming the flow to be steady, the transverse component of the Navier-Stokes equation in polar coordinates can be reduced to

$$\left[\frac{\partial^2 v_\theta'}{\partial r'^2} + \frac{1}{r'}\frac{\partial v_\theta'}{\partial r'} - \frac{v_\theta'}{r'^2}\right] = 0 \qquad (50)$$

with the boundary conditions,

$$v_{r'}' = 0 \quad ; \quad v_\theta' = a\omega \quad \text{at} \quad r' = a$$

$$v_{r'}' \to 0 \quad ; \quad v_\theta' \to 0 \quad \text{as} \quad r' \to \infty$$

The solution of the above equation that satisfies the boundary conditions is

$$v_\theta' = \frac{a^2\omega}{r'} \quad \text{and} \quad v_{r'}' = 0$$

where a is the radius of the rotating cylinder and ω is the angular speed.

Using equation (32), one can now write

$$\frac{\partial\psi'}{\partial\theta} = 0 \quad \text{and} \quad \frac{\partial\psi'}{\partial r'} = -\frac{a^2\omega}{r'}$$

and using dimensionless variables one obtains

$$v_\theta = \frac{1}{r} \quad \text{and} \quad v_r = 0 \tag{51a}$$

everywhere in the flow field. Using the modified polar coordinates, the above stream function derivatives can be written as

$$\frac{\partial\psi}{\partial\theta} = 0 \quad \text{and} \quad \frac{\partial\psi}{\partial\xi} = -1 \tag{51b}$$

Differentiating equation (44a) partially with respect to θ and comparing with the above, one obtains

$$F_n = f_n = 0$$

Again, differentiating equation (44a) partially with respect to ξ and comparing with equation (51b) yields

$$\frac{\partial F_o}{\partial\xi} = -2 \; ; \quad \frac{\partial F_n}{\partial\xi} = 0 \quad \text{and} \quad \frac{\partial f_n}{\partial\xi} = 0$$

Integration of $\partial F_o/\partial \xi = -2$ yields

$$F_o = -2\xi + C$$

At $\xi = 0$; $F_o = 0$ ($\because \psi = 0$). $\therefore C = 0$

Hence $F_o = -2\xi$

Substitution of equation (51a) in the vorticity equation (37) gives $\zeta = 0$ everywhere in the flow field which results in $G_o = g_n = G_n = 0$ at time $t = 0$. Since there is no temperature difference between the cylinder surface and the surrounding fluid, then $\phi = 0$ everywhere in the flow field which leads to

$$H_o = h_n = H_n = 0.$$

3.4 THE SECOND PHASE

In the second phase of motion, the cylinder surface is assumed to be heated instantaneously to a temperature T_s. The thermal boundary layer develops along with the velocity boundary layer in time until reaching the steady state conditions. The instantaneous temperature rise at $t = 0$ results in $\phi = 1$ on the cylinder surface and $\phi = 0$ everywhere in the flow field. From equation (44c), the following conditions are obtained

$$\left.\begin{aligned} &H_o = 2\ ,\quad H_n = h_n = 0 \quad \text{at} \quad \xi = 0 \\ &H_o = h_n = H_n = 0 \qquad \text{as} \quad \xi \to \infty \end{aligned}\right\} \tag{52}$$

For the above mentioned conditions, the equations (45)-(47) are integrated numerically using the Crank-Nicholson finite difference implicit scheme. The time development of velocity and temperature fields is obtained by advancing the solutions of ψ, ζ and ϕ in time subjected to the boundary conditions (48).

3.5 FINITE DIFFERENCE FORMULATION

The finite difference methods are more practical and universally applicable amongst all the numerical techniques available. The set of differential equations in the present problem are solved using a Crank-Nicholson finite difference scheme. When using a finite difference scheme to solve a partial differential equation (subjected to associated initial and boundary conditions), a network of grid points is first established throughout the solution domain specified by the range of the independent variables. These finite difference methods are approximate in the sense that derivatives at a point are approximated by difference quotients over a small interval i.e $\partial F_o/\partial \xi$ is replaced by $\delta F_o/\delta \xi$ where δx is small. The solution is propagated

forwards from one time level to another in a step by step fashion. The technique employed in this work is stable, flexible and highly accurate.

The finite difference approximation is accomplished by expanding the Taylor's series about a typical grid point and then the resulting series is truncated to obtain the difference formula of the derivatives. The partial differential equations are transformed to a set of algebraic equations, which are then solved to give the numerical values of the unknown function at various grid points.

Both explicit and implicit methods are used for the solution of partial differential equations. The explicit solution of the simple one dimensional, time dependent heat conduction equation

$$\frac{\partial T}{\partial t} = \alpha \frac{\partial^2 T}{\partial x^2}$$

has the restriction $0 < \alpha\Delta t/(\Delta x)^2 < 1/2$ in order to have a stable solution. In other words, for given values α and Δx, if the time step Δt exceeds the above range, the numerical calculations become unstable due to the amplification of errors [35]. Hence implicit methods are more commonly used since they overcome this difficulty at the expense of a somewhat more complicated calculational procedure.

3.6 CRANK-NICHOLSON IMPLICIT METHOD

Crank-Nicholson implicit method is one of the most important of all the implicit methods since it reduces the dependency on time increment. For the case of pure conduction mentioned above, this method is convergent and stable for all the values of the ratio $\alpha\Delta t/(\Delta x)^2$ [35]. The ordinary finite difference approximation for $\partial T/\partial t$ has a discretization or the truncation error of $O(\Delta t)$. The discretization error is defined as the difference between the exact solution of PDE at any grid point and the finite difference approximation at that gridpoint [35]. The Crank-Nicholson method reduces this discretization error to $O[(\Delta t)^2]$.

A geometric interpretation can be obtained by referring to Figure. 2

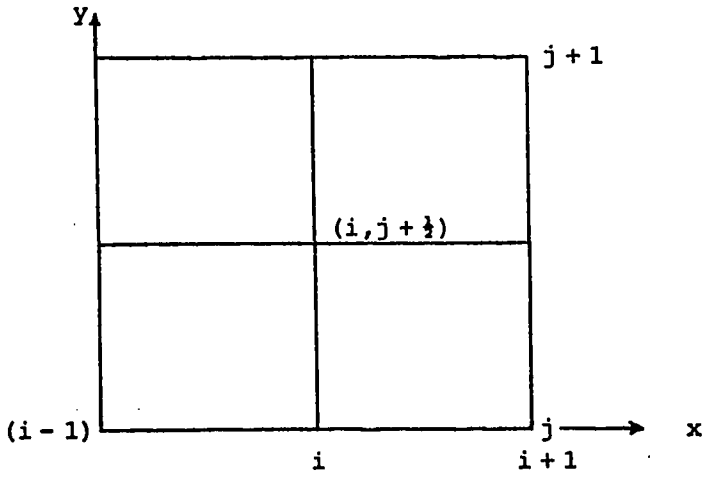

Figure 2. Geometrical representation of mesh points.

The reduced dependency on time increment can be accomplished by writing the finite difference equations for the derivatives $\partial T/\partial t$ and $\partial^2 T/\partial x^2$ at the half-way point $(i, j+1/2)$. In other words, the finite difference approximation of the derivatives are obtained by taking the mean of the finite differences on $(j+1)^{th}$ and j^{th} time steps. This can be represented mathematically as

$$\left(\frac{\partial T}{\partial t}\right)_{i,j} \cong \frac{T_{i,j+1} - T_{i,j}}{(\Delta t)} + O[(\Delta t)^2] \tag{53}$$

and

$$\left(\frac{\partial^2 T}{\partial x^2}\right)_{i,j} \cong \frac{1}{2}\left[\frac{T_{i+1,j} - 2T_{i,j} + T_{i-1,j}}{(\Delta x)^2} + \frac{T_{i+1,j+1} - 2T_{i,j+1} + T_{i-1,j+1}}{(\Delta x)^2}\right] \tag{54}$$

If there are (N-1) internal mesh points along each time row, the Crank-Nicholson method can be written generally as

$$\left.\begin{aligned}
b_1 u_1 - c_1 u_2 \quad &\ldots\ldots\ldots\ldots\ldots\ldots\ldots\ldots\ldots\ldots = d_1 \\
-a_2 u_1 + b_2 u_2 - c_2 u_3 \quad &\ldots\ldots\ldots\ldots\ldots\ldots\ldots\ldots\ldots\ldots = d_2 \\
&\vdots \qquad \vdots \qquad \vdots \\
&\qquad - a_i u_{i-1} + b_i u_i - c_i u_{i+1} \quad \ldots\ldots\ldots = d_i \\
&\qquad\qquad\qquad\qquad\qquad\qquad\qquad\qquad\qquad\qquad\qquad\qquad \vdots \\
&\qquad\qquad\qquad\qquad\qquad\qquad\qquad\qquad\qquad\qquad - a_{N-1} u_{N-2} + b_{N-1} u_{N-1} = d_{N-1}
\end{aligned}\right\} \tag{55}$$

where a's, b's, c's and d's are necessarily the known functions. The set of algebraic equations thus obtained form a tridiagonal matrix which is to be solved for every value of n between 1 and N.

3.7 CONVERGENCE, CONSISTENCY AND STABILITY

The problem of convergence and the stability of the adopted numerical technique is one of major factors to be considered in the solution of partial differential equations. The different conditions which are to be met in order to obtain a fairly good approximation to the solution of the corresponding partial differential equation using finite difference scheme are controlled by these factors.

Errors are introduced due to the truncation of the Taylor's series which is used to approximate the derivatives in the differential equations. The smaller the truncation error, the faster is the convergence of numerical solution to the exact solution of the differential equation. The finite difference solution is said to be convergent when the exact solution of the finite difference equations used to approximate the partial differential equations tend to the exact solution of partial differential equation as the grid spacing in time and distance approach the limit zero. The magnitude of these errors at any mesh point depends upon the spatial grid size Δx and time step size Δt. Since the Crank-Nicholson method has a discretization error of

$O[(\Delta x)^2+(\Delta t)^2]$, the convergence is obtained faster due to small truncation errors. Moreover, a larger value of Δt can be used in conjunction with this method, as it is second order correct and therefore a given elapsed time can be traversed in a fewer number of time steps.

The discretization errors can be furthur reduced by decreasing the mesh size Δx and time step size Δt, but this leads to an increase in the number of equations to be solved as well as the number of time steps. The method of improvement is therefore restricted by such factors as time, cost, degree of accuracy, computer storage capacity, etc.

Consistency is one of the fundamental requirements since it is of utmost importance that the finite difference scheme chosen indeed represents the actual differential equations. It is measured in terms of the difference between the differential equation and the difference equation. A finite difference scheme is said to be consistent with a system of differential equations when the former becomes identical with the latter in the limit as the mesh size approaches zero [36].

Stability is the most important aspect which has to be considered prior to the selection of a finite difference scheme for the solution of a set of partial differential equations. This problem is concerned mainly with the unstable growth or stable decay of errors in the

the arithmetical operations needed to solve the finite difference equations. Since each calculation is carried out to a finite number of decimal places or significant figures, therefore a 'round-off' error is introduced everytime and the solution actually computed is not the exact solution of the partial differential equations. A set of finite difference equations are stable when the cumulative effect of the rounding errors is negligibly small.

The magnitude of the round-off errors at a particular step is not as important as the propagation of this error as the solution continues. There is an upper limit (as $\Delta t \to 0$) to the extent to which this error, whether present in the initial conditions, or brought in via the boundary conditions, or arising due to errors in calculations, can be amplified in computations. Carnahan [35] has pointed out that according to Ritchmyer [37] stability is both a necessary and sufficient condition for convergence provided that a consistency criterion is satisfied for a linear partial differential equation. According to Kaplan [38], stability does not necessarily mean that the deviation between the true solution to a certain partial differential equation and its finite difference approximation will be in any sense small. Rather, it implies the boundedness of the finite difference solution, at a given time t as $\Delta t \to 0$. The rounding errors are not similar to discretization errors since they increase with decrease in mesh size due to more

numerical computations and therefore the chances of propagation of these errors also increases.

3.8 FINITE DIFFERENCE EQUATIONS

The solution of ψ, ζ and ϕ are advanced in time by solving the three sets of differential equations (45)-(47) using Crank-Nicholson finite difference implicit scheme and a step-by-step integration scheme. At any time t, it is reqired to obtain $G_o(\xi,t)$, $G_n(\xi,t)$ and $g_n(\xi,t)$ to determine the distribution of vorticity, the functions $H_o(\xi,t)$, $H_n(\xi,t)$ and $h_n(\xi,t)$ to determine the dimensionless temperature distribution and the functions $F_o(\xi,t)$, $F_n(\xi,t)$ and $f_n(\xi,t)$ to determine the stream function provided that all these functions are known at a time level $(t-\Delta t)$,where Δt is the time increment. The finite difference equations are first obtained and then an iterative method of solution is utilized since the resulting equations are non-linear.

The following section deals with the formulation of finite difference equations using Crank-Nicholson implicit method. The formulation procedure for the equation (45c) is described in detail and a similar procedure can be used for the solution of other equations. The governing equation (45c) is

$$2e^{2\xi}\frac{\partial G_n}{\partial t} = \left(\frac{4}{Re}\right)\left(\frac{\partial^2 G_n}{\partial \xi^2} - n^2 G_n\right) - n\, f_n \frac{\partial G_o}{\partial \xi} + n\, g_n \frac{\partial F_o}{\partial \xi} + S_{n_2}$$

Let us write the above equation as,

$$\frac{\partial G_n}{\partial t} = q_n(\xi, t) \quad \text{where}$$

$$q_n(\xi,t) = \frac{e^{-2\xi}}{2}\left[\frac{4}{Re}\left(\frac{\partial^2 G_n}{\partial \xi^2} - n^2 G_n\right) - n\, f_n \frac{\partial G_o}{\partial \xi} + n\, g_n \frac{\partial F_o}{\partial \xi} + S_{n_2}\right]$$

Then according to Crank-Nicholson method, one can use equations (53) and (54) to write the above equation as,

$$\frac{G_n(\xi,t) - G_n(\xi,t-\Delta t)}{(\Delta t)} = \frac{1}{2}\left[q_n(\xi,t) + q_n(\xi,t-\Delta t)\right]$$

where

$$q_n(\xi,t) = \frac{e^{-2\xi}}{2}\left[\left(\frac{4}{Re}\right)\left\{\frac{G_n(\xi+\Delta\xi,t) - 2G_n(\xi,t) + G_n(\xi-\Delta\xi,t)}{(\Delta\xi)^2} - n^2 G_n(\xi,t)\right\}\right.$$

$$- n\, f_n(\xi,t)\left\{\frac{G_o(\xi+\Delta\xi,t) - G_o(\xi-\Delta\xi,t)}{2(\Delta\xi)}\right\}$$

$$\left. + n\, g_n(\xi,t)\left\{\frac{F_o(\xi+\Delta\xi,t) - F_o(\xi-\Delta\xi,t)}{2(\Delta\xi)}\right\} + S_{n_2}(\xi,t)\right]$$

After simplifications and rearranging, one obtains

$$-e^{-2\xi}\left(\frac{4}{Re}\right)G_n(\xi+\Delta\xi,t) + \left[\frac{4(\Delta\xi)^2}{\Delta t} + 2e^{-2\xi}\left(\frac{4}{Re}\right)\right]G_n(\xi,t) - e^{-2\xi}G_n(\xi-\Delta\xi,t)$$

$$= \frac{4(\Delta\xi)^2}{\Delta t}\,G_n(\xi,t-\Delta t) - \frac{4n^2}{Re}\,(\Delta\xi)^2\,e^{-2\xi}\,G_n(\xi,t)$$

$$+ e^{-2\xi}(\Delta\xi)^2\left[-n\,f_n(\xi,t)\left\{\frac{G_o(\xi+\Delta\xi,t) - G_o(\xi-\Delta\xi,t)}{2(\Delta\xi)}\right\}\right.$$

$$\left. + n\,g_n(\xi,t)\left\{\frac{F_o(\xi+\Delta\xi,t) - F_o(\xi-\Delta\xi,t)}{2(\Delta\xi)}\right\} + S_{n_2}(\xi,t)\right]$$

$$+ 2(\Delta\xi)^2 q_n(\xi,t-\Delta t) \qquad (56)$$

In general, the above equation can be simply written as

$$A(\xi)G_n(\xi+\Delta\xi,t) + B(\xi)G_n(\xi,t) + C(\xi)G_n(\xi-\Delta\xi,t)$$

$$= D_n(\xi,t-\Delta t) + E_n(\xi,t) \qquad (57)$$

where $A(\xi) = C(\xi) = -e^{-2\xi}\left(\frac{4}{Re}\right)$,

$$B(\xi) = \left[\frac{4(\Delta\xi)^2}{\Delta t} + \frac{8e^{-2\xi}}{Re}\right],$$

$D_n(\xi,t-\Delta t)$ = Known function at time $(t-\Delta t)$,

$E_n(\xi,t)$ = Function which depends upon the

solution at time t.

$\Delta\xi$ = Increment along ξ-direction.

Δt = Increment along t-direction.

It is clear from equation (57) that the left hand side contains three unknown function values which are to be evaluated at time t and the right hand side contains the known functions at time $(t-\Delta t)$ represented by the term D_n in the equation. However, the term $E_n(\xi,t)$ on the right hand side of the equation is an unknown quantity since it depends upon the solution at time t. A method similar to the one used by Badr [11,12] is utilised to overcome this difficulty. An iterative process was used in which the functions $E_n(\xi,t)$ are assumed initially to be same as $E_n(\xi,t-\Delta t)$. It is then corrected according to the most recently available values. The iteration process is stopped when the difference in the solution of $G_n(\xi,t)$ between two successive iterations is within a certain allowable limit i.e

$$\left| G_n^{m+1}(\xi,t) - G_n^{m}(\xi,t) \right| < 10^{-4} \qquad (58)$$

where the superscript m denotes the iteration number.

3.9 INTEGRATION PROCEDURE

The procedure used here involves the integration of equations (45) and (47) numerically using Crank-Nicholson finite difference implicit scheme discussed earlier subject to the boundary conditions (48) and the integral conditions (49). In theory, the equations (45)-(47) should be integrated in the region $\xi = 0$ to $\xi = \infty$. However, since the problem is solved numerically, the conditions at ∞ are applied at $\xi = \xi_m$ where ξ_m defines the distance away from the cylinder surface at which ζ and ϕ have negligibly small values ($\approx 10^{-10}$). For example, if ξ is chosen to be 10, then the actual radial distance is e^{10} times the radius of the cylinder.

The solution is started at time $t = 0$, when there is only rotation but no temperature difference between the cylinder surface and the surrounding quiescent fluid. The initial velocity distribution is obtained analytically (equation (51)) and is utilized for the calculation of different functions in equation (44). The next phase starts with the instantaneous heating of the cylinder surface to a temperature T_s. The solution is marched in time since the thermal and velocity boundary layers start developing until reaching the steady conditions (indicated by constant value of average Nusselt number).

Even though the Crank-Nicholson method is stable for all values of ratio $\Delta t/(\Delta\xi)^2$, a small time step (Δt) is chosen for the accuracy requirements. Moreover, at the start of the second phase of motion, the thermal boundary layer is very small in thickness which means that the gradient $\partial H_o/\partial\xi$ is very large near the solid boundary. This also requires the use of even smaller time steps at the start of the second phase of motion to obtain higher accuracy. The mesh size is kept constant in ξ-direction ($\Delta\xi = 0.1$) during the second phase of motion.

At the start of the second phase of motion, the number of terms N in the Fourier series was 2. This number was allowed to increase with time whenever any of the last non-zero terms in the series reaches a certain small value. However, the maximum number of terms used was 20 in all the cases considered. The problem was dealt with in four stages. In the first stage, the integration was started with a time step of $\Delta t = 0.00005$ to reach $t = 0.0001$. In the second stage, the integration was performed in 10 steps of $\Delta t = 0.001$ followed by the third stage in which $\Delta t = 0.01$ was used to reach $t = 0.1$ and finally the fourth stage was carried out for time step $\Delta t = 0.05$ till the steady conditions are reached.

The numerical solution is started at $t = 0$ where the initial conditions of all the functions are known. A

generalised finite difference equation similar to equation (57) is written for all the equations and then applied at every individual mesh point in the range $\xi = \Delta\xi$ to $\xi = \xi_m$. The mesh point $\xi = 0$ was excluded because of the difficulties in calculating the derivatives on the surface of the cylinder. The integral conditions (49a), (49b) and (49c) are utilized for calculating $G_o(0,t)$, $g_n(0,t)$ and $G_n(0,t)$ respectively on the cylinder surface. Simpson's integration rule is used to evaluate the integral condition (49a). To ensure the continuity of pressure around the cylinder surface, integral condition (49a) must be satisfied.

To prove that the above condition is sufficient, consider the transverse component of the Navier-Stokes equation subjected to the boundary conditions (48) on the cylinder surface which results in

$$F_\theta - \frac{1}{r'}\frac{\partial p'}{\partial \theta} - \mu\left(\frac{\partial \zeta'}{\partial r'}\right)_{r'=a} = 0 \qquad (59)$$

where

$$\left(\frac{\partial \zeta'}{\partial r'}\right)_{r'=a} = -\left[\frac{\partial^2 v_\theta'}{\partial r'^2} + \frac{1}{r'}\frac{\partial v_\theta'}{\partial r'} - \frac{v_\theta'}{r'^2}\right]$$

To examine the pressure distribution, let us introduce the dimensionless pressure p defined as

$$p = \frac{p'}{\frac{1}{2}\rho a^2 \omega^2} \tag{60}$$

Introduce also the dimensionless variables in equation (59) and then transform the resulting equation into modified polar coordinates (ξ,θ) which yields the following relation between the pressure and the vorticity field

$$\frac{\partial p}{\partial \theta} = \frac{Gr}{Re^2}\cos\theta - \frac{4}{Re}\left(\frac{\partial \zeta}{\partial \xi}\right)_{\xi=0} \tag{61}$$

The equation (61) when integrated between 0 and 2π gives

$$p_{2\pi} - p_o = \frac{-4\pi}{Re}\left(\frac{\partial G_o}{\partial \xi}\right)_{\xi=0} \tag{62}$$

The problem is now reduced to prove that to satisfy the integral condition (49a), it is sufficient to ensure

$$\left(\frac{\partial G_o}{\partial \xi}\right)_{\xi=0} = 0 \tag{63}$$

The governing equation (45a) when integrated on both

sides from $\xi = 0$ to $\xi = \infty$ yields

$$\frac{2}{Re}\left(\frac{\partial G_o}{\partial \xi}\right)_{\xi=0} = \int_0^\infty S_o(\xi,t)d\xi - \frac{\partial}{\partial t}\int_0^\infty e^{2\xi} G_o \, d\xi \qquad (64)$$

The function $S_o(\xi,t)$ and the value of the integral conditions (49a) are substituted in the above equation which results in the condition (63) on the cylinder surface.

The value of the function $G_n(0,t)$ is assumed to be exactly same as $G_n(0,t-\Delta t)$. Application of equation (57) at every mesh point in the range $\Delta\xi \leqslant \xi \leqslant \xi_m$ results in a set of algebraic equations. These algebraic equations form a tridiagonal matrix problem which is to be solved each time to obtain the values of the function $G_n(\xi,t)$. The solution is required subjected to the boundary conditions (48) and must also satisfy the integral condition (49c). Crout's reduction technique [39] is employed for the solution of this tridiagonal system since it is more advantageous over Gauss reduction technique. The main advantage being the minimization of recording or storing the auxiliary data such as repeated rewriting of modified equations or arrays. After an approximation to the solution of equation (57) is obtained by this process, the value of function $G_n(0,t)$ is calculated to a better approximation by using the integral condition (49c). A two step formula approximating the

integrand as a polynomial over three successive points x_m, x_{m+1} and x_{m+2} similar to the one used by the Filon [40] is utilized. The conventional numerical quadrature requires a very fine grid to produce sufficiently accurate results. Moreover, the numerical quadrature produced results which were inaccurate when n was large and the periodic function had many zeroes in the range [11,33]. For stability, a relaxation technique similar to that used by Collins and Dennis [33] is employed. According to this technique

$$G_n^{m+1}(0,t) = r_f\, G_n(0,t) + (1 - r_f) G_n^{m}(0,t) \qquad (65)$$

where 'r_f' is the relaxation factor chosen empirically such that $0 < r_f < 1$. $G_n(0,t)$ is the value of iterate assumed at time level $(t-\Delta t)$, $G_n^{m}(0,t)$ is the present value of the function obtained from the condition (49c) and $G_n^{m+1}(0,t)$ is the average of the next iterate. The convergence condition (58) is now checked using the most recent available value of the function $G_n(0,t)$. If the convergence condition is not satisfied, the process is repeated using this new value of $G_n(0,t)$ until the convergence is achieved. In the present case, $r_f = 0.9$ was chosen.

Once a better approximation is obtained for each of the functions $G_o(\xi,t)$, $G_n(\xi,t)$ and $g_n(\xi,t)$, the next step is to solve equations (46). This is done in order to obtain $F_o(\xi,t)$, $F_n(\xi,t)$ and $f_n(\xi,t)$ and hence the value of stream

function ψ at any time t. A direct solution for the equation (46a) can be easily obtained using the closed type quadrature formulae in terms of ordinates as described by Hildebrand [39] to obtain higher accuracy. Step by step integration scheme similar to the one used by Dennis and Chang [41] is utilized to solve equations (46b) and (46c) numerically. This scheme involves the assumption of two first order equations for the functions $P_n(\xi,t)$ and $Q_n(\xi,t)$ such that

$$\left.\begin{aligned} P_n(\xi,t) &= f_n'(\xi,t) + n f_n(\xi,t) \\ \text{and} \\ Q_n(\xi,t) &= f_n'(\xi,t) - n f_n(\xi,t) \end{aligned}\right\} \qquad (66)$$

where the prime denotes differentiation with respect to ξ. These functions now should satisfy the equation (46c). Upon substitution one can get

$$P_n'(\xi,t) - n P_n(\xi,t) = r(\xi,t) \qquad (67a)$$

$$Q_n'(\xi,t) + n Q_n(\xi,t) = r(\xi,t) \qquad (67b)$$

where $r(\xi,t)$ is the right side of the equation (46c). The initial conditions are $P(0) = Q(0) = 0$. The other boundary conditions for the present problem are

$$P(\xi,t) = Q(\xi,t) = 0 \qquad \text{at} \quad \xi = 0$$

$$P(\xi,t) \to 0;\ Q(\xi,t) \to 0 \qquad \text{as} \quad \xi \to \infty$$

The right hand side $r(\xi,t)$ is known at all the grid points in the interval $\xi = 0$ to $\xi = \xi_m$. Expressing equations (67a) and (67b) by simple forward differences resulted in an error growth which was unacceptable [41]. This was due to the unwanted increasing exponential part of the complementary function. Equation (67a) is now integrated in the increasing ξ direction subject to the initial conditions at $\xi = 0$ and equation (67b) is integrated backwards with the conditions existing at $\xi = \xi_m$ where ξ_m is used to approximate the boundary at infinity. The solution $f_n(\xi,t)$ can be obtained simply as

$$f_n'(\xi,t) = \frac{P_n(\xi,t) + Q_n(\xi,t)}{2} \tag{68}$$

A check of the results obtained from equation (68) can now be made by observing whether

$$f' = 0 \qquad \text{at} \quad \xi = 0 \qquad \text{and}$$

$$f' \to 0 \qquad \text{as} \quad \xi \to \infty$$

within an acceptable numerical tolerance. The function $f_n(\xi,t)$ can be obtained by utilizing the closed type numerical quadrature formula [39]. The formulae used for the calculation of $f_n(\xi,t)$ are the one step formula to effect the first step of integration from the initial point $\xi_o (= 0)$ to the next adjacent point $\xi_1 (= \Delta\xi)$, but using a

parabolic approximation to $r(\xi,t)$ over the points ξ_o, ξ_1, $\xi_2(= 2\ \Delta\xi)$ and the two step formula over the successive points ξ_n, ξ_{n+1}, ξ_{n+2}. A parabolic approximation for $r(\xi,t)$ is utilised. A direct finite difference scheme was not used due to stability requirements. Since the value of step size in ξ-direction remains constant regardless of n, the error at fixed ξ increases rapidly with n which makes the use of central finite difference scheme unsuitable [41]. Moreover, the exponential term in the complementary function of the equation (46b) and (46c) increases with increasing n. Hence the error growth associated with this also increases [41]. The same procedure is adopted for finding $F_n(\xi,t)$.

The solution procedure for the calculation of each of $H_o(\xi,t)$, $H_n(\xi,t)$ and $h_n(\xi,t)$ is similar to the solution of equations (45). The equation (47) is more easy to solve since there are no integral conditions to be satisfied. The conditions existing at the end points are known completely. The Crank-Nicholson difference scheme is used to obtain a set of algebraic equations at different grid points from which a tridiagonal matrix is readily obtained. This is solved for every value of n between 1 and N. The convergence criteria is similar to the one used in equation (58).

Once the values of different functions are obtained at each mesh point at time t, the values of the stream function ψ, vorticity ζ and dimensionless temperature ϕ can be

obtained.

3.10 LOCAL AND AVERAGE NUSSELT NUMBERS

The convective transport coefficients can be expressed in terms of dimensionless groups. One of the most important being the Nusselt number which is defined as

$$Nu = hL_x/k \tag{69}$$

where L_x is the characteristic length which is the diameter of the cylinder in the present case. The coefficient of heat transfer h can be obtained from Newton's law of cooling

$$\dot{q} = h(T_s - T_\infty) \tag{70a}$$

The Fourier's law of conduction is

$$\dot{q} = -k(\partial T/\partial r')_{r'=a} \tag{70b}$$

where $\dot{q}$ is the rate of heat transfer per unit area. From the above definition, one can obtain the local Nusselt number Nu as

$$Nu = -2\left(\frac{\partial \phi}{\partial \xi}\right)_{\xi=0}$$

$$= -2\left[\frac{1}{2}\frac{\partial H_o}{\partial \xi} + \sum_{n=1}^{N}\left\{\frac{\partial h_n}{\partial \xi}\sin n\theta + \frac{\partial H_n}{\partial \xi}\cos n\theta\right\}\right]_{\xi=0} \tag{71}$$

The average Nusselt number $\overline{Nu}$ is defined as

$$\overline{Nu} = 2a\bar{h}/k \tag{72a}$$

where $\bar{h}$ is the average heat transfer coefficient obtained by integrating the local heat transfer coefficient over the whole cylinder surface such as

$$\bar{h} = \frac{1}{2\pi} \int_0^{2\pi} h d\theta \tag{72b}$$

The average Nusselt number can be obtained similarly as

$$\overline{Nu} = -\left(\frac{\partial H_o}{\partial \xi}\right)_{\xi=0} \tag{72c}$$

The various first order derivatives on the surface ($\xi = 0$) for calculating the distribution of the local Nusselt number Nu and the average Nusselt number $\overline{Nu}$ are calculated using more accurate finite difference formulae since the ordinary forward difference formulae have a leading error of $O(\Delta\xi)$. The first order derivatives are represented in forward difference to $O[(\Delta\xi)^2]$ through the following formula

$$\left(\frac{\partial U}{\partial \xi}\right)_{i,j} = \frac{-3U_{i,j} + 4U_{i+1,j} - U_{i+2,j}}{2(\Delta\xi)} \tag{73}$$

CHAPTER 4

ACCURACY OF THE RESULTS

The accuracy of the solution obtained depends mainly upon the accuracy of the mathematical model as well as the numerical technique utilized to solve the problem. The accuracy of the numerical technique used in this work can be tested by comparing the results obtained with the theoretical and experimental data available in the literature.

Two tests were performed to ascertain the validity of the results obtained. They are

1) Conduction-Convection transition.

2) Experimental verification.

4.1 CONDUCTION-CONVECTION TRANSITION

The phenomenon of transition from conduction to convection was first observed experimentally for the case of heat transfer from a suddenly heated horizontal cylinder. In that case it was observed that initially the heat transfer was purely due to conduction and at a later time, the natural convection dominates [25-29]. In the present case of a isothermally heated horizontal cylinder rotating in a quiescent fluid, the conductive heat transfer is observed initially, followed by a convective mode of heat transfer which prevailed until reaching steady state. In

order to compare between the solution of the present problem at small times and the solution of the conduction problem, consider the transient conduction equation in cylindrical coordinates

$$\frac{\partial T}{\partial t'} = \frac{k}{\rho c}\left[\frac{\partial^2 T}{\partial r'^2} + \frac{1}{r'}\frac{\partial T}{\partial r'} + \frac{1}{r'^2}\frac{\partial T}{\partial \theta^2}\right] \tag{74}$$

Due to axisymmetry, the equation is reduced to

$$\frac{\partial T}{\partial t} = \frac{k}{\rho c}\left[\frac{\partial^2 T}{\partial r'^2} + \frac{1}{r'}\frac{\partial T}{\partial r'}\right] \tag{75}$$

The initial and boundary conditions are

$$T = T_\infty \quad \text{at} \quad t = 0, \quad \text{and}$$

$$T = T_s \quad \text{at} \quad r' = a$$

$$T \to T_\infty \quad \text{as} \quad r' \to \infty \quad \text{for} \quad t > 0$$

The above equation is written in a dimensionless form using the same dimensionless variables used earlier. The resulting equation along with the initial and boundary conditions is

$$\frac{\partial \phi}{\partial t} = \frac{2}{Pe}\left[\frac{\partial^2 \phi}{\partial r^2} + \frac{1}{r}\frac{\partial \phi}{\partial r}\right] \tag{76}$$

where

$\phi = 0$ at $t = 0$, and

$\phi = 1$ at $r = 1$

$\phi \to 0$ as $r \to \infty$ for $t > 0$

The modified polar co-ordinates (ξ, θ) are used here again to account for the boundary conditions prevailing at an infinite distance from the surface of the cylinder. Accordingly we use

$$\xi = \ln r$$

The equation (76) along with the initial and boundary conditions now takes the form

$$e^{2\xi} \frac{\partial \phi}{\partial t} = \frac{2}{Pe} \frac{\partial^2 \phi}{\partial \xi^2} \qquad (77)$$

where Peclet number, $Pe = Re.Pr$

Reynolds number, $Re = 2a^2 \omega/\nu$

and Prandtl number, $Pr = \mu c/k$

The initial and boundary conditions now become

$\phi = 0$ at $t = 0$, and

$\phi = 1$ at $\xi = 0$

$\phi = 0$ as $\xi \to \infty$ for $t > 0$

Crank-Nicholson implicit method is used to write the finite difference equations for the differential equation (77). The solution is advanced in time subjected to the above initial and the boundary conditions. Figure 3 shows a comparison between the results obtained from the present work and the numerical solution of pure transient conduction problem. The results are computed for the case of Pr = 0.7, Re = 50 and Gr = 1250 in the present work whereas for pure transient conduction, the solution is obtained for Pr = 0.7 and Re = 50. It can be clearly seen that initially pure conduction theory and the present study agree very well. However, at a certain time, the pure conduction results deviate considerably from the present study. This clearly shows that there is a limit to pure conduction heat transfer after which the heat transfer by natural convection becomes more dominant. The convective process is delayed for a certain period of time following the sudden temperature rise allowing the pure conduction to influence the heat transfer process. This delay in convection is termed as 'delay time'. The results obtained in the present work for the case of rotating isothermally heated horizontal cylinder and the experimental results obtained for the case of stationary isothermally heated horizontal cylinder [25-29] show that whether the cylinder is stationary or rotating, the initial heat transfer is due to pure conduction only followed by a transition region after which the convection process

dominates.

The transition from pure conduction to natural convection which begins at the limit of pure conduction is either a monotonically decreasing transient or may occur in form of an overshoot, a phenomenon wherein the Nusselt number decreased even below its steady state value which can be clearly observed from Figure 4. It can also be observed from the Figures 3 and 4, the delay time of pure conduction can be identified with minimum of the average Nusselt number. The same conclusions were obtained for the case of heat transfer from an isothermally heated stationary horizontal cylinder [27]. Moreover, the isotherms which are presented in the next chapter further confirm this phenomenon since they are concentric circles around the cylinder axis, a result which has been experimentally observed [25-29].

4.2 EXPERIMENTAL VERIFICATION

To check the accuracy of the results obtained by the present method, the numerical computations were made for Re = 840, Pr = 0.7 and Gr = 9.8×10^5, the values used are the same as the experimental work [16]. It was shown in [16] that at Reynolds number greater than 840, the interference lines begin to oscillate and the free convection chimney starts disappearing due to the development of unsteadiness in the laminar flow. Figure 5 shows the steady state isotherms obtained from the present method around the

surface of the rotating cylinder. A marked similarity can be observed if Figure 5 is compared with the experimentally obtained steady state interference photograph [16]. The interference lines or the isotherms around the rotating cylinder are similar to the isotherms around an isothermally heated horizontal cylinder in free convection flow, the difference being the shifting of plume or the chimney in the direction of rotation. The flow caused by rotation of the cylinder was a laminar flow. As predicted by the experimental results [16] at Re=840, the position of the breakaway region of the flow is horizontal. It was also noted from numerical computations that the limit of initial pure conduction was the point where the minimum average Nusselt number occurred. The delay time was appreciably shorter and the transition from the pure conduction region to natural convection was in the form of an overshoot.

The results obtained from the present study were also compared with the experimental correlation deduced by Hatton et.al [22]. The average Nusselt numbers, $\overline{Nu}$ obtained from the present theory were compared with the following empirical correlation

$$Nu \left[\frac{T_f}{T_\infty}\right]^{-0.154} = 0.384 + 0.59\ Ra^{0.184}$$

where $[T_f/T_\infty]^{-0.154}$ is a temperature correction factor and

Ra is the Rayleigh number.

The comparison between the present method and Hatton's correlation is presented in Table 2. The results show about 10% difference at low Rayleigh numbers. The difference decreases with an increase in Rayleigh number. The differences between the present results and the empirical correlation are believed to be due to the following reasons

(a) In theory, the flow is considered two dimensional since the cylinder end effects are neglected.

(b) The temperature effects on the fluid properties were neglected and hence no temperature correction factor was applied.

(c) The above empirical correlation is for the case of low-speed air flow over a stationary horizontal cylinder whereas the results obtained from the present work are for an isothermally heated horizontal cylinder rotating slowly in a quiescent fluid.

(d) The uncertainty in the experimental measurements especially at low Rayleigh numbers.

CHAPTER 5

RESULTS AND DISCUSSIONS

Based on the governing equations of motion and energy it is clear that the thermal field and accordingly the rate of heat transfer are dependent on Reynolds number, Re, Grashoff number, Gr and the Prandtl number, Pr. Since the Prandtl number is fixed at 0.7, the Reynolds number, Re and Grashoff number, Gr mainly influence the velocity and temperature fields. Hence the parameter Gr/Re^2 which represents the ratio between buoyant and inertial forces has significant effect on the numerical computations. The full mass, momentum and energy equations are solved simultaneously for various values of Reynolds number, Re while the Grashoff number, Gr is varied in the range $0 < Gr/Re^2 < 1.5$ for every value of Re. The integration was not performed for higher values of the ratio Gr/Re^2 because of the excessive amount of computer time required to satisfy the convergence condition (58) and also because of the large storage capacity required.

The mathematical model introduced in Chapter 3 was used to predict the time development of velocity and thermal boundary layers around the rotating cylinder. The values of stream function ψ, vorticity ζ and the temperature ϕ in the flow field were obtained at different time levels from the start of motion until the steady state. The time required to

reach steady state varied from one case to another depending on Re and Gr.

Figure 4 shows the time variation of the average Nusselt number $\overline{Nu}$ following a sudden rise in cylinder surface temperature for a few of the cases considered. The figure shows that $\overline{Nu}$ has its maximum value at t = 0, however, the value decreases with an increase in time until reaching its final steady value. This is due to the fact that immediately following the step temperature rise of the cylinder surface, the thermal boundary layer thickness is very small and is confined to the immediate neighborhood of the cylinder surface. The temperature gradient near the cylinder surface is very high which leads to conduction dominated heat transfer regime. With the increase of time, the thermal boundary layer thickness increases and $\overline{Nu}$ decreases accordingly. From the figure it is also clear for the cases considered that the transition from conduction to convection occurs in the form of an overshoot. As the value of parameter Gr/Re^2 is increased for a particular value of Re, the present calculation show a decrease in convection delay and a decrease in time required to reach the steady state. For small values of the parameter $Gr/Re^2 (\leq 0.3)$, the transition from conduction to convection was a monotonically decreasing transient and hence no overshoot was obtained for these cases.

The numerical values of the average Nusselt number $\overline{Nu}$ at different values of Re and Gr are shown in Table 3. It is clear from the numerical results obtained that the value of $\overline{Nu}$ increases as Gr increases for a particular value of Re. This behavior can be explained on the basis that the buoyant forces increase as the value of Gr increases and therefore the $\overline{Nu}$ also increases. At low values of Gr, the rotation effects are more dominant over the natural convection and hence the heat transfer from the isothermally heated rotating cylinder to the surrounding quiescent ambient is mainly by conduction (characterized by the concentric isotherms around the rotating cylinder). The thermal boundary layer thickness is large and accordingly the average Nusselt number $\overline{Nu}$ is small. Increase in the value of Gr causes the natural convection effects to increase thereby increasing the average Nusselt number $\overline{Nu}$.

The ratio Gr/Re^2 also has significant effect on the development of velocity and thermal boundary layers. Figures 6a, 6b and 6c show the variation of vorticity ζ on the cylinder surface for the cases when Re = 10, 50 and 100 and for different values of Grashoff number, Gr. The figures show that the surface vorticity and accordingly the velocity gradient increases significantly with the increase of Gr. At very small Gr, the vorticity ζ is very small around the cylinder surface. The figures also clearly show that the vorticity has its maximum value near $\theta = 180^\circ$ on the surface

of the cylinder. This is mainly because the buoyant forces are opposing the flow due to the counterclockwise rotation of the cylinder thereby causing the velocity gradient to reach a maximum value. The surface vorticity has a maximum negative value near $\theta = 0^{\circ}$ since the buoyant forces there are aiding the flow due to the rotation of cylinder. The region of lower velocities to the left of vertical diameter ($90^{\circ} < \theta < 270^{\circ}$) have a positive velocity gradient whereas the region of higher velocities to the right of vertical diameter have a negative velocity gradient on the cylinder surface.

Figures 7a, 7b and 7c show the variation of local Nusselt number Nu around the cylinder surface for the cases when Re = 10, 50 and 100 respectively. Different values of the ratio Gr/Re^2 were taken in each case to show the effect of Grashoff number,Gr on the local Nusselt number distribution over the cylinder surface. The figures clearly show that the value of local Nusselt number Nu increases with the increase of Gr around the cylinder surface. The maximum and minimum values of the local Nusselt number Nu approach $\theta = 180^{\circ}$ at low values of Gr. This is expected since the rotation effects are dominant over the natural convection. As the value of Gr is increased, the maximum and minimum values of the local Nusselt number Nu shift contineously towards $\theta = 270^{\circ}$ and $\theta = 90^{\circ}$ respectively. It may be expected that at a sufficiently high value of Gr and a low value of the Re, the maximum and minimum values of the local Nusselt number Nu

will be at $\theta = 270^{\circ}$ and $\theta = 90^{\circ}$ respectively in which case the heat transfer becomes independent of Re and the flow field approaches that of the natural convection heat transfer from a horizontal isothermally heated stationary cylinder. This is due to the fact that an increase in Gr causes the natural convection effects to increase whereas the rotation effects are comparatively small. The values of Re and Gr considered by Shimomura [23] and and J.A.Filo [24] do not lie in the range considered in the present study. However, the general shape of the experimental and analytical Nusselt number Nu distribution correspond well with the Nusselt number distribution obtained from the present study.

The time development of vorticity around the cylinder surface is shown in Figures 8a, 8b and 8c for Re = 10 and Gr = 140, Re = 50 and Gr = 1250 and Re = 100 and Gr = 10000 respectively. The surface vorticity increases with increase in time since the velocity gradient increases. The maximum absolute values of the surface vorticity occur near $\theta = 0^{\circ}$ and $\theta = 180^{\circ}$ since the maximum positive and maximum negative velocity gradients occur near these points.

The time variation of local Nusselt number Nu around the cylinder surface are shown in Figures 9a, 9b and 9c. It is clear from these figures that the local Nusselt number Nu around the cylinder surface decreases continously with increase of time until the heat transfer due to natural

convection becomes more dominant over the heat transfer due to initial pure conduction. In the initial phase of pure conduction, the value of the local Nusselt number Nu around the cylinder surface decreases since the thermal boundary layer thickness increases. After the emergence of natural convection, the local Nusselt number Nu increases a little around the cylinder surface. The final steady conditions show that the maximum and minimum values of the local Nusselt number Nu continue to occur near $\theta = 270^{\bullet}$ and $\theta = 90^{\bullet}$ respectively since the thermal boundary layer thickness is minimum near $\theta = 270^{\bullet}$ and maximum near $\theta = 90^{\bullet}$.

The distribution of local Nusselt number Nu around the cylinder surface (Figures 9a, 9b and 9c) also clearly shows the initial pure conduction mode which is evident from the straight line plot (due to uniform heat transfer coefficient) at t = 1 in all the cases considered. As the time increases, the deviation from the uniformity of heat transfer coefficient starts appearing and the value of the local Nusselt number Nu around the cylinder surface starts decreasing due to increase of thermal boundary layer thickness with time.

The time development of the streamline pattern for the different cases considered are shown in Figures 10,11 and 12. Initially since the rotation effects are dominant over the natural convection, the streamlines are concentric

circles around the rotating cylinder axis. As the time increases, the velocity field is subjected to both natural convection and rotation. Velocities to the left of the vertical diameter ($90^{\circ} < \theta < 270^{\circ}$) are lesser when compared to the velocities on the right of the vertical diameter. This is due to the fact that the buoyant forces are opposing the rotation in the region to the left of vertical diameter whereas they are aiding the rotation in the region towards the right. The vortex formation which was non-existent at the beginning, begins to develop as the time increases. The size of the vortex formed increases with increase in time due to combined effect of the natural convection and the rotation of the cylinder. The vortex formation is enhanced further if Re and Gr increase. The heat transfer across the vortex boundries to the main fluid outside the vortex is by pure conduction.

Due to the rotation of the cylinder, it can be clearly seen that there always exists a thin layer of fluid which adheres to the cylinder surface and rotates with it. This layer of fluid isolates the cyliner from the rest of the flow field. The stagnation points do not lie on the surface of the cylinder but occur within the flow at certain other locations called the 'saddle points'. The exact location of the saddle points is determined by first drawing the locus of points which have zero radial velocity V_r and the locus of points which have zero transverse velocity V_θ around the

cylinder surface. The points where the two locii intersect around the cylinder surface are the saddle points. From equation (42), we have

$$V_r = e^{-\xi} \frac{\partial \psi}{\partial \theta}$$

and

$$V_\theta = -e^{-\xi} \frac{\partial \psi}{\partial \xi}$$

The stream function ψ (equation (44a)) is substituted which leads to

$$\left.\begin{aligned} V_r &= e^{-\xi} \sum_{n=1}^{N} (n f_n \cos n\theta - n F_n \sin n\theta) \\ \text{and} \\ V_\theta &= -e^{-\xi} \left[\frac{1}{2} \frac{\partial F_o}{\partial \xi} + \sum_{n=1}^{N} \left(\frac{\partial f_n}{\partial \xi} \sin n\theta + \frac{\partial F_n}{\partial \xi} \cos n\theta \right) \right] \end{aligned}\right\} \quad (78)$$

where F_o, F_n and f_n are all functions of ξ and t.

The locii of zero radial velocity V_r and the zero transverse velocity V_θ around the cylinder surface are shown in Figure 13 for the case when Re = 50 and Gr = 750. The saddle point S and the points of zero vorticity A and B are shown at steady state conditions. The exact angular location of the saddle points around the cylinder for Re = 50 and at different values of Gr are listed in table 4. It is clear from the values obtained that at low Gr, the

rotation are effects are stronger and therefore the saddle point which is situated in the region of lower velocities to the left of vertical diameter is deflected to a maximum value towards $\theta = 270^{\circ}$. As the value of Gr increases for the same Reynolds number, Re, the saddle point starts returning back towards $\theta = 180^{\circ}$. This behaviour of the saddle point clearly shows the role played by natural convection when Re is held constant and Gr is increased.

The time development of the thermal field around the rotating cylinder for the same above cases are shown in Figures 14, 15 and 16. At small times, the heat transfer regime is influenced by only conduction and hence the isotherms are concentric circles which can be clearly seen at $t = 1$ and $t = 5$ for all the cases considered. Following that, the isotherms develop with time until reaching the steady conditions. After the initial conduction mode, the isotherms become asymmetrical. The isotherms are convected upwards in the upper region whereas they remain adhered to the surface of the cylinder in the lower region. As the time is increased further, the convective effects are more significant until finally a mushroom-shaped steady state plume is formed. The isotherms obtained in the present study are similar to the experimentally obtained isotherms for the case of isothermally heated stationary horizontal cylinder except for the plume which shifts in the direction of rotation. The shifting of the plume increases with an

increase in Reynolds number, Re. If $\phi = 0.01$ is considered as the edge of the thermal zone bounding the cylinder, the effect of increasing the Gr while keeping the rotation effects constant are shown in Figure 17. It is clear from the figure that at low values of Gr, the thermal field is dominated by conduction (the isotherm $\phi = 0.01$ plotted is approximately concentric) and therefore the thermal boundary layer thickness is large. As the value of Gr is increased, natural convection becomes stronger and accordingly the thermal boundary layer thickness starts decreasing below the cylinder while increasing above it.

CONCLUSIONS

The problem of heat convection from an isothermally heated horizontal cylinder rotating in a quiescent medium is investigated for different values of Reynolds number while the Grashof number is varied in the range $0 < Gr/Re^2 < 1.5$, the Prandtl number $Pr = 0.7$ is held constant. The highest value of the Reynolds number, Re considered in the present study is 840. The study is based on the solution of full mass, momentum and energy equations simultaneously for different values of Reynolds number and the Grashof number. A mathematical model was constructed to find the time development of the velocity and thermal fields.

Transient heat transfer from a horizontal rotating cylinder subjected to a sudden rise in temperature clearly occurs in three well defined stages. An initial pure conduction stage, followed by a convective transition and, finally, to the state of steady free convection. The convective transition from pure conduction to steady free convection occurs either as a monotonically decreasing transient with no overshoot or in the form of an overshoot depending upon the value of the parameter Gr/Re^2.

The results obtained were compared with the previous empirical correlations where a good agreement was found. In the considered range, for a particular value of Reynolds

number, it is found the velocity and thermal fields are strongly influenced by the Grashof number. The average Nusselt number increases with increase in Grashof number due to increase in the buoyant forces for a particular value of the Reynolds number. The details of the steady velocity and thermal boundary layers were obtained and accordingly the variation of vorticity and the local Nusselt number around the rotating cylinder surface were plotted for different cases. The resulting values of the average Nusselt number were tabulated and compared with the Hatton's correlation. The agreement between the two was satisfactory.

The streamline and isotherm patterns were plotted to show some of the details of the velocity and thermal fields. It was clear that due to rotation of the cylinder, there always exists a layer of fluid which rotates with the cylinder and hence the stagnation points are no longer situated on the cylinder surface but at some other locations called the saddle points. The ratio Gr/Re^2 again has considerable influence on the location of the saddle points around the cylinder surface. The isotherms obtained clearly show the initial pure conduction mode and are similar to the experimentally obtained isotherms for the case of isothermally heated stationary horizontal cylinder except for the plume which shifts in the direction of rotation.

Re	Gr	Ra	$\overline{Nu}$ Hatton's correlation	$\overline{Nu}$ Present study
3.0	3.0	2.10	1.060	0.947
3.0	4.5	3.15	1.112	0.991
3.0	6.3	4.41	1.159	1.047
5.0	8.0	5.60	1.194	1.092
10.0	10.0	7.00	1.228	1.162

Table 2. Comparison between $\overline{Nu}$ obtained from the present work and Hatton's experimental correlation.

Re	Gr	$\overline{Nu}$
10	10	1.170
10	50	1.634
10	100	1.896
10	140	2.015
50	250	1.770
50	1250	2.907
50	2500	3.411
50	3500	3.682
100	1000	2.225
100	5000	3.757
100	10000	4.525
100	14000	4.823
200	4000	2.580
200	20000	4.932

Table 3. Values of $\overline{Nu}$ for the case of Pr = 0.7.

Re	Gr	θ_s in deg.
50	250	216
50	750	207
50	1250	201
50	2500	194
50	3500	189

Table 4. Exact location of the saddle point in the flow field around the cylinder surface.

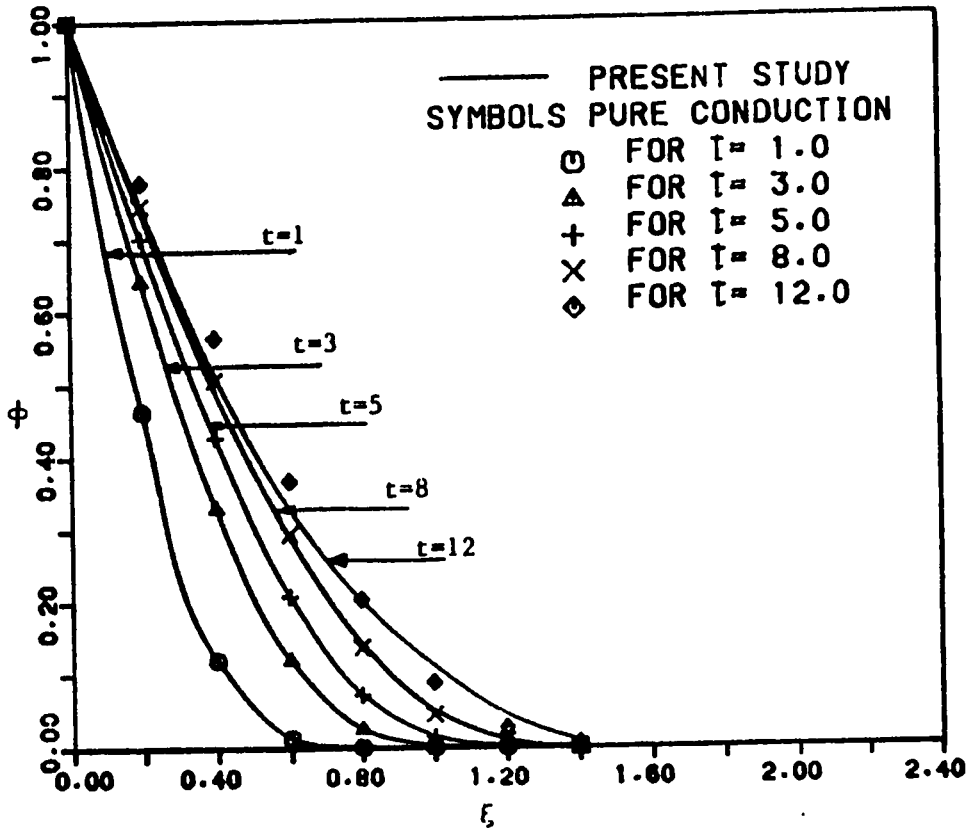

Fig. 3. Comparison of temperature distribution obtained from the present work and the transient pure conduction for Re=50, Pr = 0.7 and Gr = 1250.

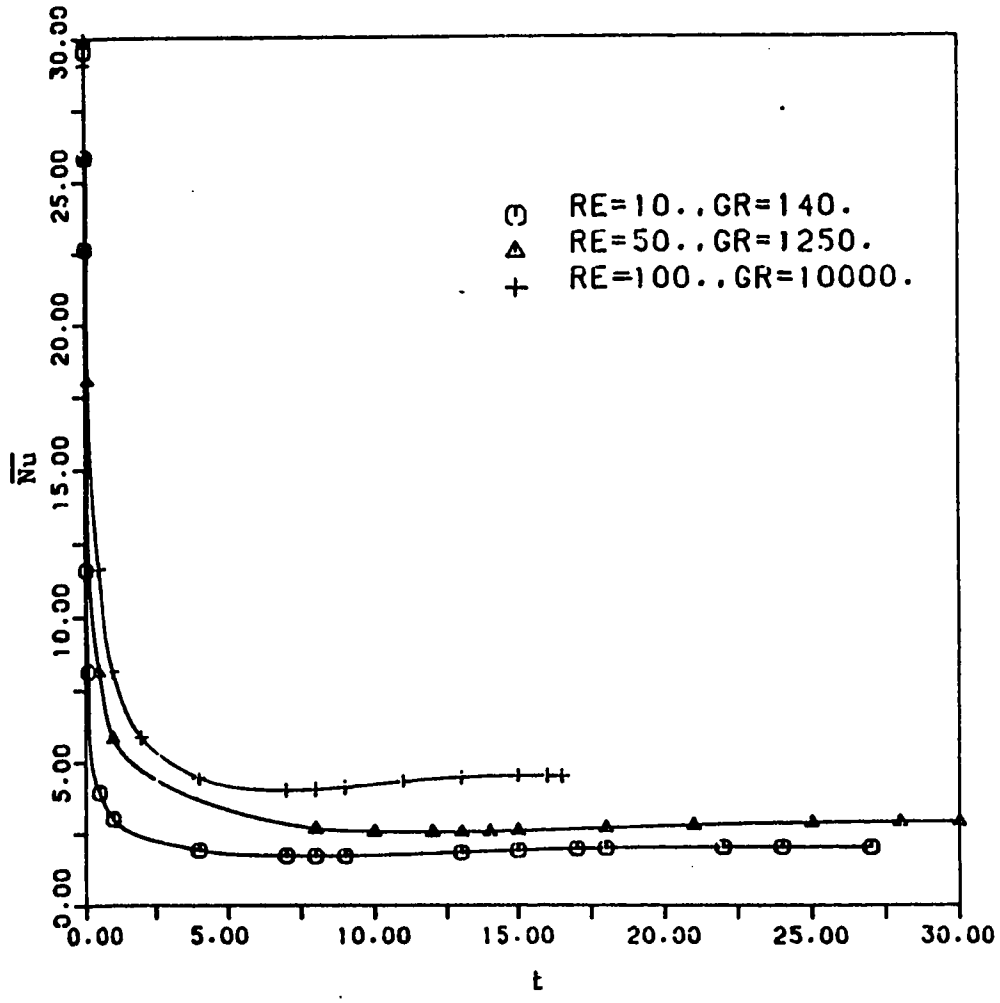

Fig. 4. Transient decay of $\overline{Nu}$ for the case of Pr = 0.7.

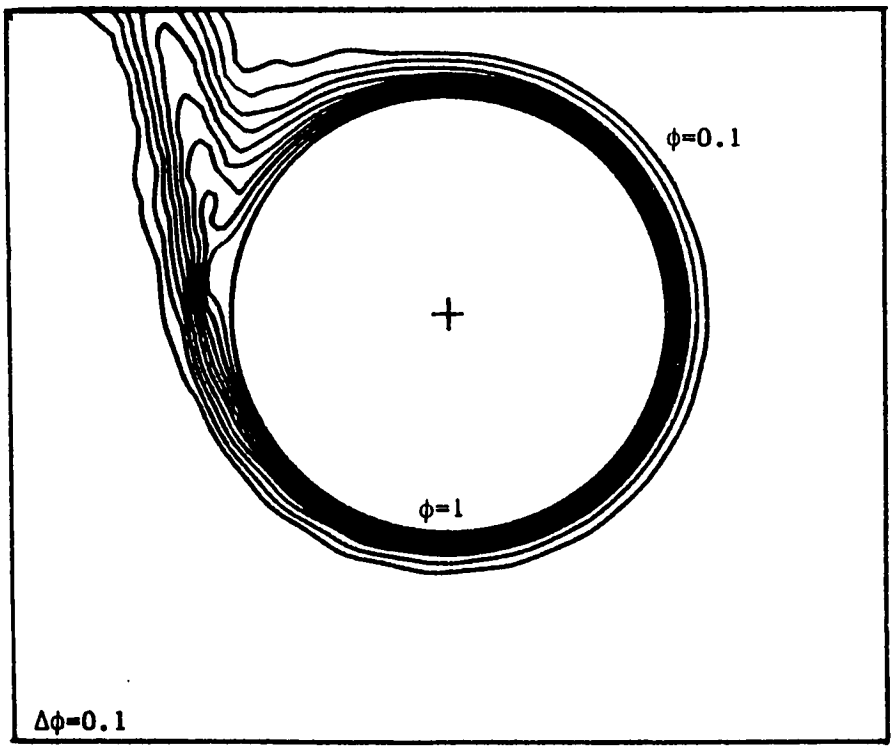

Fig. 5. Isotherm pattern for the case of Re = 840, Pr = 0.7 and Gr = 9.8×10^5.

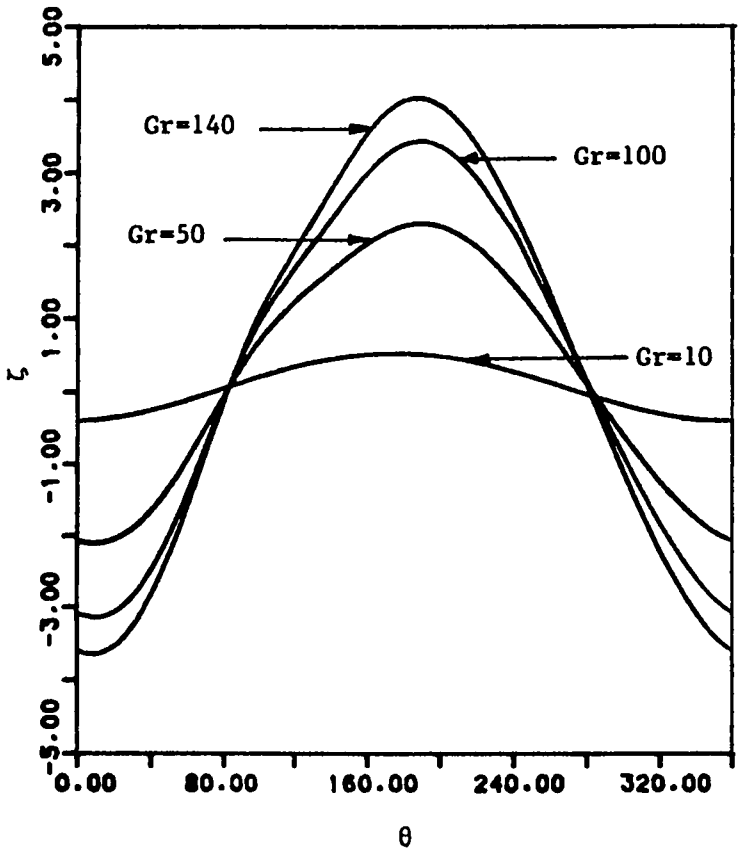
Gr=140
Gr=100
Gr=50
Gr=10
5.00
3.00
1.00
-1.00
-3.00
-5.00
ζ
0.00
80.00
160.00
240.00
320.00
θ

(a)

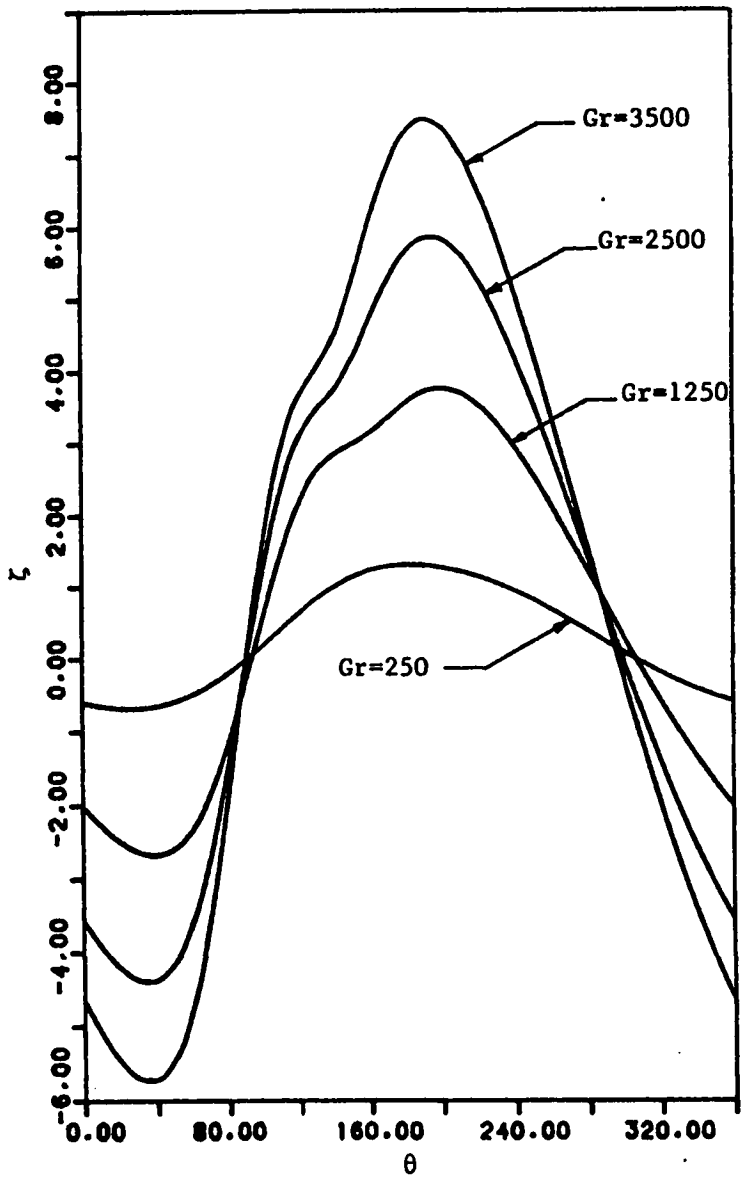
Gr=3500
Gr=2500
Gr=1250
Gr=250
8.00
6.00
4.00
2.00
0.00
-2.00
-4.00
-6.00
ζ
0.00
80.00
160.00
240.00
320.00
θ

(b)

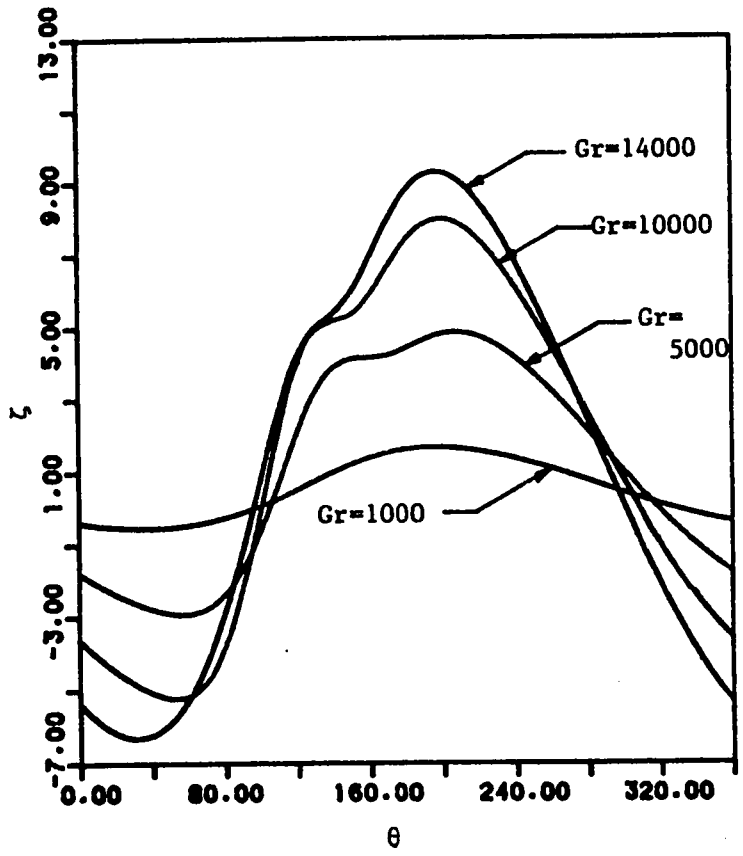

(c)

Fig. 6. Vorticity distribution on the cylinder surface for the case of

(a) Re = 10
(b) Re = 50
(c) Re = 100.

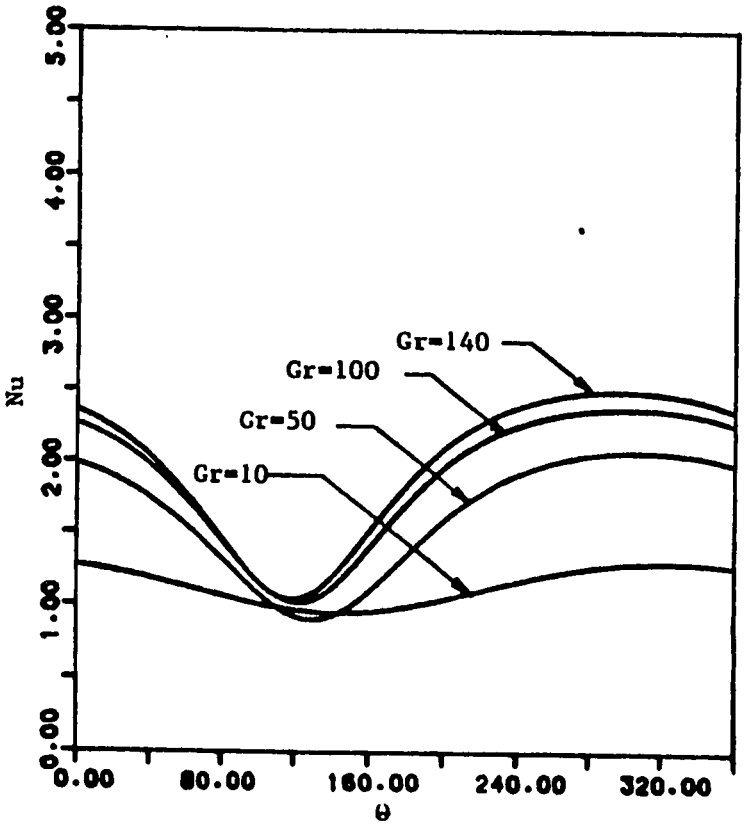
5.00
4.00
3.00
2.00
1.00
0.00
Nu
Gr=140
Gr=100
Gr=50
Gr=10
0.00
80.00
160.00
240.00
320.00
θ

(a)

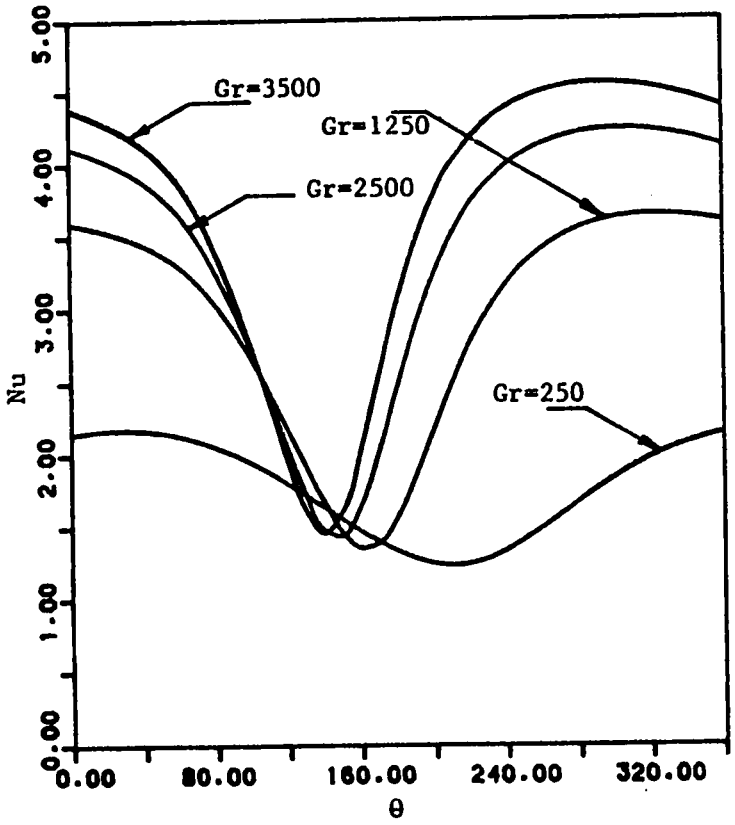
Gr=3500
Gr=1250
Gr=2500
Gr=250
Nu
θ
0.00
1.00
2.00
3.00
4.00
5.00
0.00
80.00
160.00
240.00
320.00

(b)

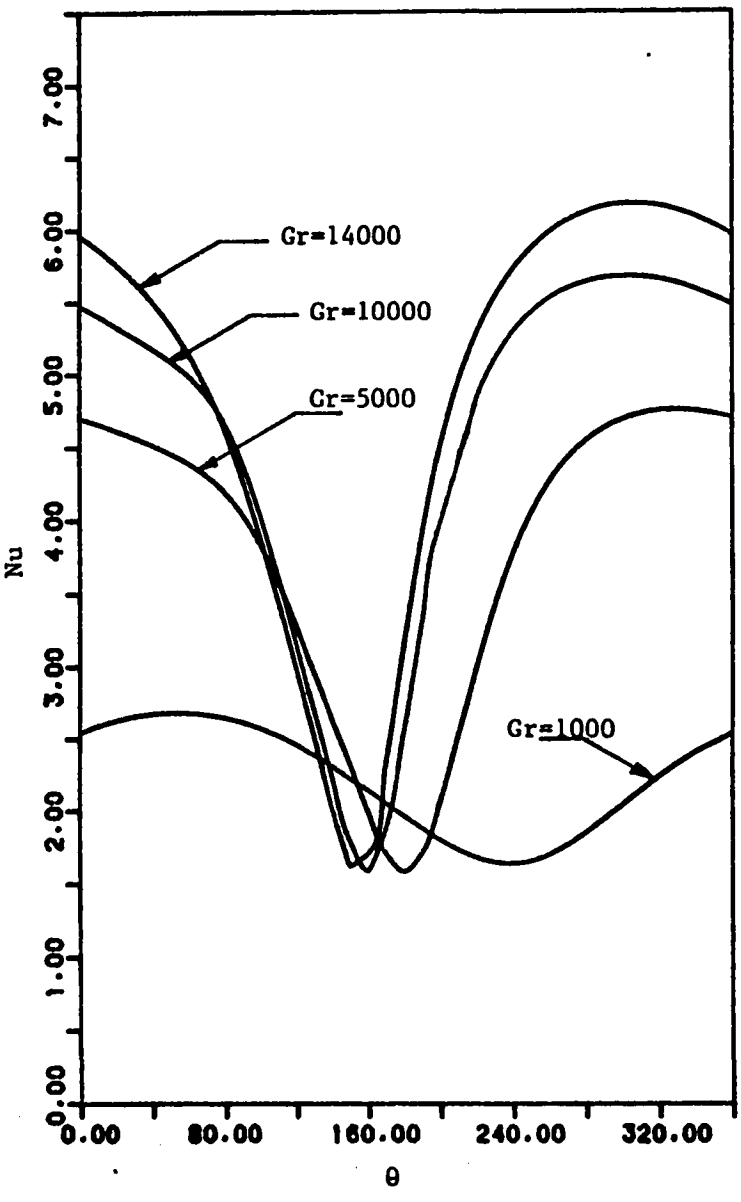

(c)

Fig. 7. Variation of local Nusselt number around the cylinder surface for the case of

(a) Re = 10
(b) Re = 50
(c) Re = 100.

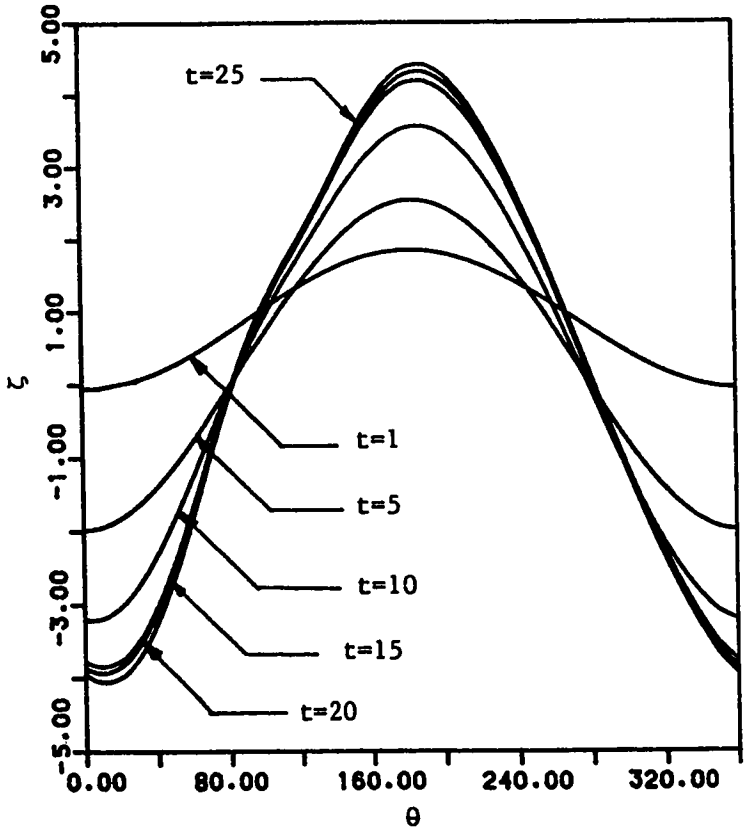
5.00
3.00
1.00
-1.00
-3.00
-5.00
ζ
t=25
t=1
t=5
t=10
t=15
t=20
0.00
80.00
160.00
240.00
320.00
θ

(a)

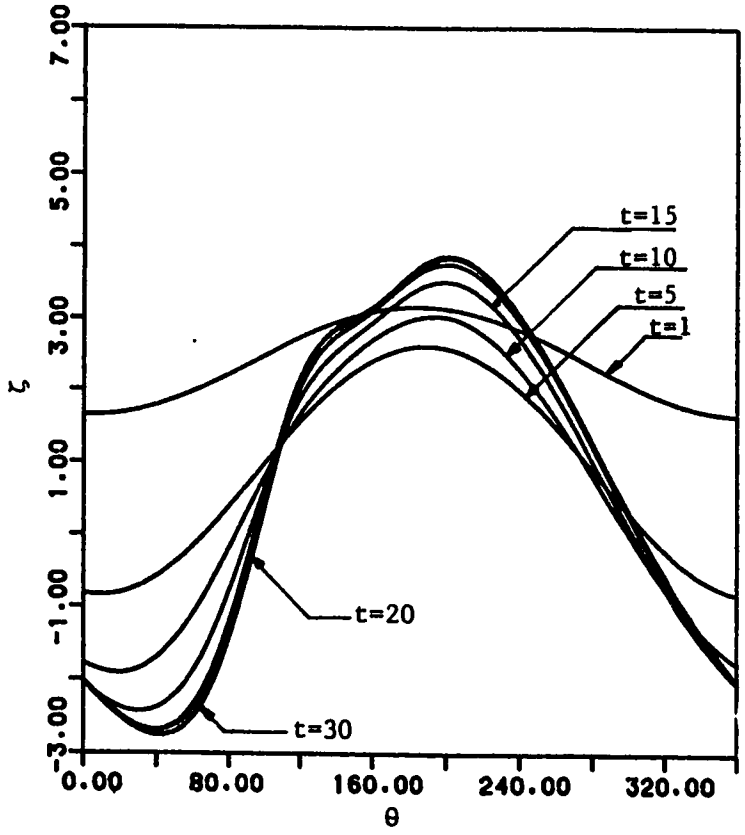
7.00
5.00
3.00
1.00
-1.00
-3.00
ζ
t=15
t=10
t=5
t=1
t=20
t=30
0.00
80.00
160.00
240.00
320.00
θ

(b)

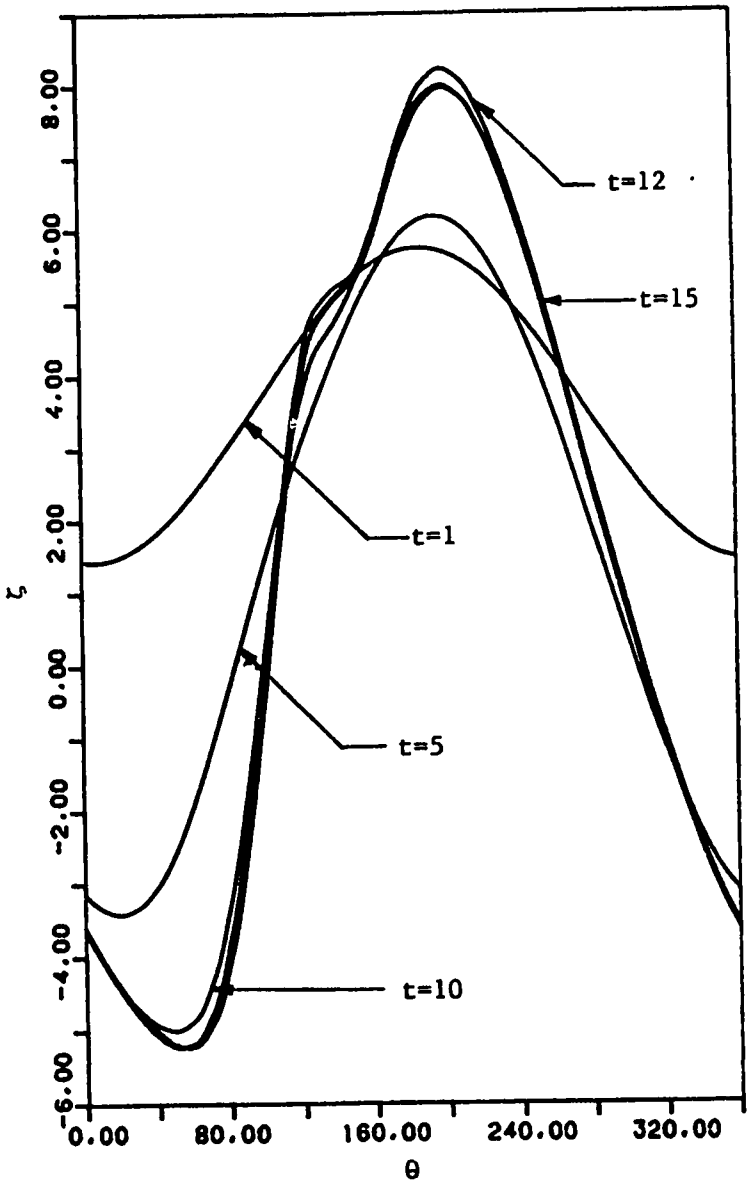

(c)

Fig. 8. The time variation of vorticity around the cylinder surface for

(a) Re = 10, Gr = 140
(b) Re = 50, Gr = 1250
(c) Re = 100, Gr = 10000.

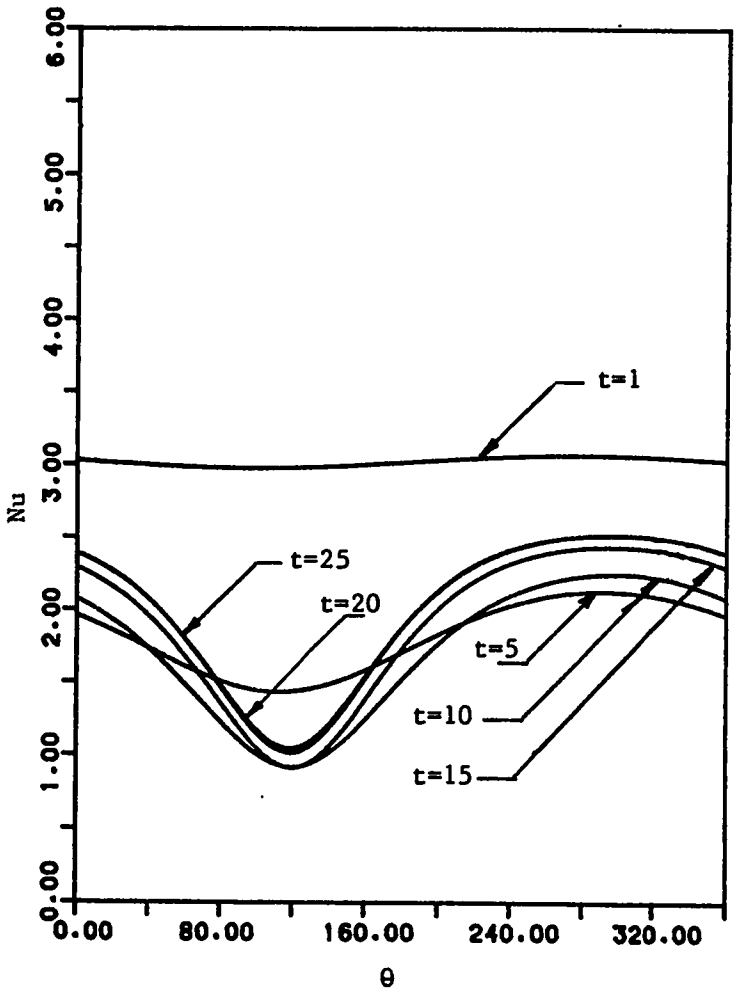
6.00
5.00
4.00
3.00
2.00
1.00
0.00
Nu
t=1
t=25
t=20
t=5
t=10
t=15
0.00
80.00
160.00
240.00
320.00
θ

(a)

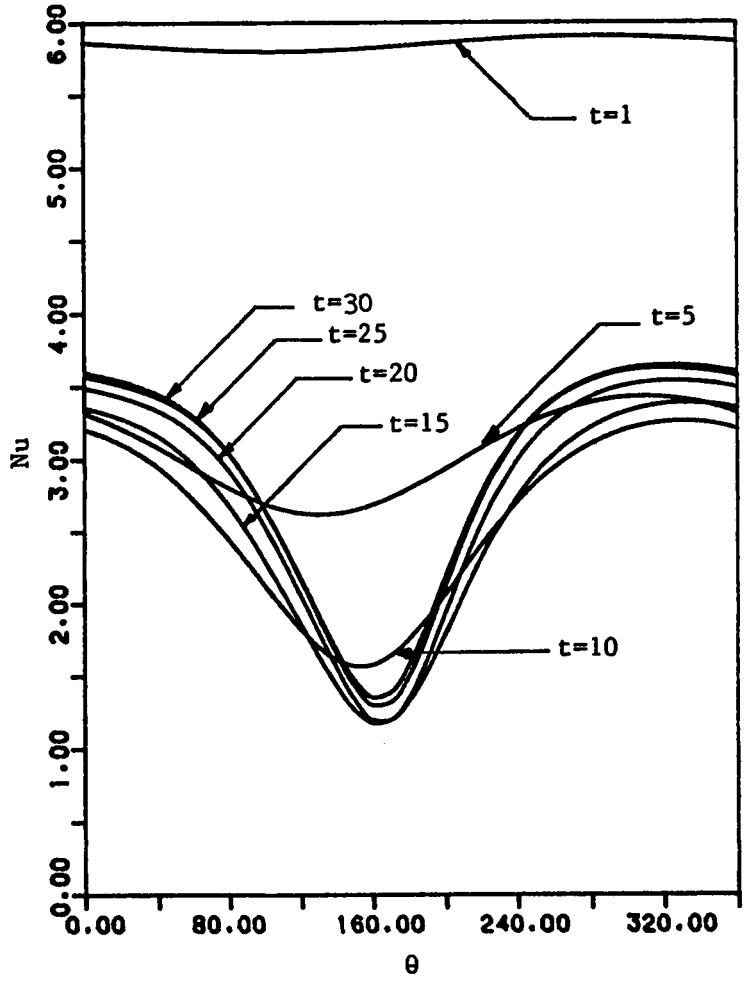
6.00
5.00
4.00
3.00
2.00
1.00
0.00
Nu
0.00
80.00
160.00
240.00
320.00
θ
t=1
t=30
t=25
t=20
t=15
t=5
t=10

(b)

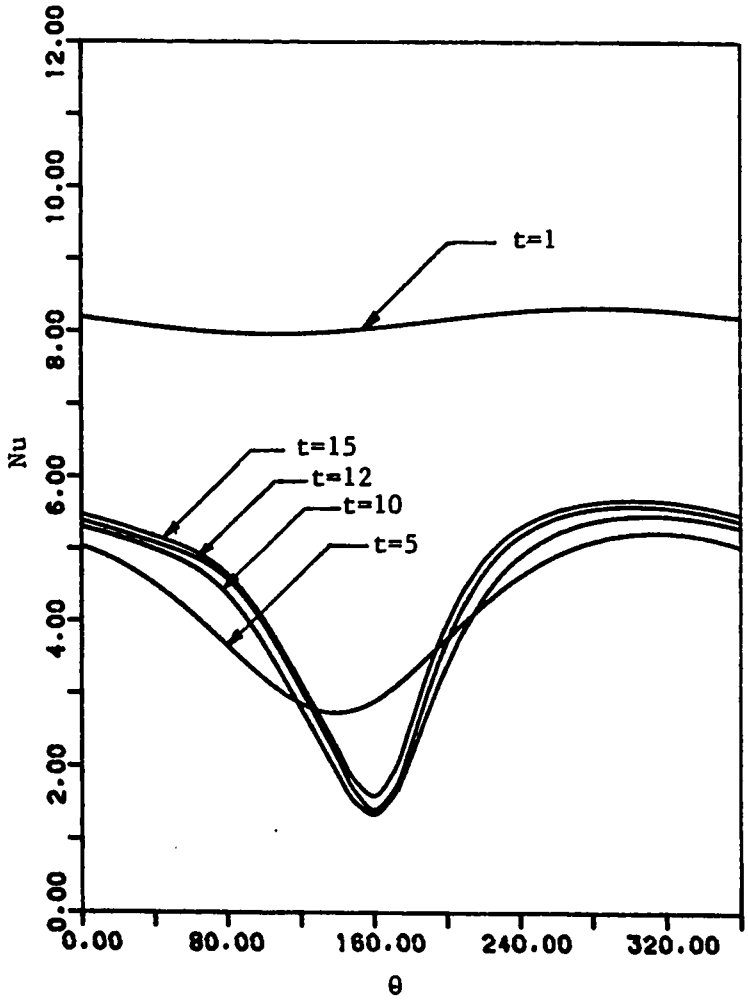

(c)

Fig. 9. Time variation of local Nusselt number around the cylinder surface for

(a) Re = 10, Gr = 140
(b) Re = 50, Gr = 1250
(c) Re = 100, Gr = 10000.

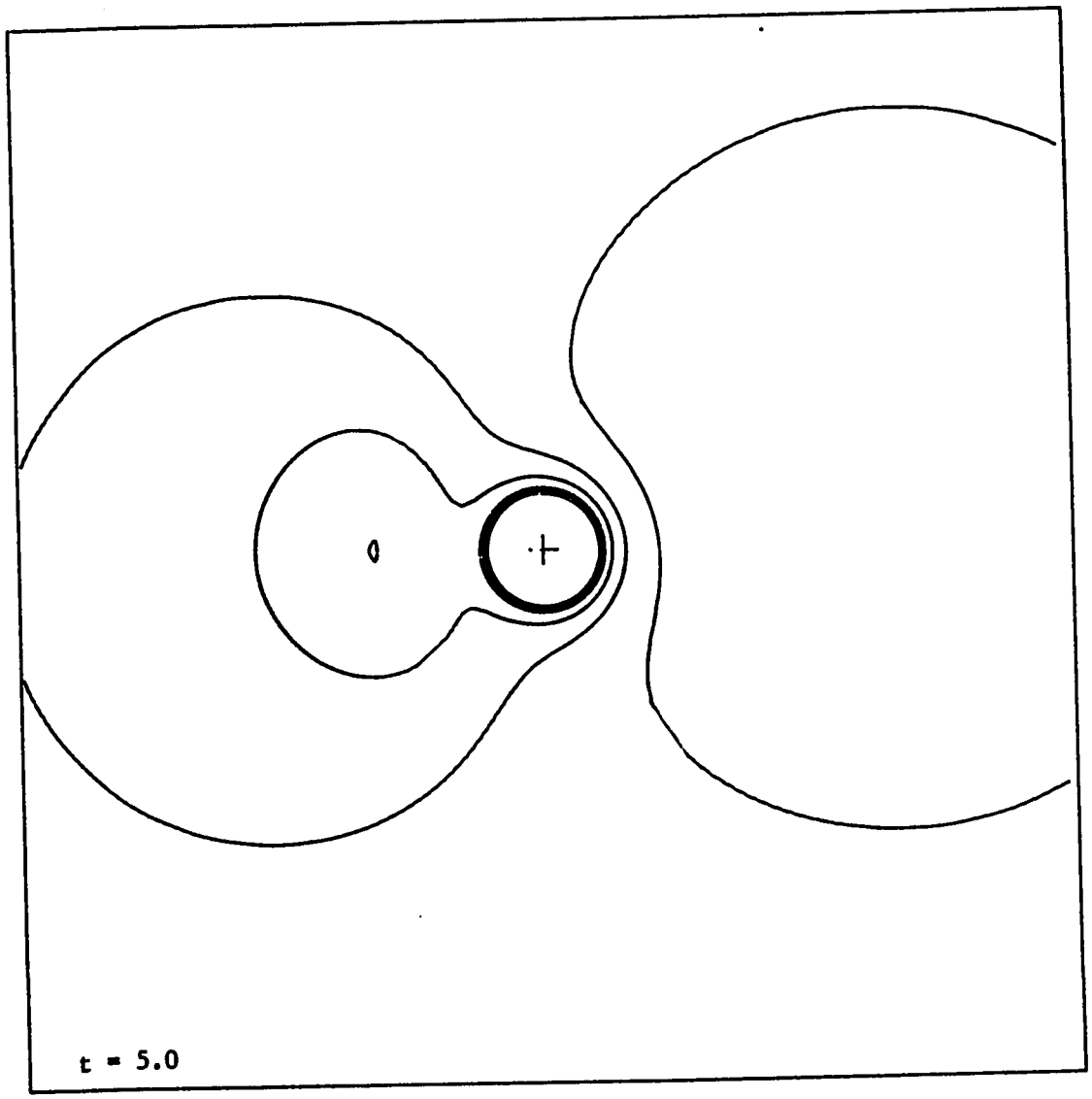

(a)

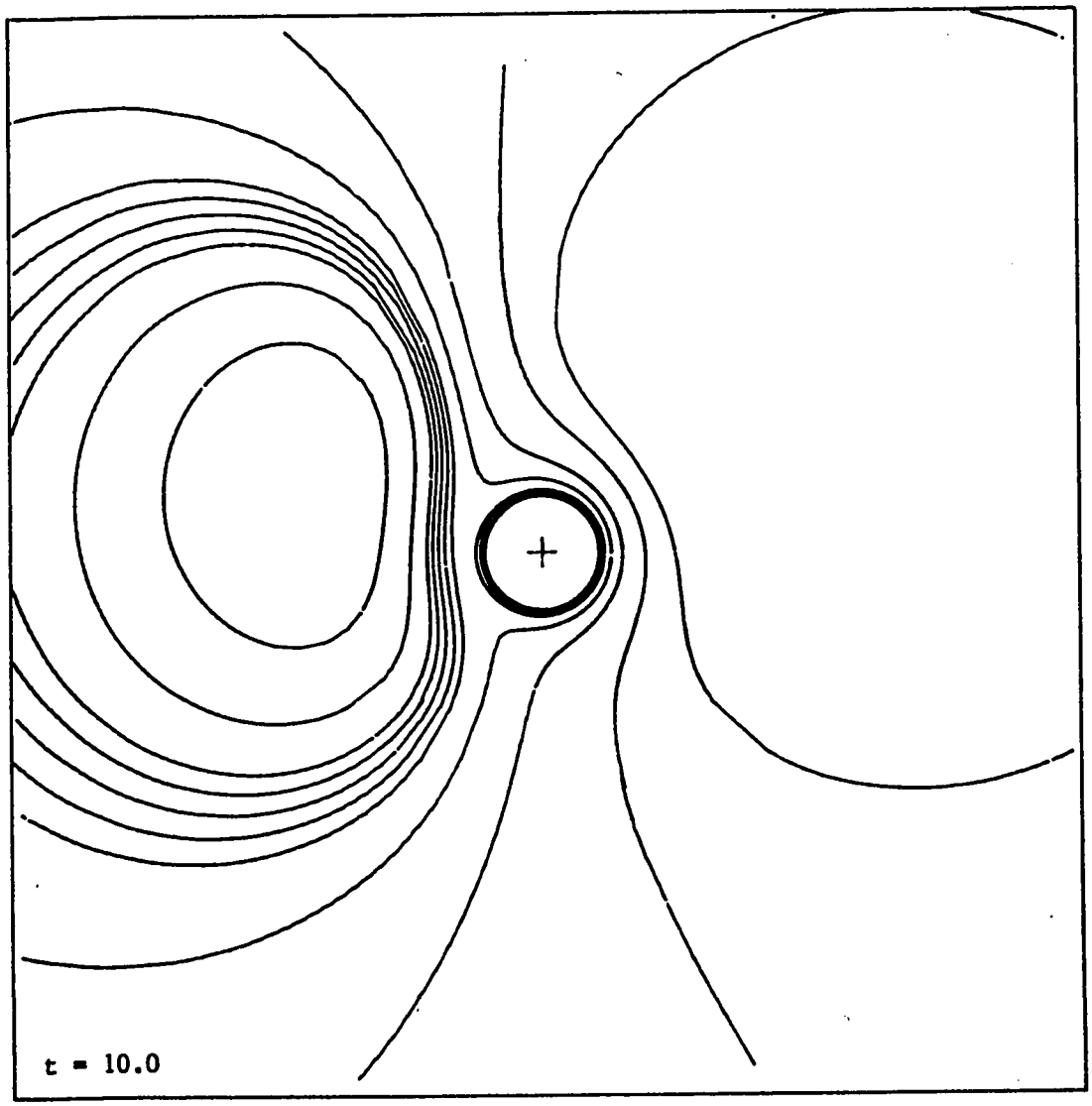

(b)

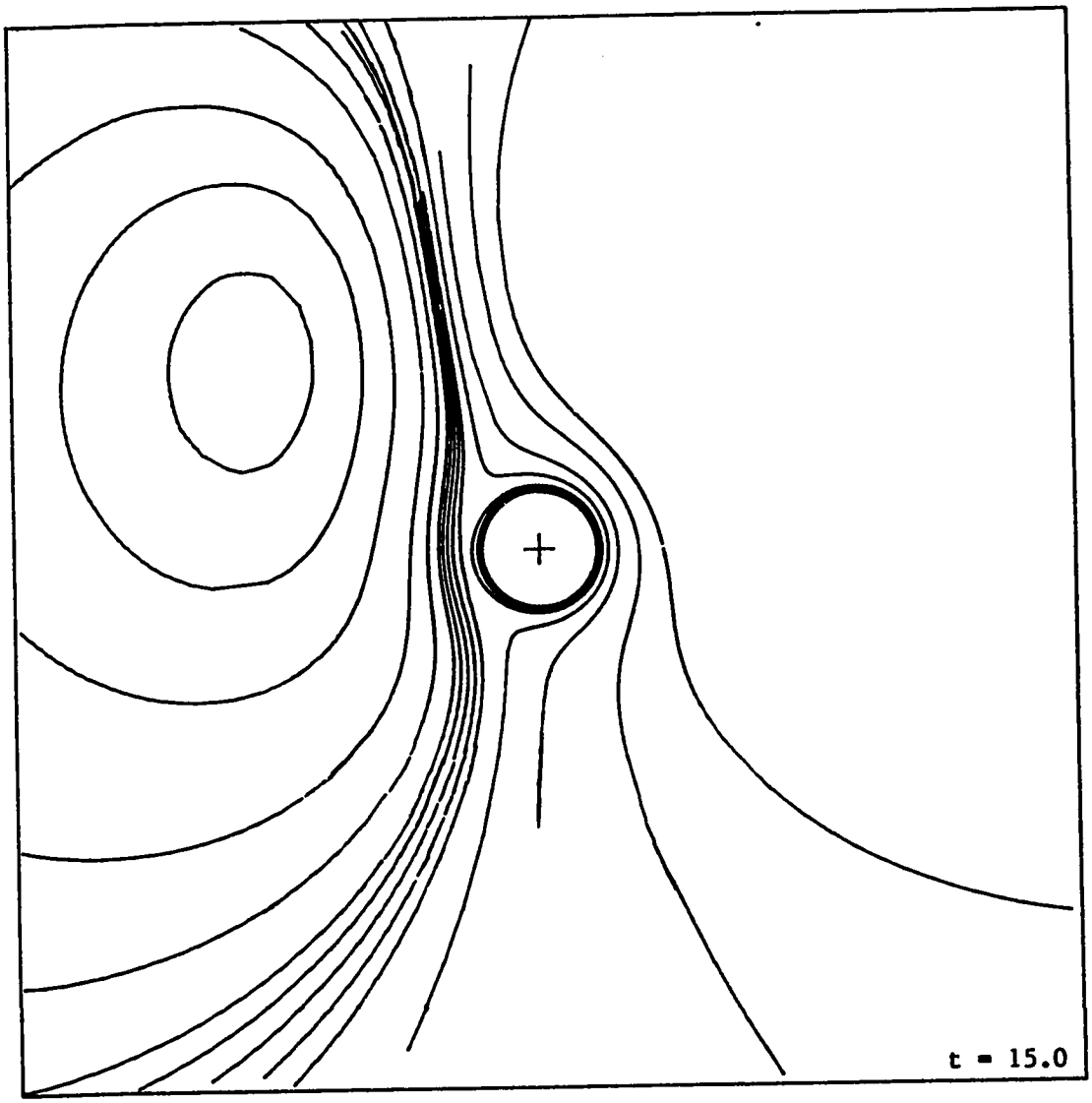

(c)

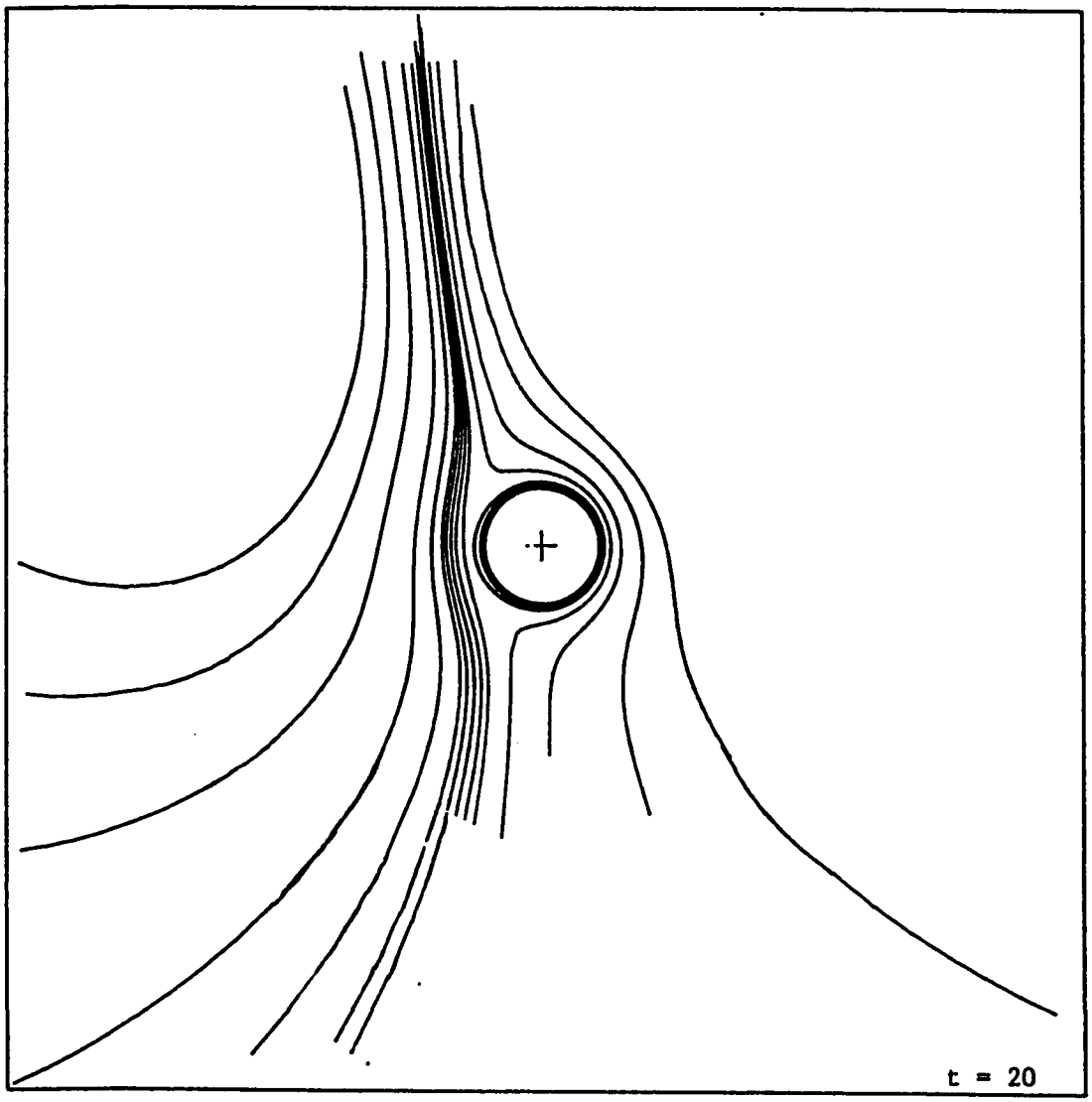

(d)

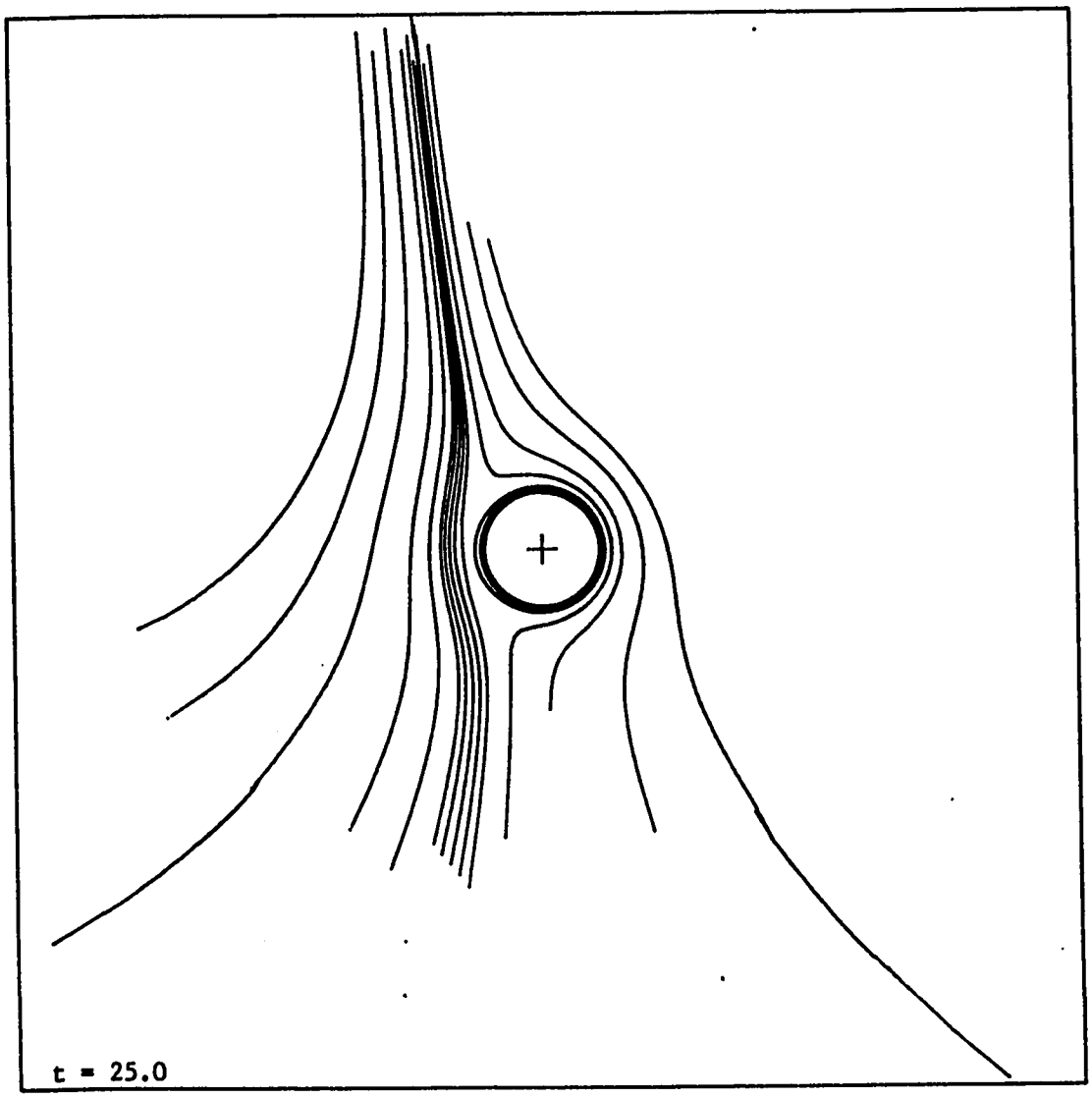

(e)

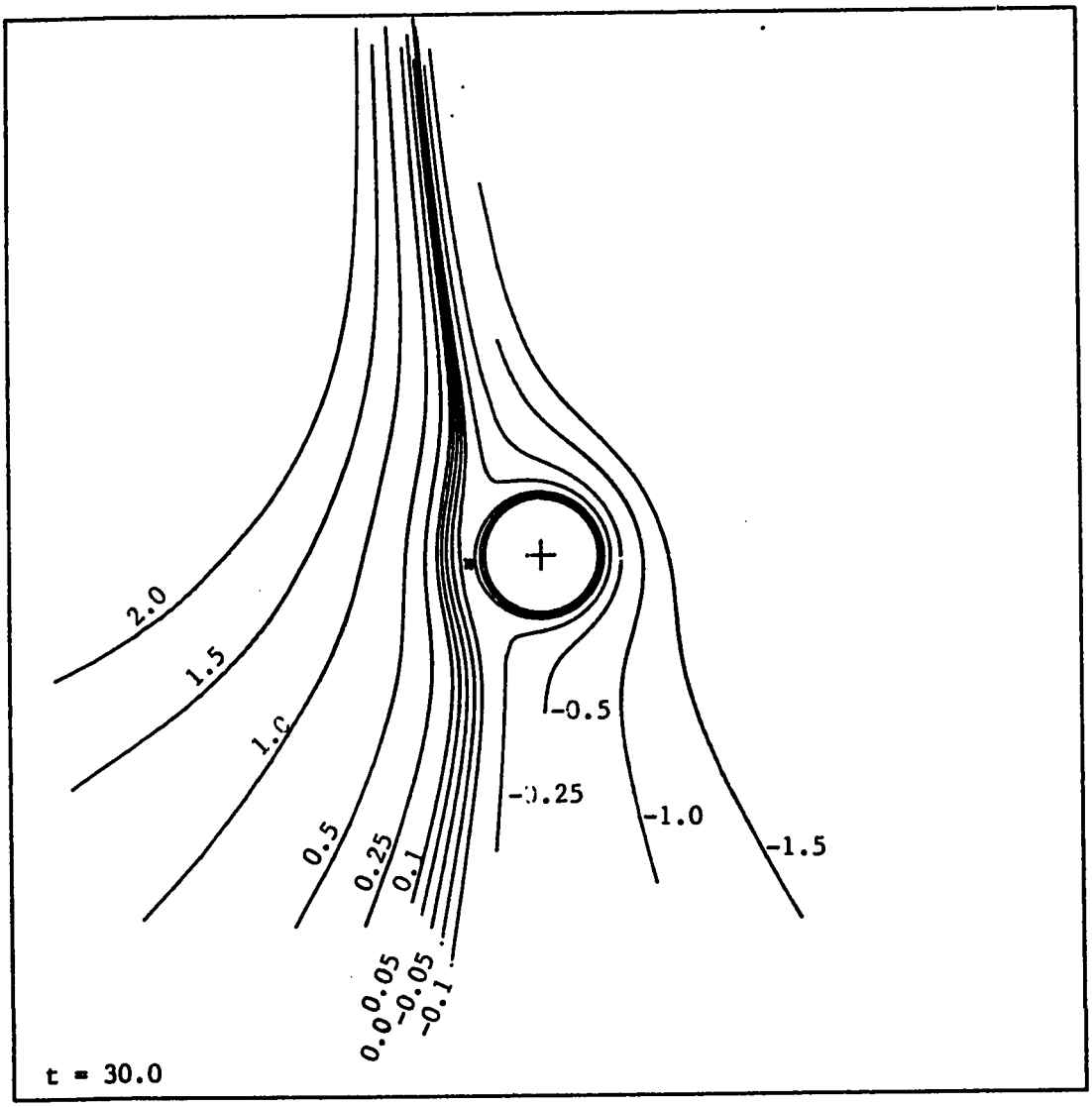

(f)

Fig. 10. The time development of the streamline pattern for the case of Re = 10, Pr = 0.7 and Gr = 140. (The streamlines plotted are -1.5, -1.0, -0.5, -0.25, -0.1, -0.05, 0.0, 0.05, 0.1, 0.25, 0.5, 1.0 and 1.5)

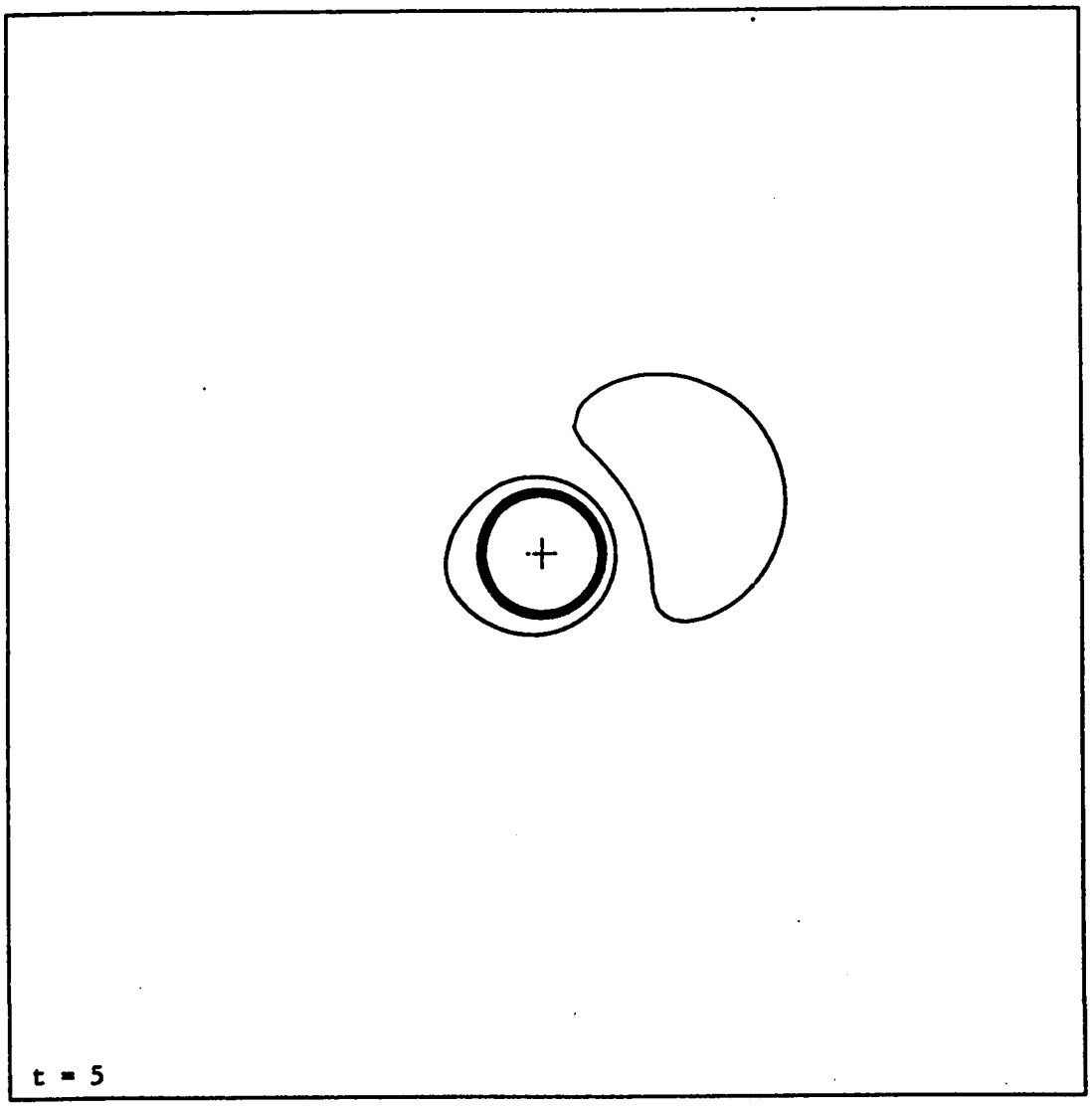

(a)

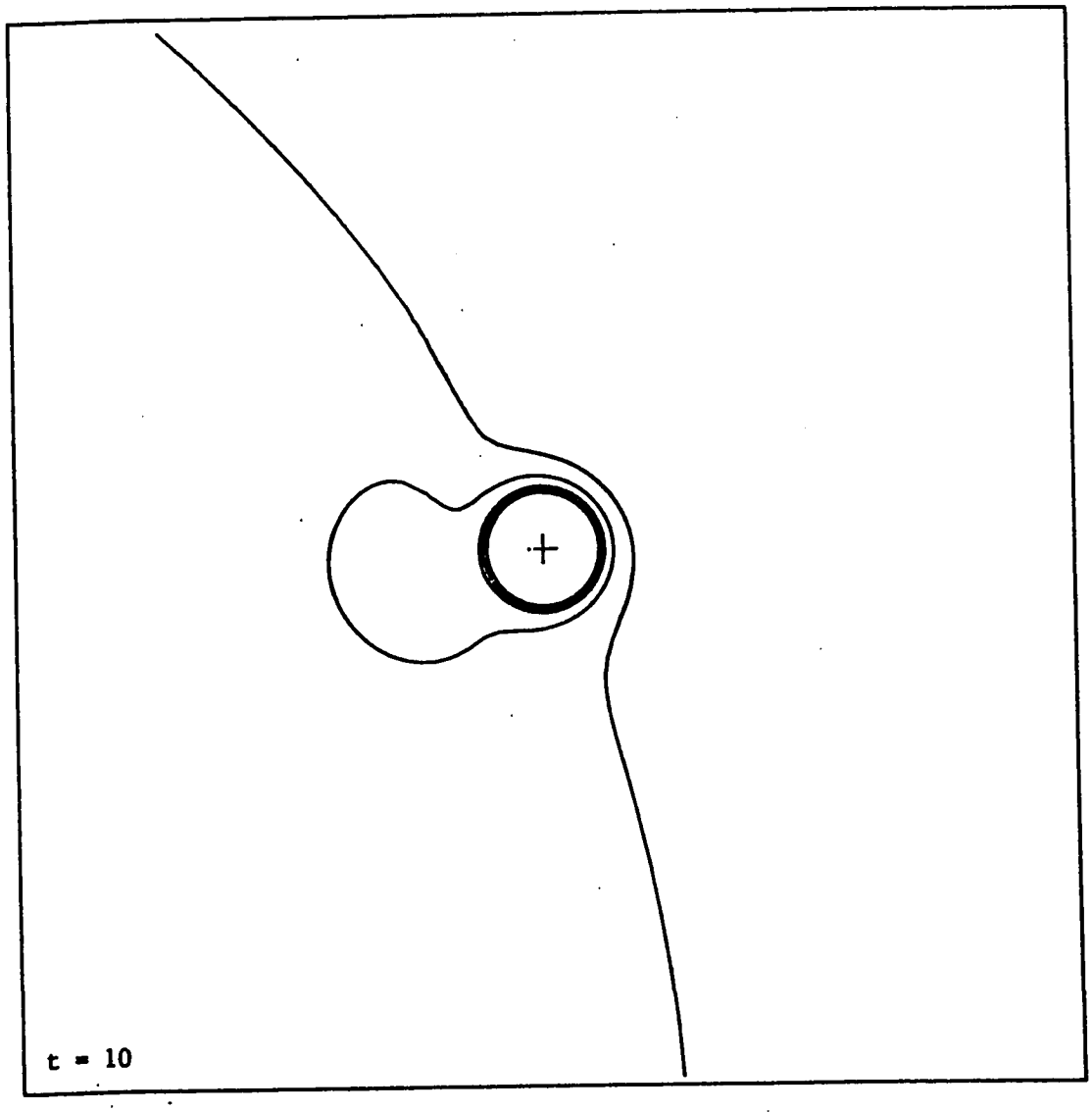

(b)

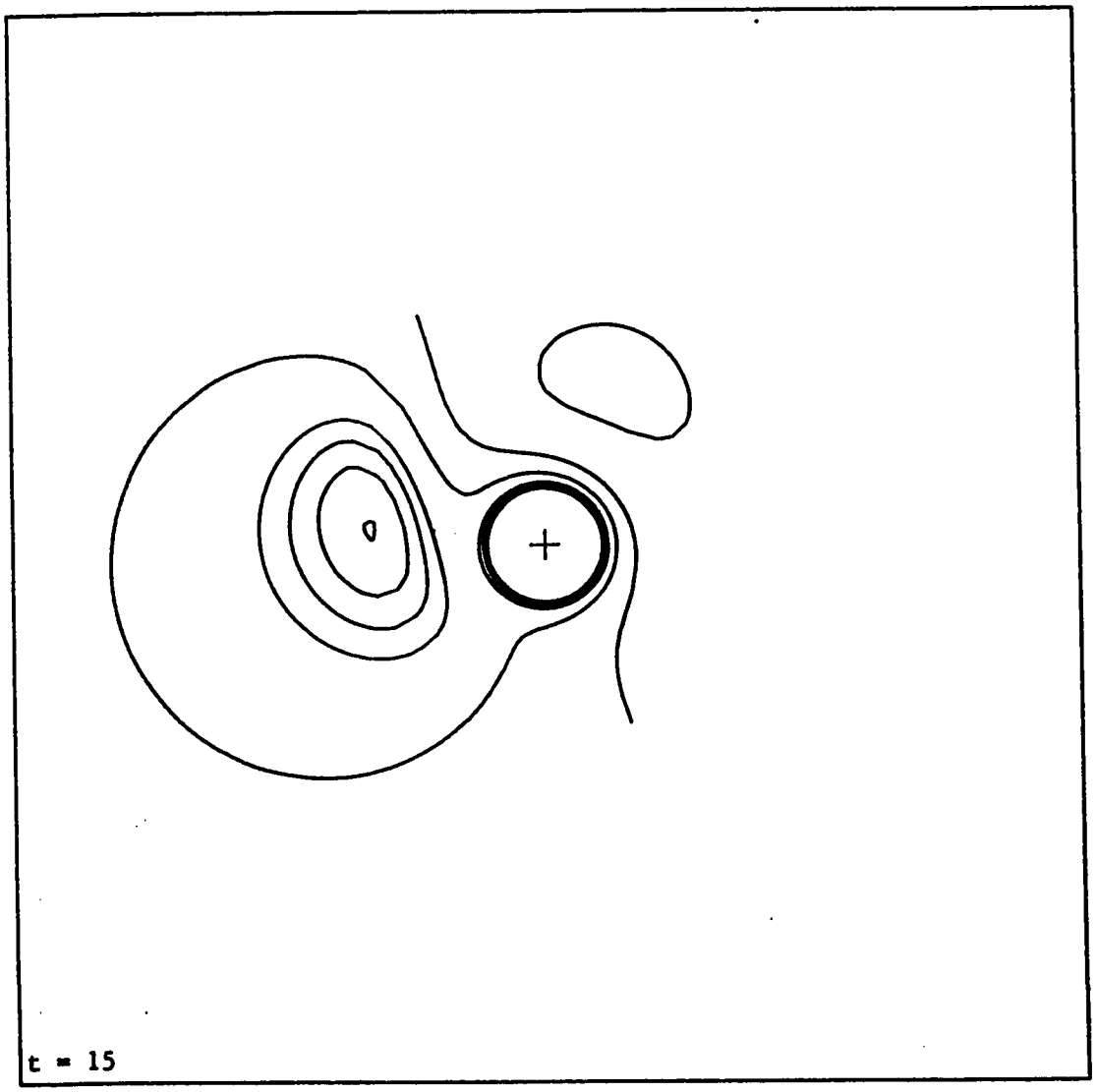

(c)

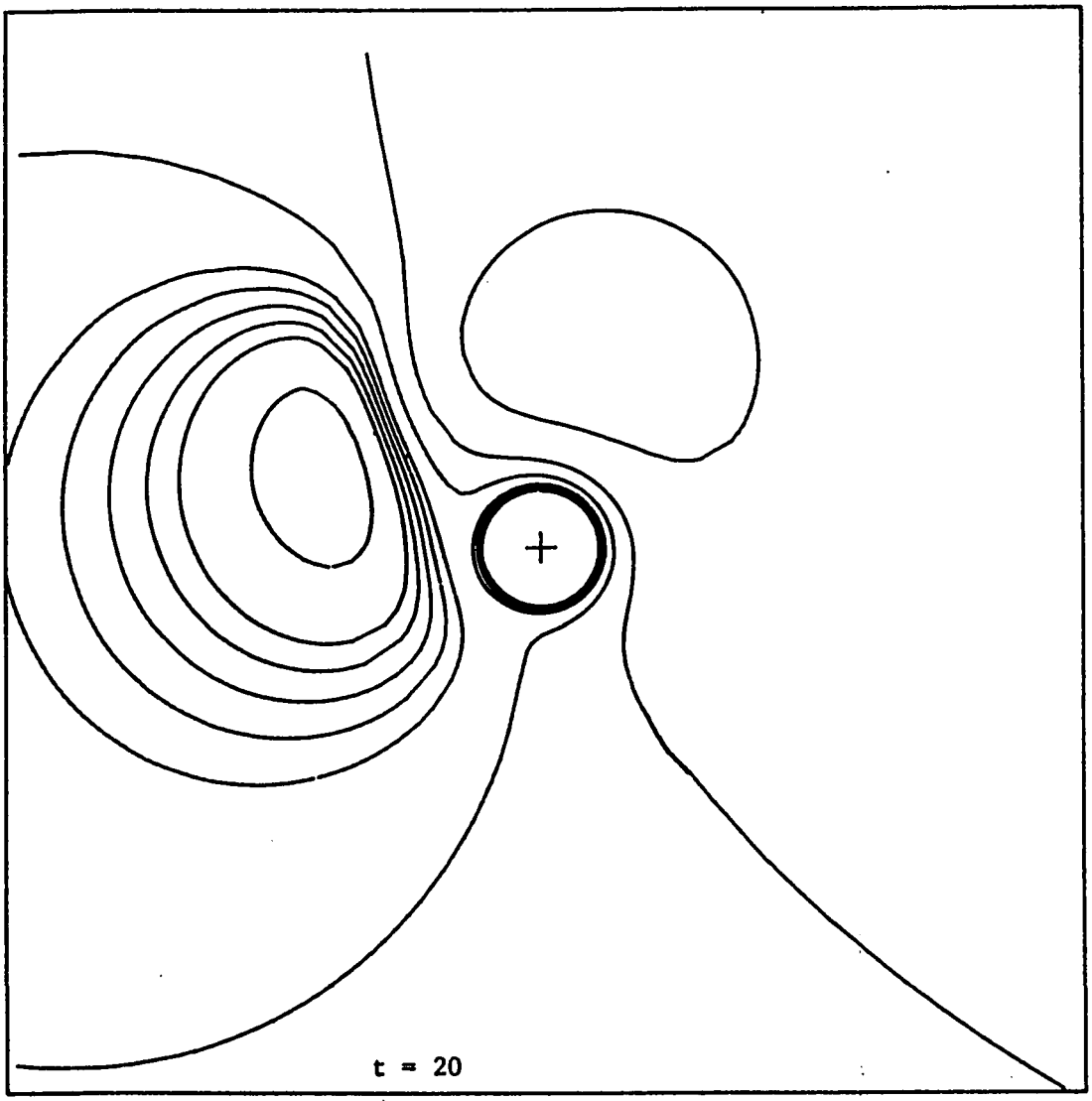

(d)

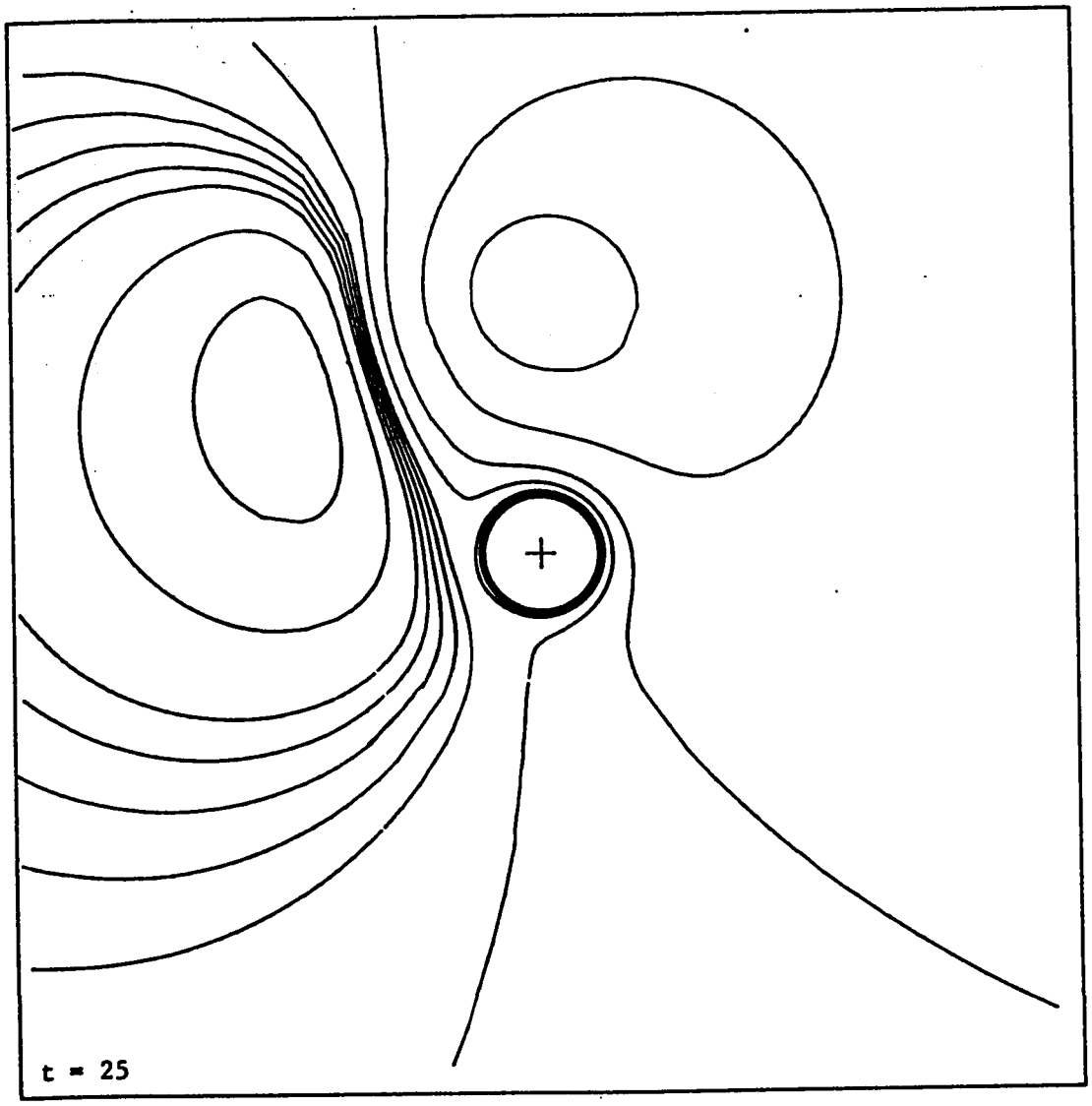

(e)

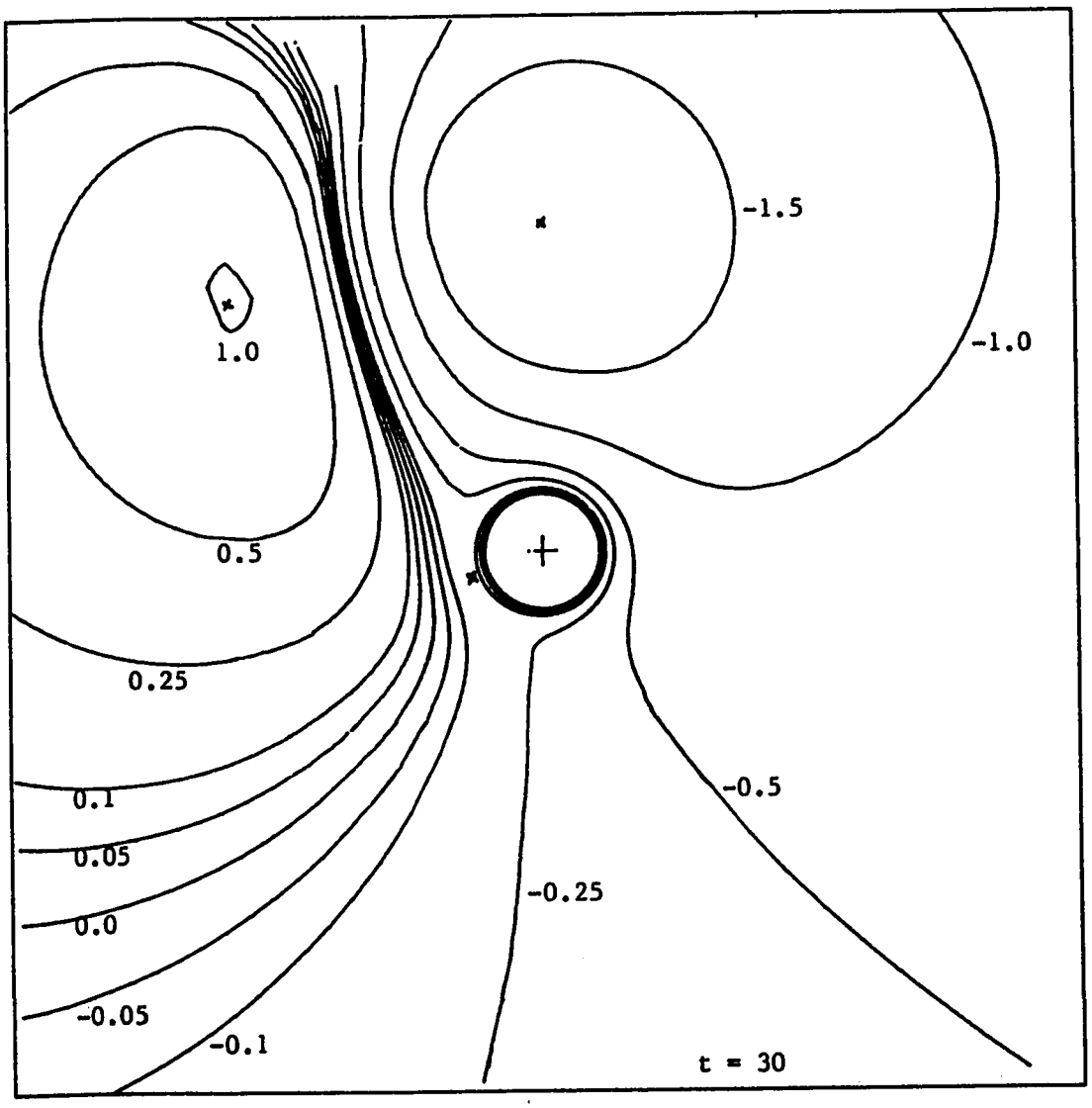

(f)

Fig. 11. The time development of the streamline pattern for the case of Re = 50, Pr = 0.7 and Gr = 1250. (The streamlines plotted are -1.5, -1.0, -0.5, -0.25, -0.1, -0.05, 0.0, 0.05, 0.1, 0.25, 0.5, 1.0 and 1.5)

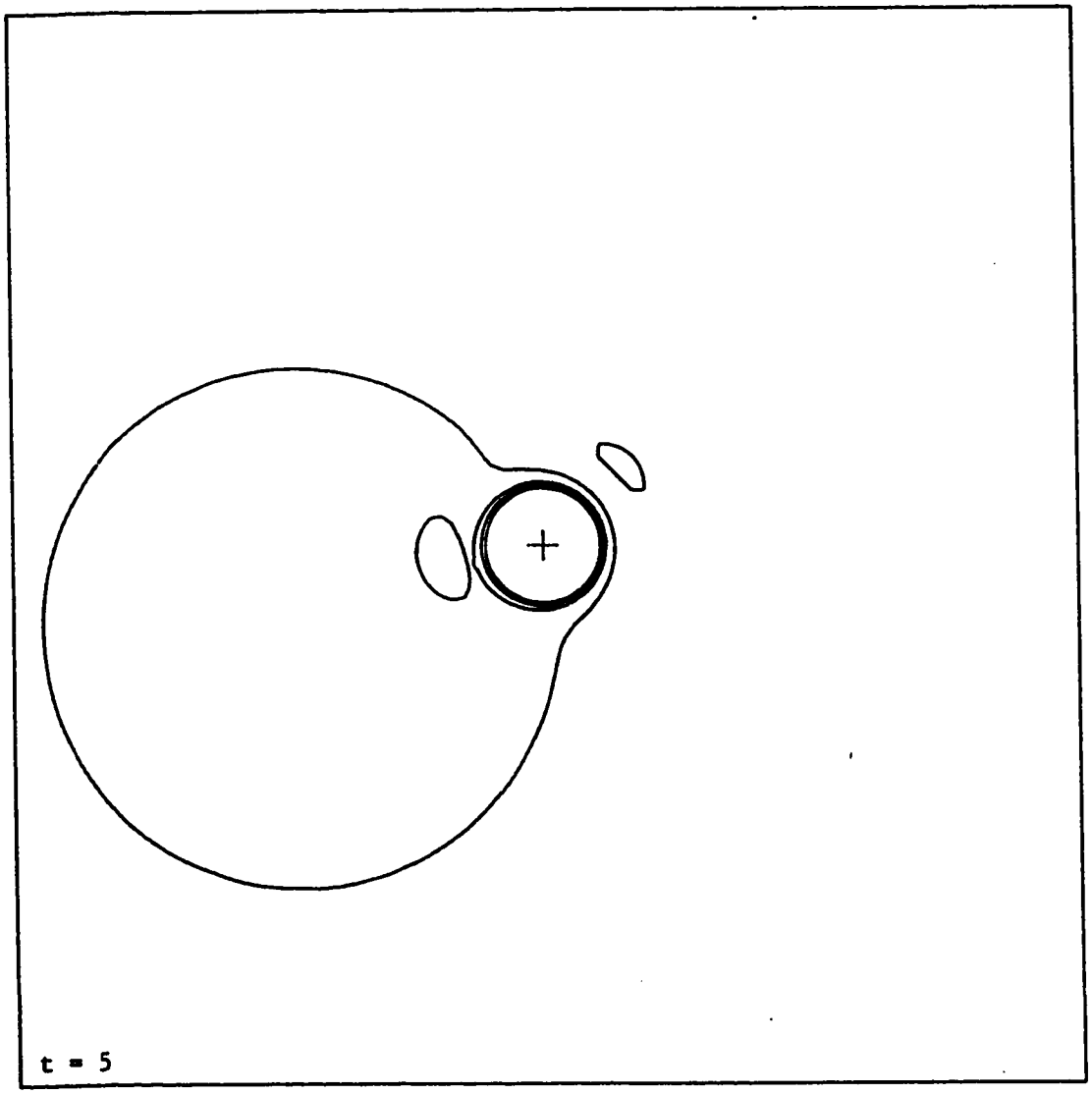

(a)

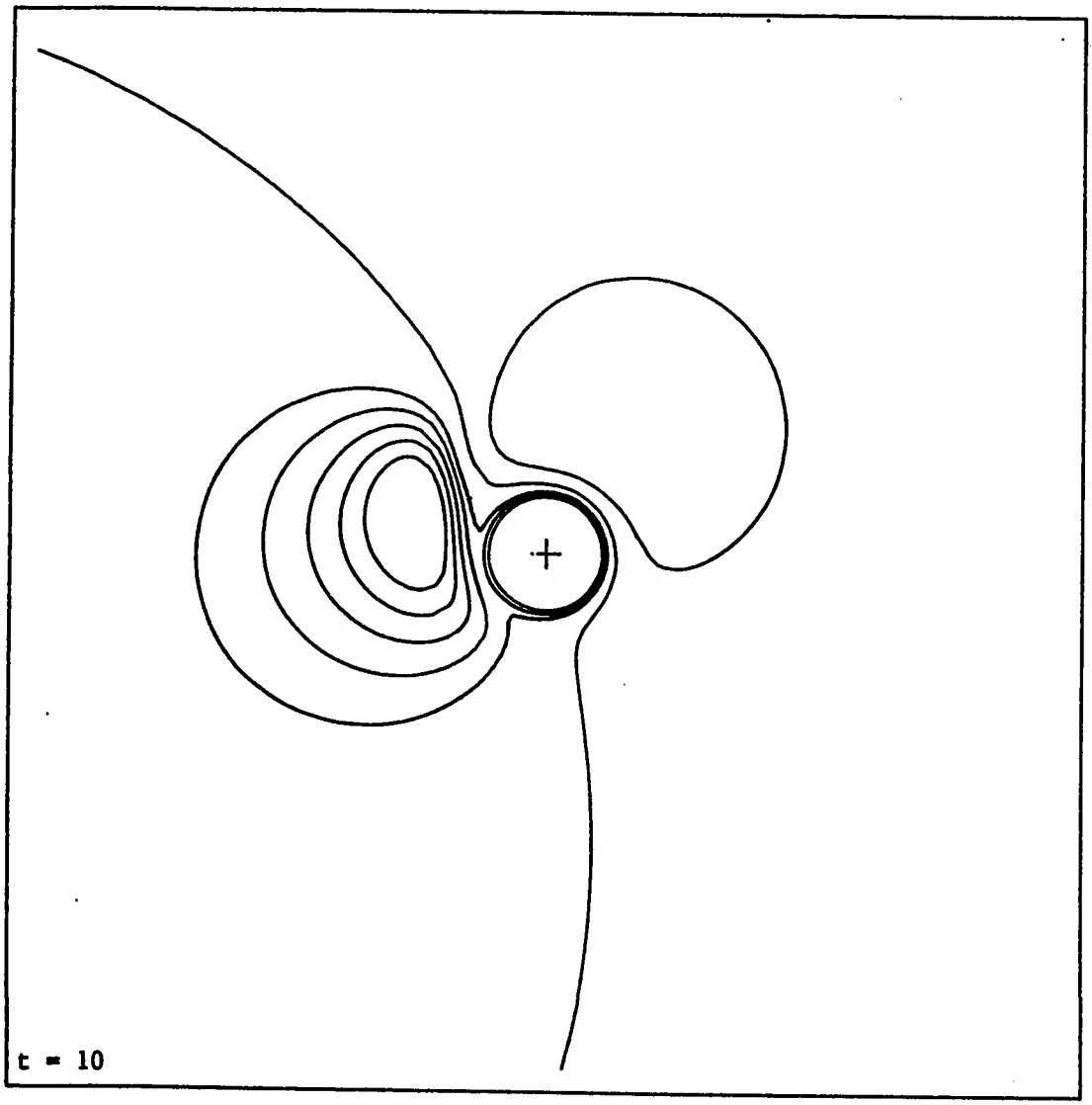

(b)

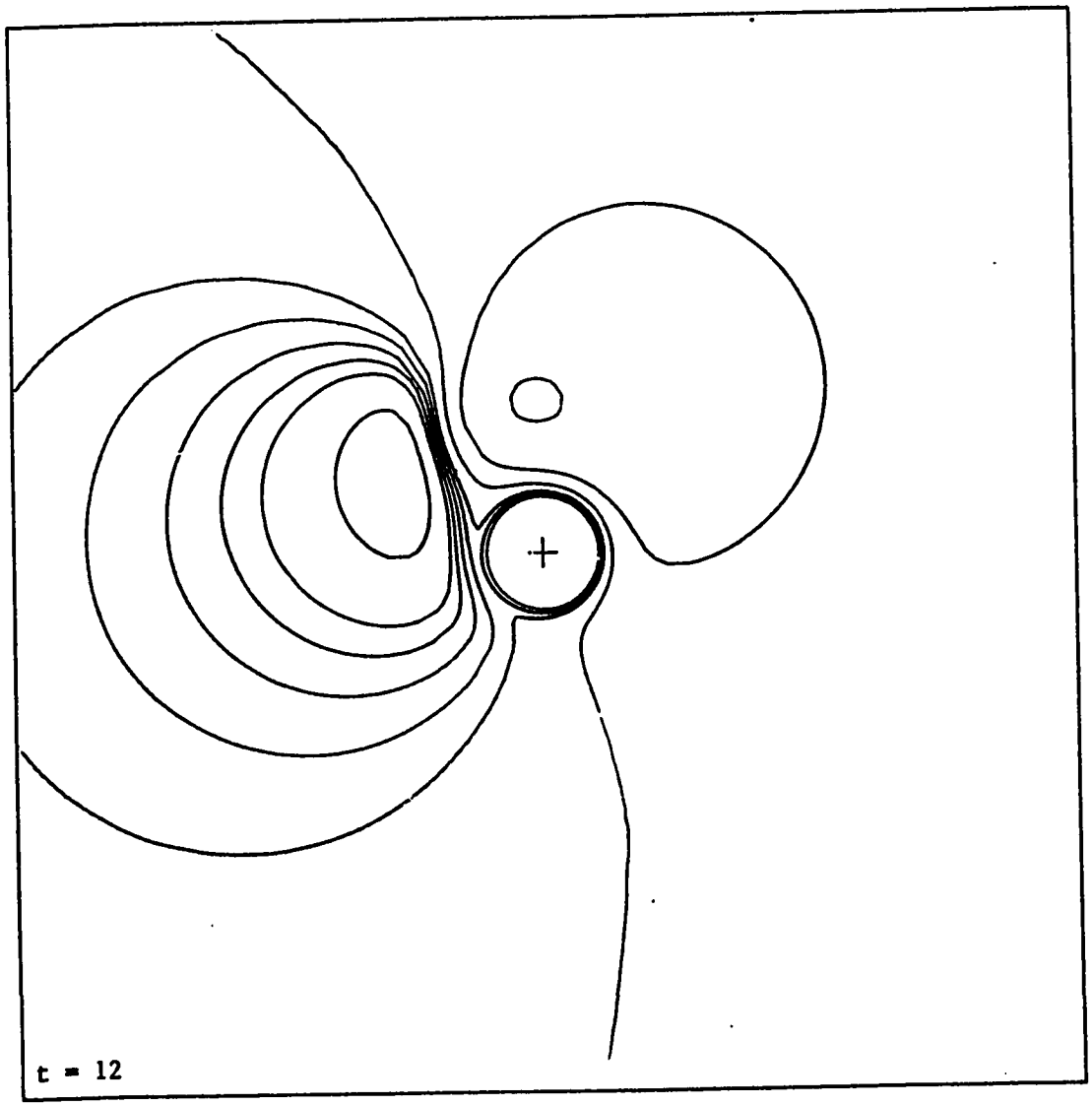

(c)

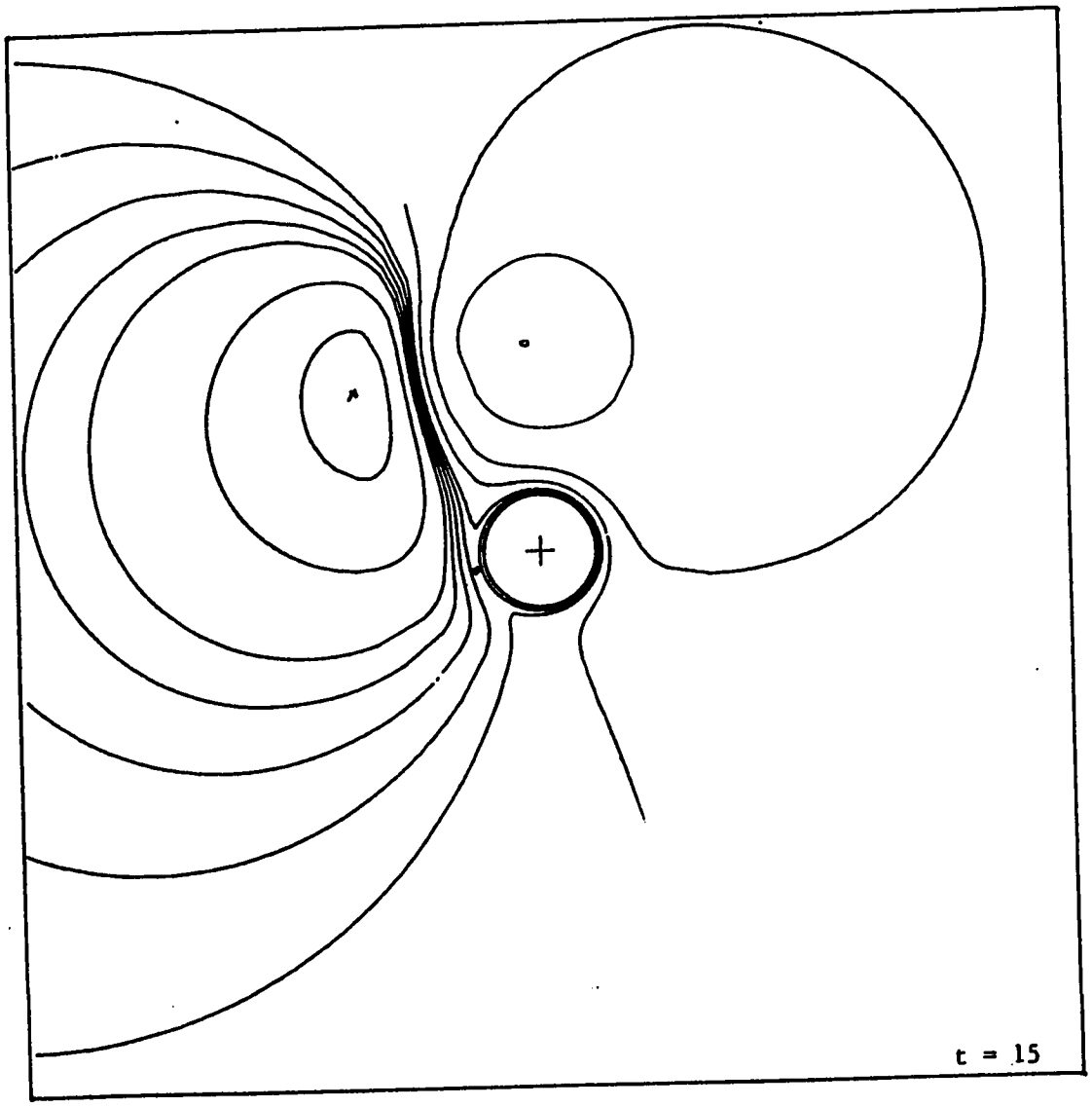

(d)

Fig. 12. The time development of the streamline pattern for the case of Re = 100, Pr = 0.7 and Gr = 10000. (The streamlines plotted are -1.5, -1.0, -0.5, -0.25, -0.1, -0.05, 0.0, 0.05, 0.1, 0.25, 0.5, 1.0 and 1.5)

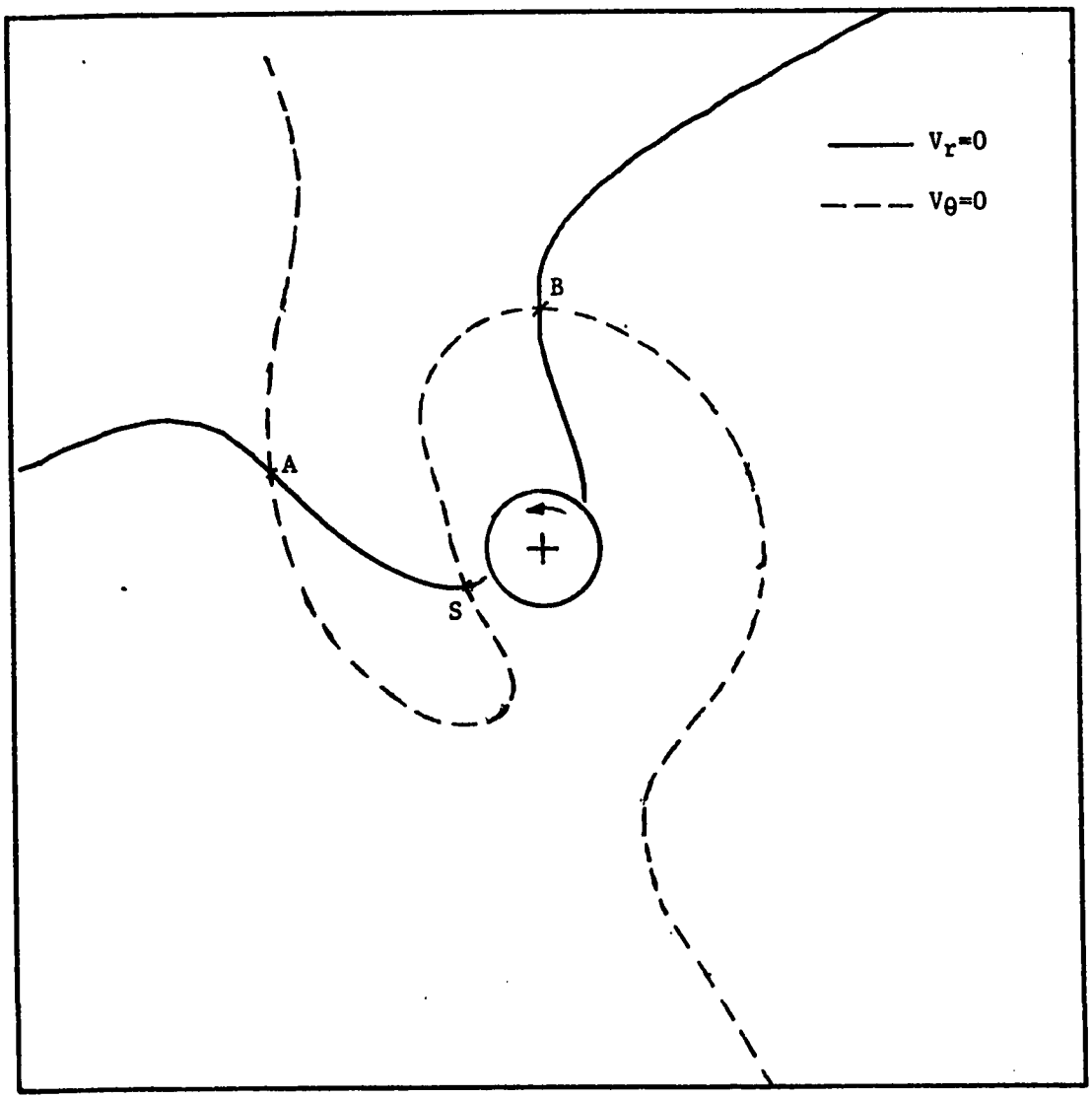

Fig. 13. Location of saddle point in the flow field around the rotating cylinder for the case of Re = 50 and Gr = 750.

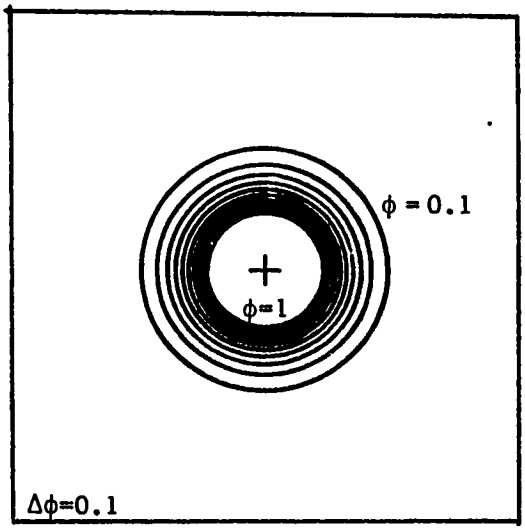

(a)

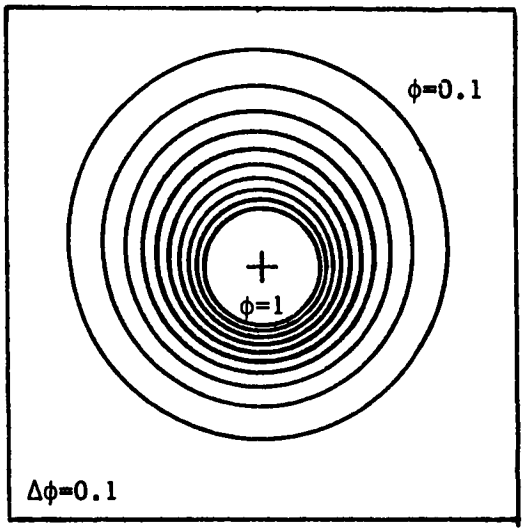

(b)

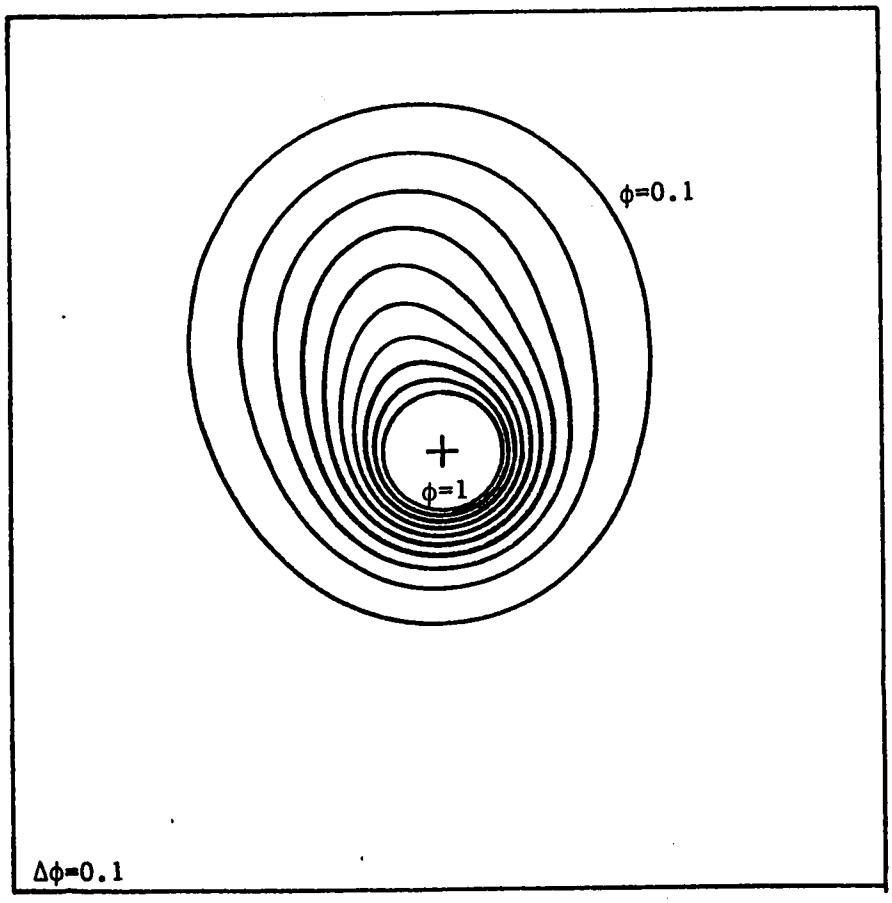

(c)

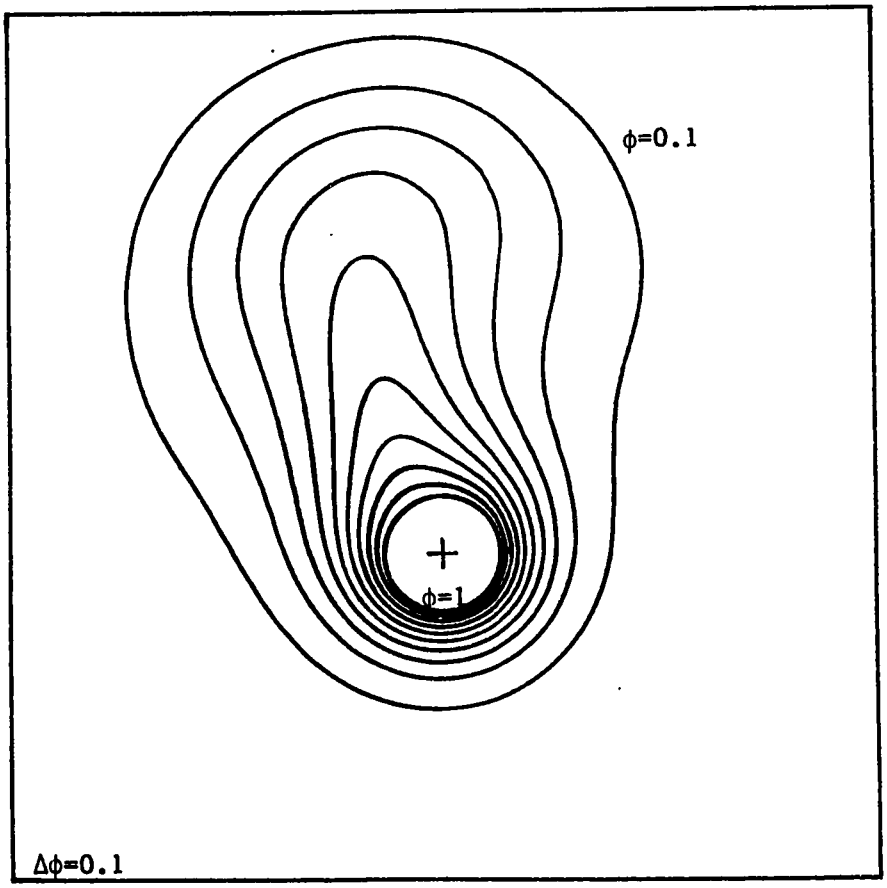

(d)

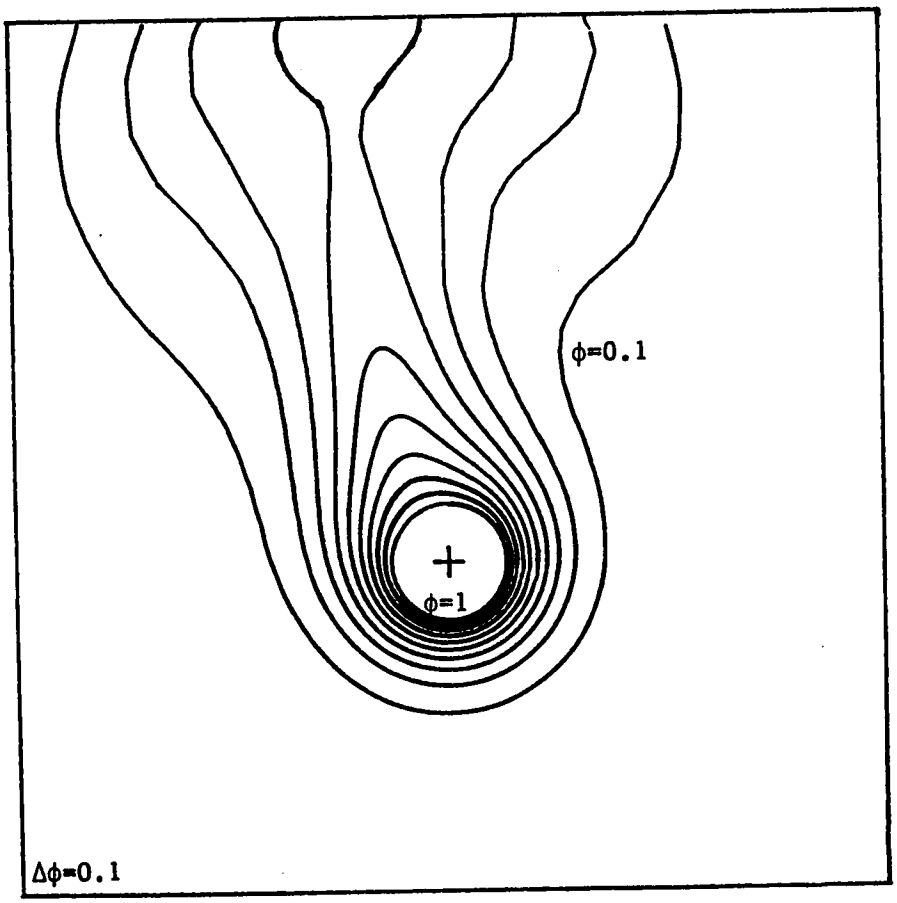

(e)

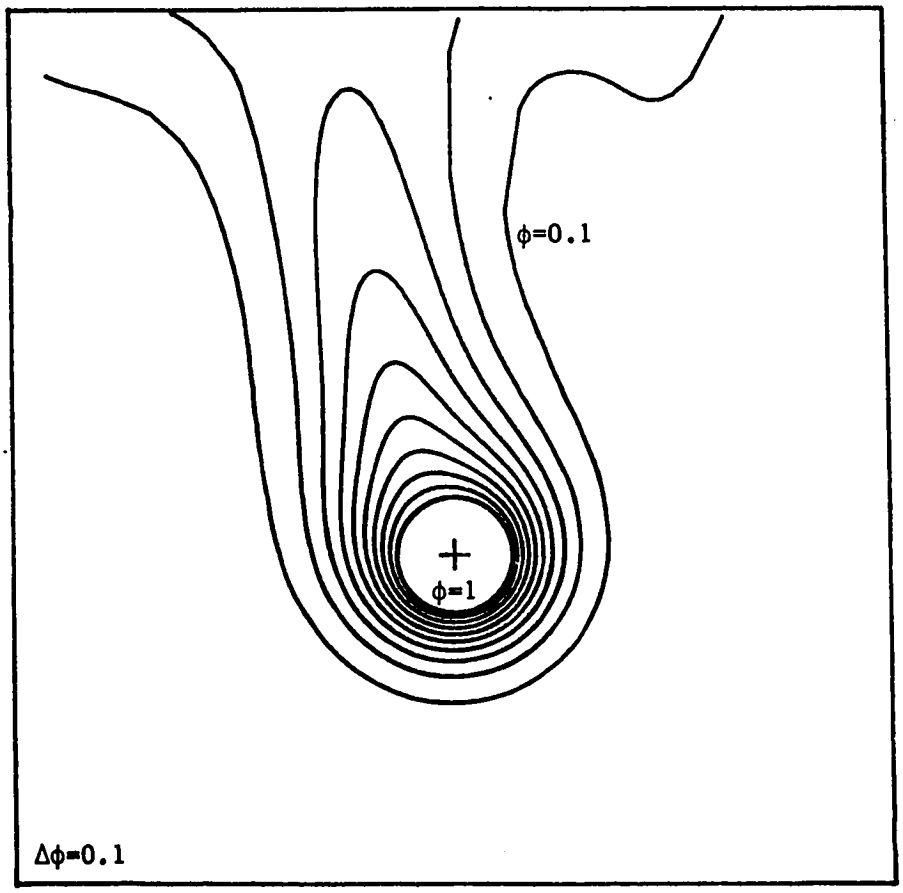

(f)

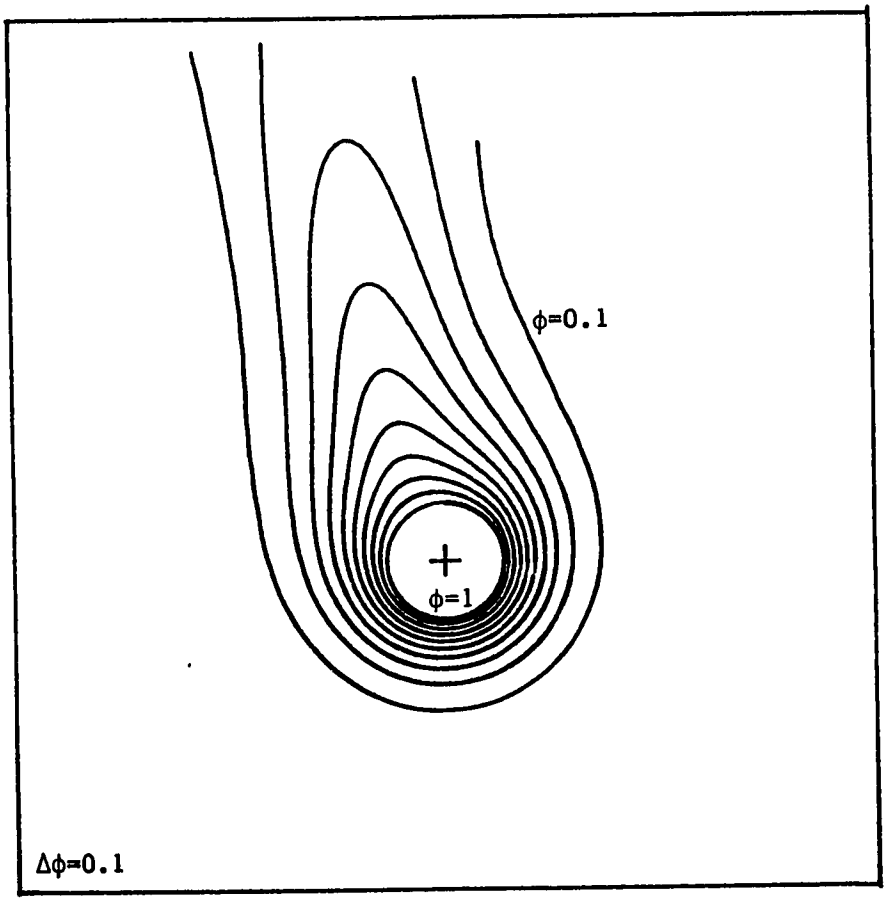

(g)

Fig. 14. The time development of the isotherm pattern for the case of Re = 10, Pr = 0.7 and Gr = 140.

(a) t = 1.0 (b) t = 5.0 (c) t = 10.0 (d) t = 15.0
(e) t = 20.0 (f) t = 25.0 (g) t = 30.0.

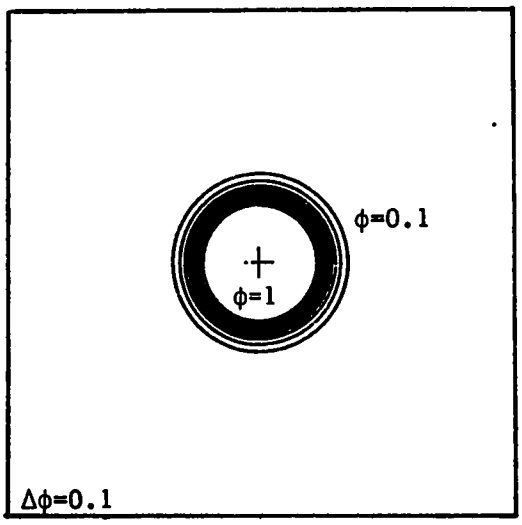

(a)

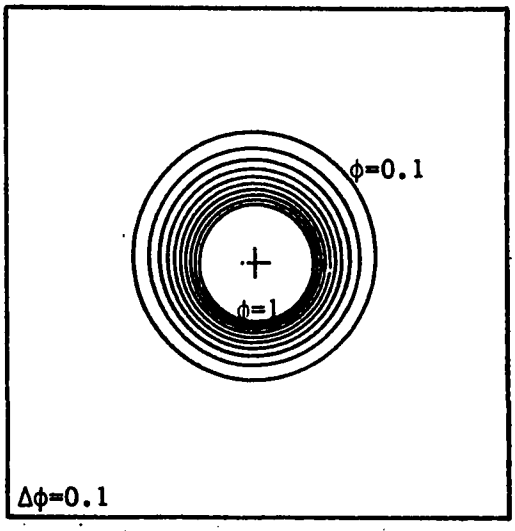

(b)

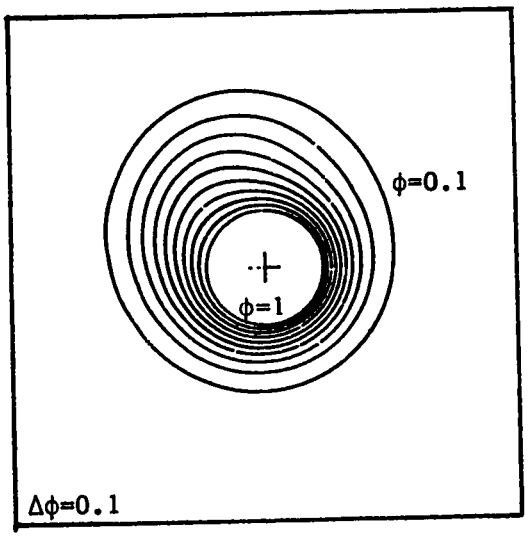

(c)

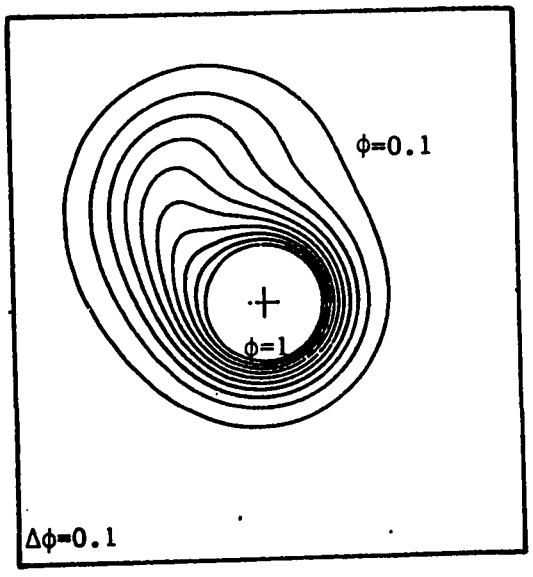

(d)

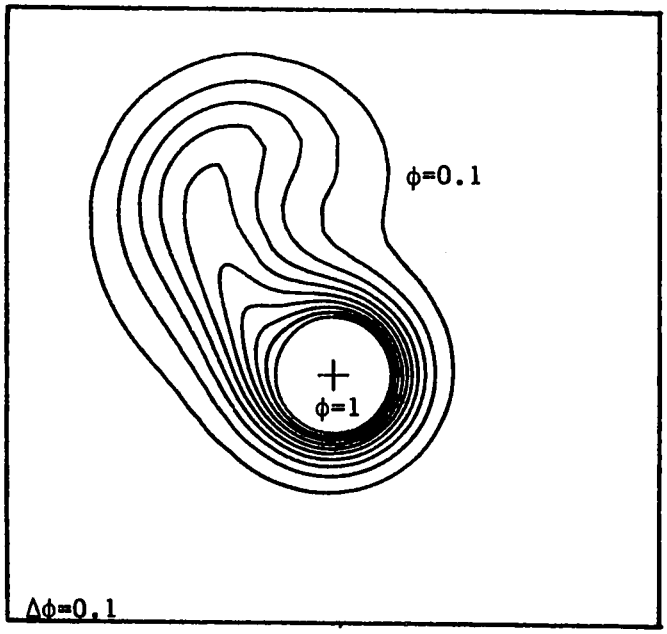

(e)

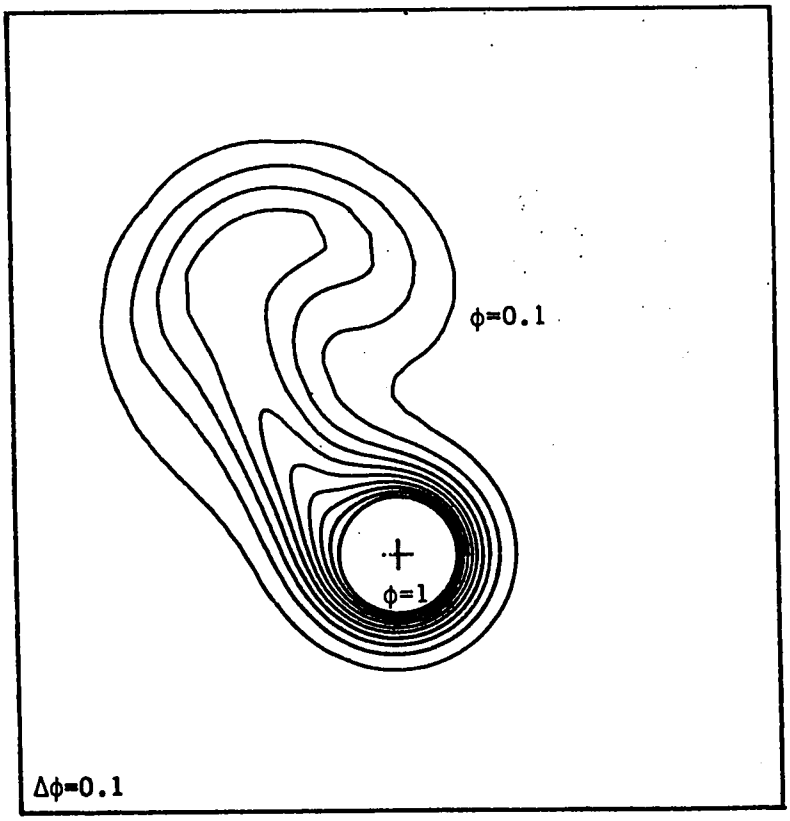

(f)

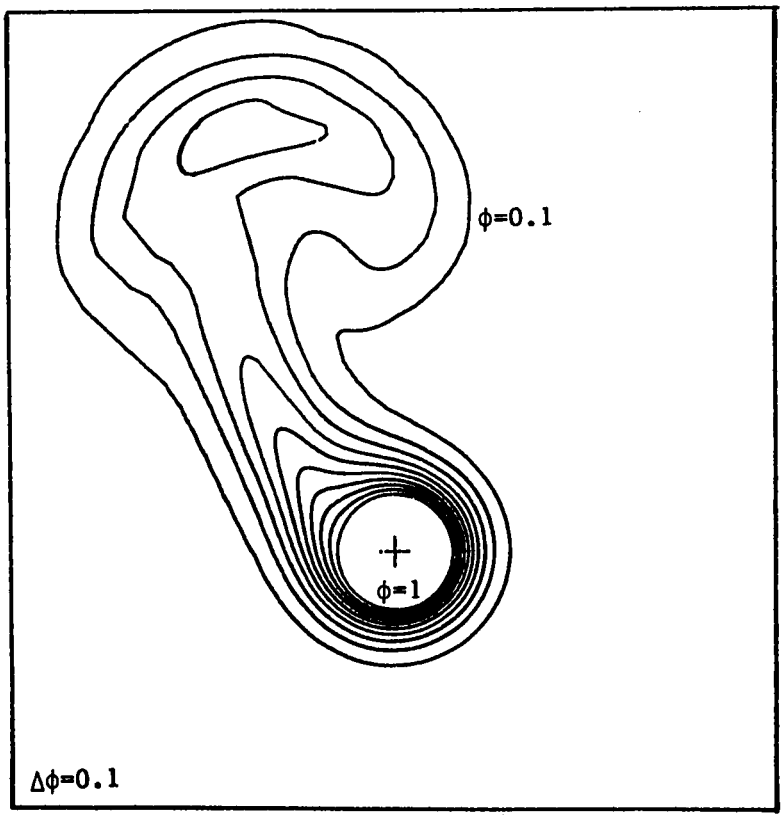

(g)

Fig. 15. The time development of the isotherm pattern for the case of Re = 50, Pr = 0.7 and Gr = 1250.

(a) t = 1.0 (b) t = 5.0 (c) t = 10.0 (d) t = 15.0
(e) t = 20.0 (f) t = 25.0 (g) t = 30.0.

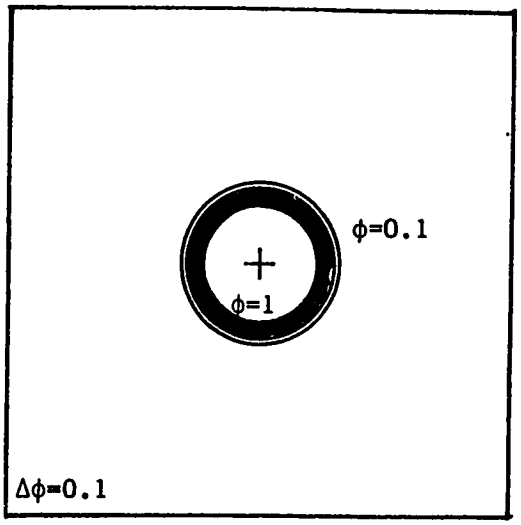

(a)

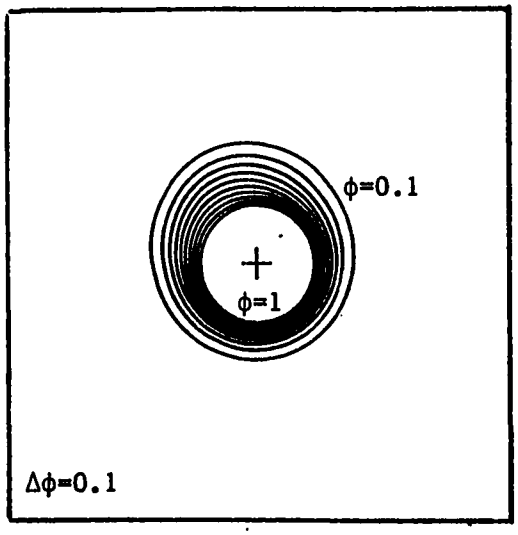

(b)

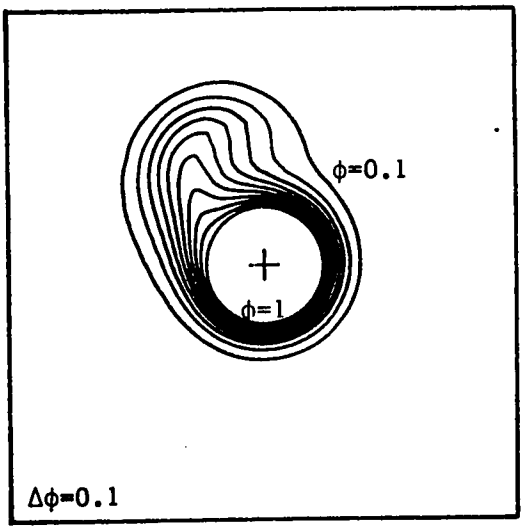

(c)

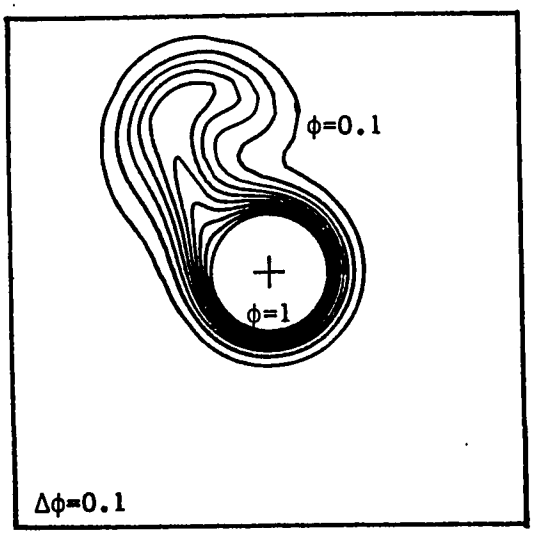

(d)

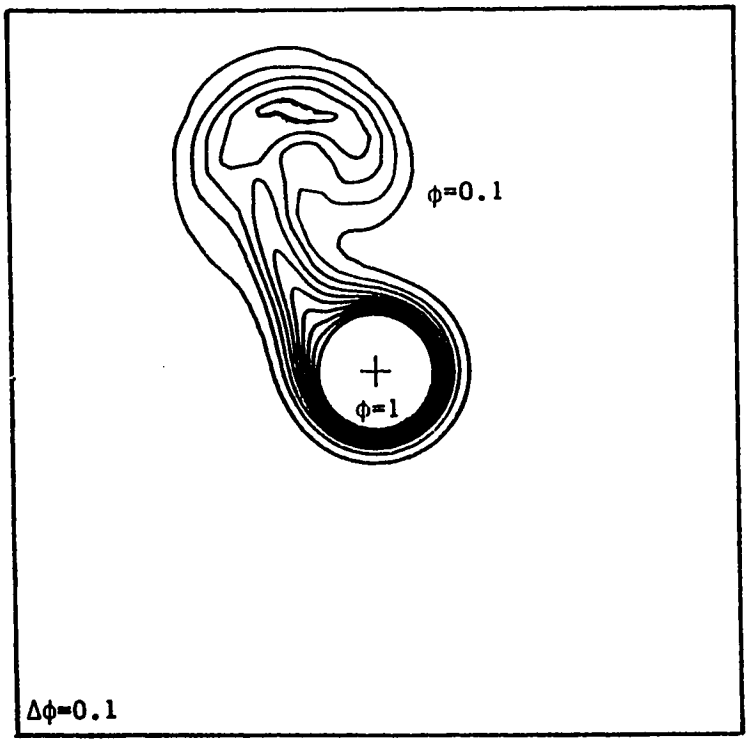

(e)

Fig. 16. The time development of the isotherm pattern for the case of Re = 100, Pr = 0.7 and Gr = 10000.

(a) t = 1.0 (b) t = 5.0 (c) t = 10.0
(d) t = 12.0 (e) t = 15.0.

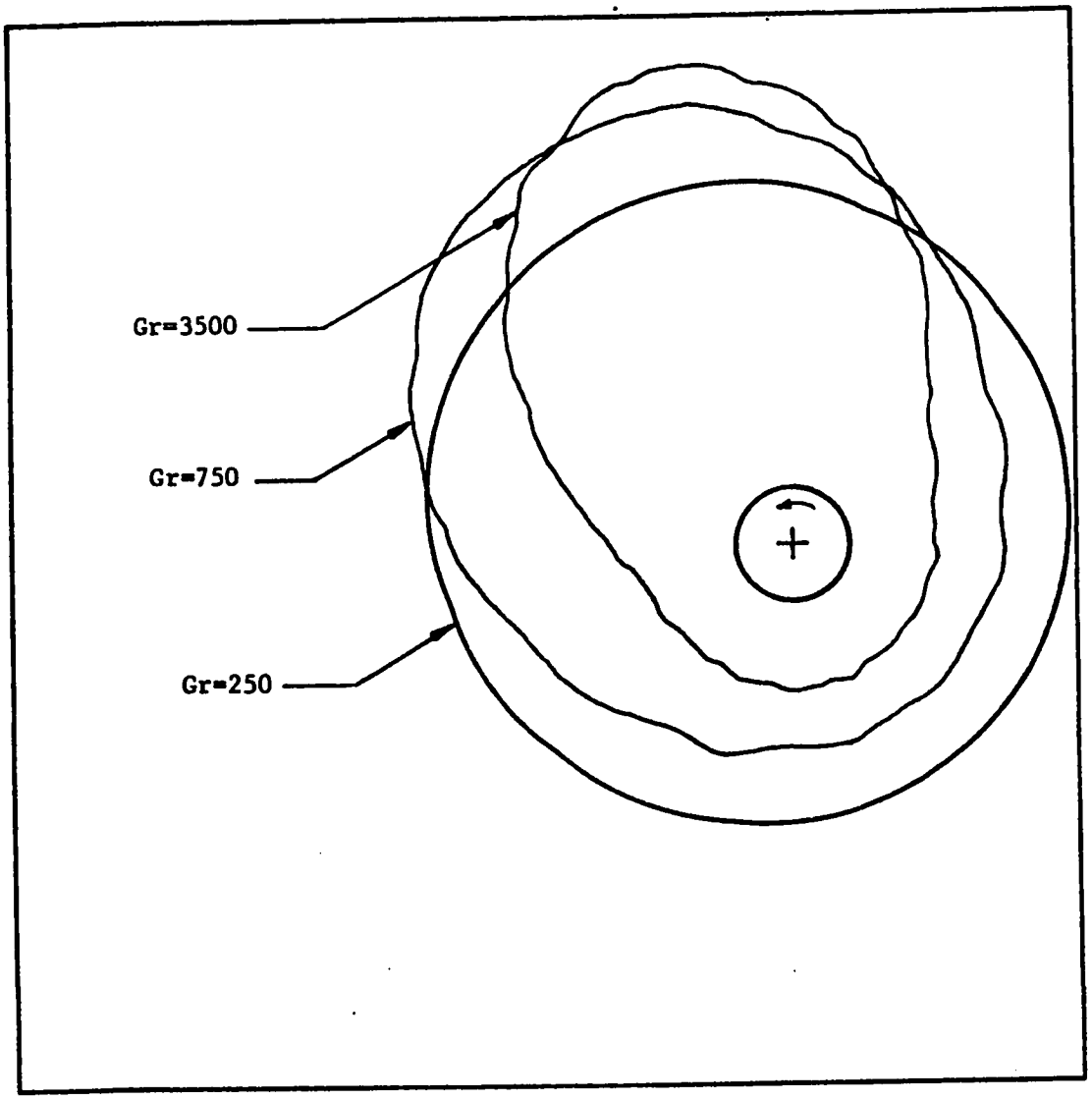

Fig. 17. The effect of Gr on the thermal boundary layer around the rotating cylinder for the case of Re = 50.

REFERENCES

[1] B.G.Vander Hegge Zijnen, Modified correlation formula for the heat transfer by natural and forced convection from horizontal cylinders, Appl. Sci. Res. A6, 129-140 (1957).

[2] J.R.Kyte, A.J.Madden and E.L.Piret, Natural convectional heat transfer at reduced pressures, Chem. Engng Prog.49, 653-662 (1953).

[3] T.Tsubouchi and H.Masuda, Heat transfer by natural convection from horizontal cylinders at low Rayleigh numbers, Report of the Institute of High Speed Mechanics, Tohoku University, 19, pp.205-219 (1967-1968).

[4] S.W.Churchill and H.H.S.Chu, Correlation equations for laminar and turbulant free convection from a horizontal cylinder, Int.J. Heat Mass Transfer, 18, 1049-1053 (1975).

[5] C.W.Rice, Free convection of heat in gases and liquids, Trans. AIEE, 42, 131-144 (1923); 43, 653-706 (1924).

[6] H.Senftleben, Die Warmeabgebe von Korperverschiedener form in Flussig keiten gasen bei freier stromung, Physik, 3, 361-373 (1951).

[7] V.T.Morgan, The overall convection heat transfer from smooth circular cylinders, Advances in Heat Transfer, 11, 199-264 (1975).

[8] G.D.Raithby and K.G.T.Hollands, Laminar and turbulant free convection from ellyptic cylinders with a vertical plate and horizontal cylinder as a special case, Trans. ASME, 98, 72-80 (1976).

[9] B. Farouk and S.I.Guceri, Natural convection from horizontal cylinder-Laminar regime, J. Heat Transfer, 103, 522-527 (1981).

[10] T.H. Kuehn and R.J.Goldstein, Numerical solution to the NavierStokes equations for laminar natural convection about a horizontal isothermal circular cylinder, Int.J. Heat Mass transfer, 23, 971-979 (1980).

[11] H.M. Badr, A theoritical study of laminar mixed convection from a horizontal cylinder in a cross stream, Int.J. Heat Mass Transfer, 26, No.5, 639-653 (1983).

[12] H.M. Badr, Laminar combined convection from a horizontal cylinder-parallel and contraflow regimes, Int.J. Heat Mass Transfer, 27, 15-27 (1984).

[13] H.M. Badr, On the effect of flow direction on mixed

convection from a horizontal cylinder, Int.J. for Numerical Methods in Fluids, (in print).

[14] I.T. Anderson and O.A.Saunders, Convection from an isolated heated horizontal cylinder rotating about its axis, Proc. Roy. Soc. of London, A, 217,555 (1953).

[15] D.Dropkin and A.Carmi, Natural convection heat transfer from horizontal cylinders rotating in air, Heat Transfer and Fluid Mechanics Institute, Stanford University (1956).

[16] G.A.Etemad, Free convection heat transfer from a rotating cylinder to ambient air with interferometric study of flow, Trans. ASME 77, 1283 (1955).

[17] G.I.Taylor, Distribution of velocity and temperature between concentric rotating cylinders, Proceedings of Royal Soc. of London, 151, A, 494-512 (1935).

[18] W.M.Kays and I.J.Bjorklund, Heat transfer from a rotating cylinder with and without cross flow, Trans. ASME, Paper no. 56-A-71 (1956).

[19] Th.Theodorsen and A.Regier, Experiments on drag of revolving discs, cylinders and streamlined rods at high speeds, NASA Technical Report 793 (1944).

[20] Kurt.M.Becker, Measurements of convective heat transfer from a horizontal cylinder rotating in a tank of water, Int.J. Heat Mass Transfer, 6, 1053-1062 (1963).

[21] R.A.Seban and H.A.Johnson, Heat transfer from a horizontal cylinder rotating in oil, NASA Memo 4-22-59W (April 1959).

[22] A.P.Hatton, D.D. James and H.W.Swire, Combined forced and natural convection with low-speed air flow over horizontal cylinders, J. Fluid Mechanics, 42, 17-31 (1970).

[23] Shimomura.R, Trans.JSME, 29, 1352 (1963).

[24] Lillian L. Goettler and J.A.Filo, Free convection from a slowly rotating horizontal cylinder ,Proc.5th.Int. Heat transfer conference . Tokyo, Sept. 3-7, 33, pp.207-211 (1974).

[25] G.A.Ostroumov, Unsteady heat convection near a horizontal cylinder, J. Tech. Phys., USSR, 1, 2627-2641 (1956).

[26] C.M.Vest and M.L.Lawson, Onset of convection near a suddenly heated horizontal wire, Int.J. Heat Mass Transfer, 15, 1281-1283 (1972).

[27] J.R.Parsons Jr. and J.C.Mulligan, Transient free

convection from a suddenly heated horizontal wire, J. Heat Transfer, 100, 423-428 (1978).

[28] J.R.Parsons Jr. and J.C.Mulligan, Onset of natural convection from a suddenly heated horizontal cylinder, J. Heat Transfer, 102, 636-639 (1980).

[29] R.E.Faw, R.P.H.Ismuntoyo and T.W.Lester, Transition from conduction to convection around a horizontal cylinder experiencing a ramp excursion in internal heat generation, Int.J. Heat Mass Transfer, 27, 1087-1097 (1984).

[30] Schlichting. R, Boundry Layer Theory , 7^{th} Edition, Mc-Graw Hill Book Company (1979).

[31] H.M.Badr and S.C.R.Dennis, Laminar forced convection from a rotating cylinder , Int.J. Heat Mass Transfer, 28, 253-264 (1985).

[32] H.M.Badr and S.C.R.Dennis, Unsteady flow past a rotating and translating circular cylinder, Proc.8th Canadian Congr. Applied Mechanics, 659-660 (1981).

[33] W.M.Collins and S.C.R.Dennis, Flow past an impulsively started circular cylinder, J. Fluid Mechanics, 60, 105-127 (1973).

[34] D.B.Ingham, Free convection boundry layer on an isothermal horizontal cylinder, ZAMP, 29, 871-883

(1978).

[35] Carnahan, Luther and Wilkes, Applied Numerical Methods, John Wiley and sons, Inc. (1969).

[36] V.Vemuri and Walter J. Karplus, Digital computer treatment of Partial Differential Equations, Prentice-Hall, Inc. (1981).

[37] R.D.Ritchmyer, Differential Methods for Initial Value Problems, Interscience, New York (1957).

[38] G.O'Brien, M.Hyman and S.Kaplan, A Study of the Numerical Solution of Partial Differential Equations, J. Math. Phys., 29, 233-251 (1951).

[39] Hildebrand, Introduction to Numerical Analysis, 2nd Edition, Mc-Graw Hill Inc., (1974)

[40] Filon, On a Quadrature Formula for Trigonometric Integrals, Proc. Roy. Soc. Edinburgh, 49, 38-47 (1928).

[41] S.C.R.Dennis and G.Chang, Numerical Integration of Navier-Stokes Equation in two dimensions, Math. Research Center, U.S. Army Tech. Rep. No.859 (1969).

APPENDICES

APPENDIX (A)

The functions S_o, S_{n_1} and S_{n_2} used in equations (45a), (45b) and 45(c) are as follows

$$S_o(\xi,t) = -e^{\xi}\frac{Gr}{2Re^2}\left[\frac{\partial H_1}{\partial \xi} + H_1\right] + \sum_{n=1}^{N} n\left(F_n\frac{\partial g_n}{\partial \xi} - f_n\frac{\partial G_n}{\partial \xi} + g_n\frac{\partial F_n}{\partial \xi} - G_n\frac{\partial f_n}{\partial \xi}\right), \quad (A1)$$

$$S_{n_1}(\xi,t) = -e^{\xi}\left(\frac{Gr}{2Re^2}\right)\left[\frac{\partial h_{n-1}}{\partial \xi} + \frac{\partial h_{n+1}}{\partial \xi} - (n-1)h_{n-1} + (n+1)h_{n+1}\right] + \sum_{m=1}^{N}\left\{\frac{\partial g_m}{\partial \xi}(K f_K - J f_J) + \frac{\partial G_m}{\partial \xi}[K F_K - (m-n)F_J] + mg_m\left[\frac{\partial f_K}{\partial \xi} - Sg_n(m-n)\frac{\partial f_J}{\partial \xi}\right] + mG_m\left(\frac{\partial F_K}{\partial \xi} - \frac{\partial F_J}{\partial \xi}\right)\right\}, \quad (A2)$$

$$S_{n_2}(\xi,t) = -e^{\xi}\left(\frac{Gr}{2Re^2}\right)\left[\delta_n\frac{\partial H_o}{\partial \xi} + \frac{\partial H_{n-1}}{\partial \xi} + \frac{\partial H_{n+1}}{\partial \xi} + (n+1)H_{n+1} - (n-1)H_{n-1}\right] + \sum_{m=1}^{N}\left\{\frac{\partial g_m}{\partial \xi}[K F_K + (m-n)F_J] - \frac{\partial G_m}{\partial \xi}(K f_K + J f_J) + mg_m\left(\frac{\partial F_K}{\partial \xi} + \frac{\partial F_J}{\partial \xi}\right) - mG_m\left[\frac{\partial f_K}{\partial \xi} + Sg_n(m-n)\frac{\partial f_J}{\partial \xi}\right]\right\}, \quad (A3)$$

where

$$K = m+n, \quad J = |m-n| \text{ and } \delta_n = \begin{cases} 1 & \text{when } n = 1 \\ 0 & \text{when } n \neq 1 \end{cases},$$

and $Sg_n(m-n)$ means the sign of the term $(m-n)$ and $Sg_n(m-n) = 0$ when $m = n$. All the functions with subscripts less than 1 and greater than N must be equated to zero.

APPENDIX (B)

The definition of the functions Z_o, Z_{n_1} and Z_{n_2} used in equations 47(a), 47(b) and 47(c) are as follows:

$$Z_o(\xi,t) = \sum_{n=1}^{N} n\left(F_n \frac{\partial h_n}{\partial \xi} - f_n \frac{\partial H_n}{\partial \xi} + h_n \frac{\partial F_n}{\partial \xi} - H_n \frac{\partial f_n}{\partial \xi}\right) , \tag{B1}$$

$$Z_{n_1}(\xi,t) = \sum_{m=1}^{N} \left\{ \frac{\partial h_m}{\partial \xi} (K f_K - J f_J) + \frac{\partial H_m}{\partial \xi} [K F_K - (m-n)F_J] \right.$$

$$\left. + m h_m \left[\frac{\partial f_K}{\partial \xi} - Sg_n(m-n) \frac{\partial f_J}{\partial \xi}\right] + m H_m \left(\frac{\partial F_K}{\partial \xi} - \frac{\partial F_J}{\partial \xi}\right)\right\} , \tag{B2}$$

$$Z_{n_2}(\xi,t) = \sum_{m=1}^{N} \left\{ \frac{\partial h_m}{\partial \xi} [K F_K + (m-n)F_J] - \frac{\partial H_m}{\partial \xi} (K f_K + J f_J) \right.$$

$$\left. + m h_m \left(\frac{\partial F_K}{\partial \xi} + \frac{\partial F_J}{\partial \xi}\right) - m H_m \left[\frac{\partial f_K}{\partial \xi} + Sg_n(m-n) \frac{\partial f_J}{\partial \xi}\right]\right\} , \tag{B3}$$

where

$$K = m+n,\ J = |m-n| \text{ and } \delta_n = \begin{cases} 1 \text{ when } n = 1 \\ 0 \text{ when } n \neq 1 \end{cases} ,$$

and $Sg_n(m-n)$ means the sign of term $(m-n)$ and $Sg_n(m-n) = 0$ when $m = n$. All the functions with subscripts less than 1 and more than N must be equated to zero.